Suppression of African horse sickness virus NS1 protein expression in mammalian cells by short hairpin RNAs

by

Helena Johanna Roos

Submitted in partial fulfilment of the requirements for the degree of
Master of Science
in the Faculty of Natural and Agricultural Sciences
University of Pretoria
Pretoria

October 2008

I declare that the dissertation, which I hereby submit for the degree M.Sc (Microbiology) at the University of Pretoria, is my own work and had not previously been submitted by me for a degree at this or any other tertiary institution.

Signature: _____

Helena Johanna Roos

Date: _____

ACKNOWLEDGEMENTS

I would like to thank the following people for their contribution:

Prof. J. Theron for guiding me and assisting me with my M.Sc project.

Prof. H. Huismans for his assistance in my project.

Liesel Stassen and Marthi Nieuwoudt for their unwavering support and contributions to the RNA interference project.

The staff and students of the Departments of Microbiology and Plant Pathology and Genetics for their contributions to this investigation.

The Microscopy staff for illuminating fluorescence and electron microscopy for me.

My family and friends for their support and encouragement towards my work.

The National Research Foundation for providing the necessary finances for this research project.

SUMMARY

Suppression of African horse sickness virus NS1 protein expression in mammalian cells by short hairpin RNAs

by

Helena Johanna Roos

Supervisor: Prof. J. Theron
Department of Microbiology and Plant Pathology
University of Pretoria

Co-supervisor: Prof. H. Huismans
Department of Genetics
University of Pretoria

for the degree M.Sc

African horse sickness virus (AHSV), a member of the *Orbivirus* genus within the *Reoviridae* family, causes an acute disease in horses with a high mortality rate. AHSV encodes four nonstructural proteins (NS1, NS2, NS3/NS3A), whose functions in the viral life cycle are not fully understood. The NS1 protein is the most abundantly expressed viral protein during AHSV infection and forms tubular structures within the cell cytoplasm. No function has been ascribed to these tubules to date, although it has been suggested that they may play a role in cellular pathogenesis. Studies aimed at understanding the function of NS1 have been hampered by the lack of a suitable reverse genetics system for AHSV. However, the phenomenon of RNA interference (RNAi) has emerged as a powerful tool whereby the function of individual genes can be studied. In mammalian cells, RNAi can be triggered by exposing cells to double-stranded RNA either via exogenous delivery of chemically synthesized small interfering RNAs (siRNAs) or endogenous expression of short hairpin RNAs (shRNAs). Consequently, the aim of this investigation was to develop a plasmid DNA vector-based RNAi assay whereby expression of the AHSV-6 NS1 gene could be suppressed in BHK-21 cell culture with shRNAs directed to the NS1 gene.

To investigate, complementary oligonucleotides corresponding to selected AHSV-6 NS1 gene sequences were chemically synthesized, annealed and cloned into the pSUPER shRNA delivery vector under control of the RNA polymerase III H1 promoter. The plasmid DNA vector-expressed shRNAs targeted sequences within the NS1 gene corresponding to nucleotides 710 to 728 (shNS1-710) and 1464 to 1482 (shNS1-1464), respectively. A NS1-eGFP chimeric gene was constructed and used towards establishing a simple assay whereby the gene silencing efficiency of different RNAi effector molecules could be evaluated by analysis of the protein level visually and quantitatively by fluorometry. The effect of the NS1-directed shRNAs on AHSV-6 NS1 protein expression was subsequently evaluated by co-transfection of BHK-21 cells with the respective recombinant pSUPER shRNA delivery vectors and the NS1 reporter plasmid pCMV-NS1-eGFP. The results indicated that shNS1-710 and shNS1-1464 suppressed NS1-eGFP expression by 19% and 9%, respectively. The potential of the NS1-directed shRNAs to suppress NS1 mRNA expression was investigated by transfection of BHK-21 cells with the respective recombinant pSUPER shRNA delivery vectors, followed by transfection with the recombinant mammalian expression vector pCMV-NS1 or infection with AHSV-6. Results obtained by semi-quantitative real-time PCR assays indicated that both NS1-directed shRNAs interfered with NS1 mRNA expression, albeit to different extents in the respective assays. Taken together, these results demonstrated that AHSV-6 NS1 gene expression can be suppressed in BHK-21 cells by plasmid DNA vector-derived shRNAs and suggests that this approach may, with further optimization, be useful in determining the function of the NS1 protein in virus-infected cells.

TABLE OF CONTENTS

LIST OF ABBREVIATIONS

AHS	African horse sickness
ATP	adenosine-5'-triphosphate
ATPase	adenosine triphosphatase
AHSV	African horse sickness virus
BHK	baby hamster kidney
β2-MG	β2-microglobulin
BLAST	Basic Local Alignment Search Tool
bp	base pair
BTV	Bluetongue virus
˚C	degree Celsius
ca.	approximately
cDNA	complementary DNA
CER	chicken embryo-related
cm^2	cubic centimeter
CMV	cytomegalovirus
CO_2	carbon dioxide
CsCl	cesium chloride
Da	dalton
DNA	deoxiribonucleic acid
DNase	deoxyribonuclease
dNTP	deoxynucleoside-5'-triphosphate
ds	double-stranded
dsRNA	double-stranded RNA
EDTA	ethylenediamine-tetra-acetic acid
eGFP	enhanced green fluorescent protein
FBS	foetal bovine serum
FCS	foetal calf serum
Fig.	figure
h	hours
IPTG	5-bromo-4-chloro-3-indolyl-β-D-galactosidase
kb	kilo-base pairs
kDa	kilodalton
L	litre
LB-medium	Luria-Bertani medium

M	molar
mA	milliampere
MCS	multiple cloning site
MEM	minimal essential medium
min	minute
ml	milliliter
mM	millimolar
MOI	multiplicity of infection
ng	nanogram
nm	nanometer
nt	nucleotide
OAc	acetate
OD	optical density
PBS	phosphate-buffered saline
pfu	plaque forming units
PCR	polymerase chain reaction
PKR	protein kinase R
pmol	picomole
PSB	protein solvent buffer
REST	Relative Expression Software Tool
RISC	RNA-induced silencing complex
RNA	ribonucleic acid
RNAi	RNA interference
RNase	ribonuclease
RNPs	ribonucleoprotein particles
rpm	revolutions per minute
RT	reverse transcription
RT-PCR	reverse transcription-polymerase chain reaction
s	seconds
SDS-PAGE	sodium dodecyl sulphate-polyacrylamide gel electrophoresis
SECs	shRNA expression cassettes
shRNA	short hairpin RNA
siRNA	small interfering RNA
ssRNA	single-stranded RNA
TEM	transmission electron microscopy
TEMED	N’,N’,N’,N’-tetramethylethylenediamine

U	units
UHQ	ultra high quality
µg	microgram
µl	microliter
µM	micromolar
UV	ultraviolet
v.	version
V	volt
VIB	virus inclusion body
v/v	volume per volume
w/v	weight per volume
X-gal	5-bromo-4-chloro-3-indolyl-β-D-galactosidase
2’,5’-AS	2’,5’-oligoadenylate synthetase

LIST OF FIGURES

LIST OF TABLES

CHAPTER 1

LITERATURE REVIEW

1.1 GENERAL INTRODUCTION

African horse sickness virus (AHSV), a member of the *Orbivirus* genus within the *Reoviridae* family, causes an acute infectious but non-contagious disease of *Equidae*. Although the mortality rate in horses is high, sometimes in excess of 90%, mules and donkeys appear to have some natural resistance to the development of acute disease, while zebras are even less susceptible (Erasmus *et al.*, 1978; Tomori *et al.*, 1992). AHSV is transmitted to susceptible animals by biting midges of the *Culicoides* genus, which become infected by feeding on animals during the febrile and viraemic stages of infection (Wetzel *et al.*, 1970; Mellor, 1994; Venter *et al.*, 2000). African horse sickness (AHS) is endemic in sub-Saharan Africa, although occasional outbreaks of the disease have occurred in North Africa and the Arabian Peninsula (Rafyi, 1961; Mirchamsy and Hazrati, 1973; Mellor, 1994). More recently, outbreaks have also occurred in southern European countries, which may be due to severe climate changes that have allowed the *Culicoides* vector to expand its host range to these increasingly warmer countries (Mellor and Hamblin, 2004). Due to its severity and ability to spread quickly and without warning from its endemic areas, AHS has been classified as a notifiable disease by the Office International des Epizooties (OIE) (Mellor and Hamblin, 2004).

Like other members of the *Orbivirus* genus, the genome of AHSV consists of ten double-stranded (ds) RNA segments (Bremer, 1976; Bremer *et al.*, 1990), which encodes seven structural proteins (VP1-VP7) that are organized into two concentric protein shells, *i.e.* the outer and inner capsids (Verwoerd and Huismans, 1969; Oellerman *et al.*, 1970). Whereas the outer capsid is composed of the two major structural proteins VP2 and VP5, the inner capsid (core particle) is composed of the two major proteins VP3 and VP7, and three minor proteins, VP1, VP4 and VP6, in addition to the dsRNA genome (Roy *et al.*, 1994). In addition to the seven structural proteins, four nonstructural proteins, NS1, NS2 and NS3/NS3A, are synthesized in AHSV-infected cells (Bremer *et al.*, 1990; Grubman and Lewis, 1992). The NS1 and NS2 proteins are synthesized abundantly in the infected cell cytoplasm (Lecastas, 1968) and are believed to be involved in virus replication, assembly and morphogenesis (Hyatt and Eaton, 1988; Kar *et al.*, 2007). In contrast, the NS3/NS3A proteins are barely detectable in infected cells and are believed to be involved in the egress of progeny virus (Hyatt *et al.*, 1989; Stoltz *et al.*, 1996).

Studies regarding the structure-function relationships of many different AHSV genes and encoded proteins have been facilitated by the baculovirus expression system (Van Staden *et al.*, 1995; Uitenweerde *et al.*, 1995; Maree and Huismans, 1997; Maree *et al.*, 1998; Van Niekerk *et al.*, 2001; De Waal and Huismans, 2005). Despite these advances, a major drawback of research with AHSV has been the lack of a suitable reverse genetics system that would allow genetic manipulation of the virus. However, the recently described phenomenon of RNA interference (RNAi) may provide a means whereby studies regarding the replication process of AHSV, interactions between the virus and host cells and the role of individual viral proteins within the context of the whole virus can be investigated. RNAi is a post-transcriptional gene silencing process in which dsRNA initiates specific cleavage of cytoplasmic mRNA (Fire *et al.*, 1998). In this process, dsRNA is cleaved into small interfering RNAs (siRNAs) of 21-23 nucleotides (nt) in length by an RNase III enzyme, commonly referred to as Dicer. The siRNAs associate with a multiprotein complex, known as the RNA-induced silencing complex (RISC), and is used as a template to guide splicing of mRNA that is homogolous in sequence to the RISC-bound siRNA strand (Meister and Tuschl, 2004; Tomari and Zamore, 2005). The efficient and sequence-specific nature of RNAi has made it a powerful tool for investigating virus gene function (Bitko and Barik, 2001; Déctor *et al.*, 2002; López *et al.*, 2005; Campagna *et al.*, 2005; Wirblich *et al.*, 2006), and it has great potential as an antiviral therapy (Haasnoot *et al.*, 2003; Tan and Yin, 2004; Colbére-Garapin *et al.*, 2005; Stram and Kuzntzova, 2006).

1.2 AFRICAN HORSE SICKNESS VIRUS

1.2.1 Taxonomic classification of AHSV

African horse sickness virus is a member of the genus *Oribivirus* within the *Reoviridae* family (Calisher and Mertens, 1998). Viruses within this family possess segmented dsRNA genomes (10-12 segments) encapsidated within single non-enveloped virus particles with a diameter of 60-80 nm and exhibit icosahedral symmetry (Matthews, 1982; Francki *et al.*, 1991; Gorman, 1992). In addition to the *Orbivirus* genus, the other eight genera of this family are *Orthoreovirus*, *Cypovirus*, *Aquareovirus*, *Rotavirus*, *Coltivirus*, *Fijivirus*, *Phytoreovirus* and *Oryzavirus*, which encompass vertebrate, arthropod and plant pathogens (Calisher and Mertens, 1998). The name “orbivirus” is derived from the Latin word “orbis”, which means ring or circle and refers to the ring-like capsomers on the surface of the inner core of the orbiviruses (Borden *et al.*, 1971). Orbiviruses differ from other members of the *Reoviridae* by

the presence of a double-layered protein capsid (Verwoerd and Huismans, 1969; Borden *et al.*, 1971), their greater sensitivity to lipid solvents and detergents (Gorman and Taylor, 1985) and they are able to replicate in both insects and vertebrates (Gorman, 1992). To date, there are 19 recognized serogroups of orbiviruses and they can be differentiated from each other based on biochemical and immunological tests (Calisher and Mertens, 1998). Viruses within each serogroup can be classified into serotypes on the basis of antibody-mediated neutralization of viral infectivity (Knudson and Monath, 1990; Brown *et al.*, 1991). There are presently nine recognized serotypes of AHSV (McIntosh, 1958; Howell, 1962).

1.2.2 Epidemiology, transmission and pathogenesis of AHS

African horse sickness (AHS) is an infectious but non-contagious viral disease of equids, with horses being the most susceptible (Tomori *et al.*, 1992). However, antibodies to AHSV have been detected in dogs, camels, donkeys, mules and zebra (Van Rensburg *et al.*, 1981; Fassi-Fihri *et al.*, 1998; El Hasnaoui *et al.*, 1998). Indeed, zebra have long been considered the natural vertebrate host and reservoir of AHSV, since they rarely exhibit clinical signs of AHSV infection (Erasmus, 1976; Barnard, 1998). Consequently, they are believed to play an important role in the persistence of the virus in Africa. Although AHS was believed to be endemic to sub-Saharan Africa, except for occasional outbreaks in North Africa and the Arabian Peninsula (Rafyi, 1961; Mirchamsy and Hazrati, 1973; Mellor, 1994), there have been, however, several outbreaks of the disease in the Persian Gulf, middle Eastern and southern European countries (Howell, 1960; Lubroth, 1988; Mellor and Hamblin, 2004). Of the nine AHSV serotypes, serotypes 1 to 8 are found in sub-Saharan Africa, while serotype 9 is more widespread and, with the exception of Spain-Portuguese outbreaks during 1989-1990, has been responsible for almost all outbreaks outside Africa (Coetzer and Erasmus, 1994).

AHSV is primarily transmitted to susceptible equide hosts via biting heamotophagous midges of the *Culicoides* genus (Wetzel *et al.*, 1970; Mellor, 1994). Different *Culicoides* species may be responsible for transmitting AHSV across various areas, but *Culicoides imicola* is believed to be the primary vector of the virus in Europe, Africa and Asia (Mellor, 1994). *C. botilinos*, which has a wide distribution in southern Africa, has also been identified as a potential vector of AHSV (Venter *et al.*, 2000) and is common in cooler highland areas where *C. imicola* is rare. Moreover, in Spain, AHSV has also been found in *C. obsoletus* and *C. pulicaris*, both of which are also the most common *Culicoides* species in central and northern Europe (Mellor *et*

al., 1983). Virus replication and therefore transmission does not occur at temperatures below 15ºC. However, it has been observed that the virus persists in vectors during extended periods of cool temperatures and when transferred to more preferable temperatures, high levels of virus replication occur (Welby *et al.*, 1996). This may have major implications for the transmission of AHSV in countries with more moderate climates, because it allows for the over-wintering of the disease in the absence of major vertebrate hosts.

After transfer of AHSV by the bite of infected *Culicoides* spp. midges, the virus is transported to the lymph nodes where initial virus replication occurs. The virus then spreads through the host via the blood (primary vireamia) and infects the target organs, the lungs, spleen, other lymphoid tissues and endothelial cells. Secondary vireamia occurs in these tissues and is of a variable duration and titer, depending on the host species, the pathogenicity of the serotype involved and the immunity of the infected animal (Coetzer and Erasmus, 1994; Mellor and Hamblin, 2004). Four forms of the disease have been described in horses, depending on the predominant system affected, *i.e.* the acute or pulmonary form, the sub-acute or cardiac form, the mixed form (both cardiac and pulmonary) and the febrile or fever form (Coetzer and Erasmus, 1994). The fever form of the disease, which is caused by less virulent strains of AHSV, develops after an incubation period of 5 to 14 days and is characterized by a mild to moderate fever and edema of the supraorbital fossae. No mortality is associated with this form of the disease and horses recover completely. The pulmonary form develops rapidly (within 4 to 5 days) and is characterized by respiratory distress, dyspnea, coughing spasms, and a frothy, fluid discharge from the animal's nostrils. The mortality rate exceeds 95%, with death and terminal hypothermia occurring 24-48 h after the occurrence of the first clinical signs. The cardiac form has an incubation period of 7 to 14 days and is characterized by a mild fever and signs of increasing subcutaneous edema of the head, neck and chest, as well as edema of the supraorbital fossae. The mortality rate may exceed 50% and death can occur within 5-7 days after the onset of the symptoms. The mixed pulmonary and cardiac form of AHS is often the most common form of the disease and the animals display symptoms of both forms of the disease. The mortality rate is 70% and death can occur within 3-6 days after the onset of the symptoms (Coetzer and Erasmus, 1994).

Although there is no efficient treatment for AHS, horses in southern Africa are vaccinated annually with polyvalent attenuated vaccines in an attempt to prevent disease and control outbreaks (Erasmus, 1976). Due to concerns regarding incomplete protection as a

consequence of interference between the virus serotypes (Erasmus, 1994) and the fact that some strains of the virus in the vaccine might only be weakly immunogenic (Laegreid, 1996), research has been undertaken to develop alternate vaccines. Subunit vaccines, based on the use of baculovirus-expressed AHSV-4 VP7 (Wade-Evans *et al.*, 1997) and the outer capsid proteins VP2 and VP5 (Martinez-Torrecuadrada *et al.*, 1996; Scanlen *et al.*, 2002), as well as BTV core- and virus-like particles (Roy *et al.*, 1992; Roy *et al.*, 1993; Roy and Sutton, 1998) have been investigated. However, the subunit vaccines have not been commercialized yet, which may be indicative of the high costs and difficulties associated with their production.

1.3 STRUCTURE AND MOLECULAR BIOLOGY OF AHSV

Bluetongue virus (BTV), the prototype virus of the *Orbivirus* genus, has been the subject of extensive molecular, genetic and structural studies. As a consequence, it represents one of the best characterized viruses. Therefore, in the following sections, information on AHSV will be supplemented with that obtained from studies undertaken on BTV.

1.3.1 The virion

The AHSV virion is non-enveloped with two concentric protein layers (Fig. 1.1) (Verwoerd and Huismans, 1969; Oellerman *et al.*, 1970). The core or inner capsid is comprised mainly of the two major proteins VP3 and VP7 and encloses the three minor proteins VP1, VP4 and VP6, and the segmented dsRNA genome. The outer shell or outer capsid is composed mainly of the two other major structural proteins VP2 and VP5 (Roy *et al.*, 1994). The overall ultrastructure of orbiviruses is typified by that of BTV of which the single- and double-shelled virus particles have been studied extensively by immunoelectron microscopy, cryo-electron microscopy and X-ray crystallography (Hewat *et al.*, 1992a; Prasad *et al.*, 1992; Grimes *et al.*, 1998; Stuart and Grimes, 2006).

Based on these analyses, it is possible to segregate the core into two distinct layers. A thin inner layer is formed from 120 molecules of VP3, arranged as 60 dimers, to form a smooth-surfaced shell. The VP3 shell is stabilized by the outer layer of the core that comprises 260 VP7 trimers, organized into pentametric and hexameric rings that protrude 5 nm from the surface with channels between them. The channels may be involved in the passage of metabolites into and from the virus particle during infection (Prasad *et al.*, 1992; Stuart *et al.*, 1998). The core contains the dsRNA genome and the three minor proteins VP1 (10 or 12

copies), VP4 (20 or 24 copies that form dimers) and VP6 (60 or 72 copies that may form hexamers), each of which play a significant role in genome RNA replication (Stuart and Grimes, 2006). The icosahedral and fibrillar outer capsid consists of 360 globular-shaped VP5 molecules arranged in 120 trimers that are located in the channels formed by the six-membered rings of the VP7 trimers. The 180 copies of VP2 form 60 triskelion-type motifs that cover all of the VP7 trimers and protrude 4 nm above the globular VP5 proteins (Hewat *et al.*, 1992a; Stuart *et al.*, 1998). A schematic diagram at the BTV particle is presented in Fig. 1.1.

1.3.2 The viral genome

The AHSV genome consists of ten dsRNA segments, which are grouped according to size into large (L1-L3), medium (M4-M6) and small (S7-S10) genome segments (Table 1.1). The molecular weight of the ten AHSV genome segments range from 2.53-0.2 × 10^6 Da, with a total molecular weight of 13 × 10^6 Da (Verwoerd *et al.*, 1972; Bremer, 1976; Gorman *et al.*, 1977). Each genome segment, except for the smallest (segment 10), encodes for a single protein (Bremer *et al.*, 1990; Grubman and Lewis, 1992). The viral genome segments contain conserved 5' (5'-GUUAAA) and 3' (ACUUAC-3') terminal hexanucleotides, a feature that is typical of viruses in the *Reoviridae* family. Furthermore, each genome segment has unique complementary inverted repeat sequences (Rao *et al.*, 1983; Cowley *et al.*, 1992), which may be of importance for initiation of transcription and/or in the sorting and assembly of genome segments during virus replication (Anzola *et al.*, 1987; Mizukoshi *et al.*, 1993).

1.3.3 The viral proteins

In tissue culture, the first BTV-specific proteins are detectable 2 h post-infection, and the rate of protein synthesis increases rapidly until 12 to 13 h post-infection after which it slows down but continues until cell death (Huismans, 1979). In addition to seven structural proteins (VP1-VP7), four nonstructural proteins are also characterized in infected cells. Nonstructural proteins NS1 and NS2 are synthesized abundantly early in infection and co-incides with two virus-specific intracellular structures, *i.e.* tubules and viral inclusion bodies (VIBs), respectively (Lecastas, 1968; Huismans and Els, 1979). However, synthesis of NS3 and the related NS3A protein is barely detectable and its expression may correlate with virus release (Van Staden *et al.*, 1995; Stoltz *et al.*, 1996).

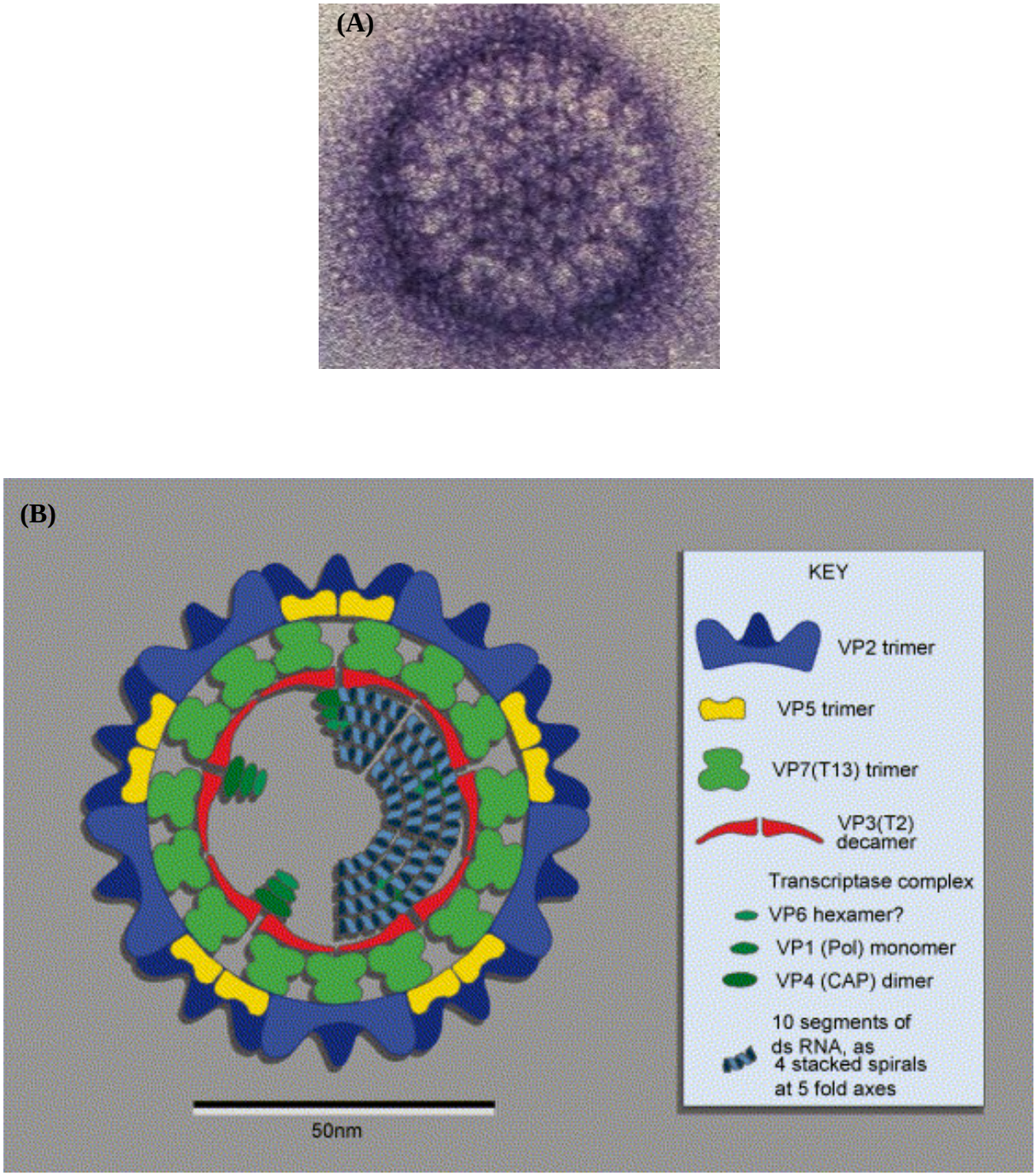

Fig. 1.1 Structure of the bluetongue virus particle. Electron micrograph of bluetongue virus (adapted from www.fao.org) (A). Schematic diagram of the structure of the bluetongue virus particle, including the two concentric protein layers and the dsRNA genome (B). The outer capsid consists of VP2 and VP5, while the core consists of the two major proteins VP3 and VP7 that encloses the three minor proteins VP1, VP4 and VP6, and the ten dsRNA genome segments (Mertens, 2000).

Table 1.1 BTV genome segments and their encoded proteins (adapted from Mertens, 2004)

Genome segment (bp)	Protein	Location	Number of amino acids	Molecular mass of proteins (Mr)	Properties	Functions
L1	VP1	Within the subcore	1305	150292	The largest protein, highly basic with a positively charged carboxyl terminus.	RNA-directed RNA polymerase responsible for RNA transcription/replication.
L2	VP2	Outer capsid	1051	122043	It forms a triskelion spike-like structure, which is found in excess in the outer layer of the core. Together with VP5 it exhibits the greatest variation in sequence between the serotypes, it determines the virus serotype and it is a neutralizing antigen, as well as a hydrophilic protein.	It possesses the viral haemagglutination and neutralization activity, is the cellular receptor protein which allows for the attachment and adsorption of the virus to the cell and is involved in the determination of virulence.
L3	VP3	Within the subcore layer	905	103269	It contains group-specific antigen determinants and it is highly conserved and hydrophobic in nature.	Controls the size and organization of the core structure.
M4	VP4	Component of the inner core	642	75826	Hydrophilic protein, which is highly conserved.	It is a methyl transferase protein that caps and methylates the mRNAs.
M6	VP5	The inner layer of the outer capsid	504	56900	It forms globular structures on the outer layer and is very variable in sequence between the serotypes.	VP5 and VP2 form the outer capsid. VP5 is involved in the permeabilization of the endosomal membrane in a pH-dependent manner during initiation of infection and it also helps determine the virus serotype.
S9	VP6	Within the subcore layer	369	38464	Hydrophilic protein with ssRNA- and dsRNA-binding ability.	May serve as a NTPase and a helicase, which unwinds the dsRNA before replication, and it binds ssRNA and dsRNA.
S7	VP7	Outer core surface	349	37916	It contains group-specific antigen determinants and is rich in hydrophobic regions.	It forms the outer core surface, which is involved in cell entry and in the high infectivity of vector insects and cells.
M5	NS1	Cytoplasm of infected cells	548	63377	Highly conserved and form tubules during replication, which consist of helically coiled ribbons of dimers.	Although the function of NS1 tubules in virus replication is unclear, it may be involved in pathogenesis.
S8	NS2	Cytoplasm of infected cells	365	41193	Only phosphorylated protein, which is largely hydrophilic and has a NTPase function.	It binds to ssRNA and may be involved in enveloping the mRNA during viral assembly and replication, and its NTPase activity might play a role in providing energy for the assortment, movement or packaging of the ssRNA that it binds.
S10	NS3 and NS3A	Cell membranes	217 206	23659 22481	NS3A is a truncated form of NS3, both proteins are glycosylated, highly variable and cytotoxic to cell.	It disrupts cell membranes allowing virus release and may be involved in determination of virulence.

1.3.3.1 Outer capsid proteins

The VP2 protein, one of the two outer capsid proteins, is the most variable of the viral proteins and is the major serotype-specific antigen (Huismans and Erasmus, 1981) and viral heamagglutinin (Cowley and Gorman, 1987). Neutralizing epitopes have been mapped on AHSV VP2 (Bentley *et al.*, 2000; Martinez-Torrecuadrada *et al.*, 2001) and antibodies raised in rabbits to VP2 of AHSV-4 have been reported to neutralize a virulent strain of AHSV-4 (Martinez-Torrecuadrada *et al.*, 1994). It has also been shown that baculovirus- and vaccinia-expressed AHSV VP2 can protect horses against a lethal challenge with the homologous virus serotype (Huismans *et al.*, 1987a; Stone-Marchat *et al.*, 1996; Scanlen *et al.*, 2002). In addition, VP2 is directly involved in the attachment of virus to cells, since removal of VP2 eliminates binding of the virus to host cells (Huismans and Van Dijk, 1990). Although the cellular receptor(s) are unknown, it has more recently been reported that VP2 binds to sialic acid moieties of cellular receptors prior to internalization of the virus particles via an early endosome (Hassan and Roy, 1999). These functional features of VP2 appear to correlate well with it being the most accessible protein on the virion surface.

In contrast to the VP2 protein, the role of VP5 in neutralization has not yet been clearly established. In contrast to BTV (Marshall and Roy, 1990), AHSV VP5 is able to induce neutralizing antibodies, albeit at lower levels than VP2 (Martinez-Torrecuadrada *et al.*, 1999). However, when used in conjunction with VP2, higher titers of neutralizing antibody, compared to immunization with VP2 only, have been reported (Martinez-Torrecuadrada *et al.*, 1996). It has been suggested that VP5 may modulate the conformation of VP2 and thus influence its protective efficacy. Recent studies on the biological activity of BTV VP5 have suggested its involvement in membrane permealizing activity (Hassan *et al.*, 2001; Forzan *et al.*, 2004). Using an experimental system for cell-surface expression of VP2 and VP5, it was shown that VP5 has the ability to interact with host cell membranes and to induce cell-cell fusion in a manner similar to that of fusion proteins of enveloped viruses. The membrane-interacting properties occur only after VP5 has undergone a low pH-triggered activation step that may result in a fusion-competent conformation of the protein (Forzan *et al.*, 2004). However, the mechanism by which VP5 mediates membrane penetration and cell fusion is unknown.

1.3.3.2 Major core proteins

The structural proteins VP3 and VP7 form the inner and outer layer, respectively, of the viral core particle. Of the two proteins, VP7 is the most abundant protein in the core particle and self-assembles into trimers (Basak *et al.*, 1992). The crystal structure of BTV VP7 has been solved and revealed that each VP7 monomer has two distinct domains, *i.e.* an outer or top domain (residues 121-249) and an inner or bottom domain that is formed by both the amino (N) (residues 1-120) and the carboxy (C) (residues 250-349) termini of the molecule (Basak *et al.*, 1992). Whereas the small top domain of VP7 forms the head region of the trimer that appears as a knobby projection on the outer surface of the core, the bottom domain attaches to the VP3 scaffold. The X-ray structure of the top domain of AHSV-4 has also been solved and revealed a structural arrangement similar to that of BTV (Basak *et al.*, 1996). Notably, the top domain of both BTV and AHSV VP7 contains a surface-exposed RGD tripeptide motif, which in the case of BTV, has been shown to be responsible for virus core attachment to *Culicoides* cells (Tan *et al.*, 2001). In contrast to BTV VP7, the VP7 protein of AHSV has been reported to form flat hexagonal crystals in the cytoplasm of virus-infected cells (Burroughs *et al.*, 1994) and when expressed by a baculovirus recombinant in *S. frugiperda* cells (Chuma *et al.*, 1992). The functional significance, if any, of the AHSV VP7 crystals is not yet known.

The VP3 protein forms a shell that surrounds the inner genomic RNA and the three minor structural proteins, and serves as a scaffold for the deposition of VP7. Co-expression of VP3 and VP7 of AHSV (Maree *et al.*, 1998) and of BTV (Tanaka and Roy, 1994) by means of recombinant baculoviruses resulted in their assembly into core-like particles that are structurally similar to virus-derived cores. The structure and assembly of the BTV VP3 subcore has been reported (Grimes *et al.*, 1998; Kar *et al.*, 2004). VP3 was reported to have three distinct domains. Whereas the “carapace” domain (residues 7-297, 588-698, 855-901) forms a rigid plate that represents the majority of the surface of the subcore shell, the “apical” domain (residues 298-587) is situated closest to the five-fold axis in the intact particle, and the “dimerization” domain (residues 699-854) is situated further away from the five-fold axis. The “dimerization” domain mediates formation of VP3 dimers, which pack together in decamers to form the icosahedral structure of the VP3 layer. Although it has been reported that BTV VP3 can bind to RNA (Loudon and Roy, 1991), it was recently reported that BTV RNAs failed to associate with the VP3 decamers (Kar *et al.*, 2004). Consequently, it was

suggested that assembly of the BTV core may begin with a complex formed by minor core proteins and the VP3 decamers, and that these assembly intermediates recruit the viral RNA prior to completion of the assembly of the VP3 subcore (Kar *et al.*, 2004).

1.3.3.3 Minor core proteins

The three minor structural proteins, VP1, VP4 and VP6, are candidates for the virus-directed RNA polymerase and associated enzymes that are responsible for transcription of the ten viral mRNAs. The largest viral protein, VP1, with a molecular mass of 150 kDa, is a highly basic protein and is present in a low molar ratio (10 to 12 copies) in the core (Stuart and Grimes, 2006). Based on its size, location, molar ratio in the core and predicted amino acid sequence, VP1 is considered to be the prime candidate for the viral RNA-dependant RNA polymerase (Roy *et al.*, 1988; Koonin *et al.*, 1989). The primary sequence of both BTV (Urakawa *et al.*, 1989) and AHSV (Vreede and Huismans, 1998) VP1 contains a GDD motif that is characteristic of other RNA polymerases. By making use of lysates prepared from *S. frugiperda* cells infected with a baculovirus recombinant expressing BTV VP1, it was shown that poly(A) synthesis can occur when the extract is provided with a poly(A) primer and poly(U) template (Urakawa *et al.*, 1989). More recently, it was reported that soluble recombinant BTV VP1 exhibited a processive replicase activity, synthesizing complete complementary RNA strands of *in vitro*-synthesized BTV ssRNA templates (Boyce *et al.*, 2004). However, the replicase activity associated with the recombinant BTV VP1 was low and exhibited little sequence specificity for BTV positive strand templates. Consequently, it was proposed that the activity of VP1 may be modulated by other viral proteins present in the assembling core particle (Boyce *et al.*, 2004).

The 5'-ends of BTV mRNA transcripts are capped and methylated during transcription, thus stabilizing the viral mRNA synthesized during virus infection (Roy, 1992). The BTV VP4 protein has been reported to possess guanylyltransferase (Le Blois *et al.*, 1992) and methyltransferase type 1 and type 2 (Ramadevi *et al.*, 1998) activities. Furthermore, BTV VP4 also binds to GTP and displays nucleoside triphosphate phosphohydrolase (NTPase) activity, which may be important for transcription and RNA processing (Ramadevi and Roy, 1998). The atomic structure at the BTV VP4 protein has recently been solved (Sutton *et al.*, 2007). The protein was shown to have an elongated structure with an array of various active sites organized in a manner that may allow the sequential catalytical activities required to

produce the cap structure on nascent RNA molecules. The protein folds into four distinct domains, delineating each enzymatic reaction. The N-terminus (residues 1-108) forms a kinase-like domain, and a 30-residue α-helix then leads into the N-terminal part of the methyltransferase type 1 domain. The protein then forms the entire methyltransferase type 2 domain before completing the methyltransferase type 1 domain, and finally forms the putative guanylyltransferase domain (Sutton *et al.*, 2007).

The third minor core protein, VP6, is a highly basic protein and capable of binding both viral and non-viral ssRNA, as well as dsRNA (Roy *et al.*, 1990; De Waal and Huismans, 2005). The nucleic acid-binding domains in BTV VP6 have been mapped to a region in the centre of the protein and to the C-terminus (Hayama and Li, 1994), while that of AHSV has been mapped a region spanning residues 190-289 (De Waal and Huismans, 2005). Sequence analysis of BTV and AHSV VP6 sequences has revealed a motif common to helicases (Roy, 1992; Turnbull *et al.*, 1996). In this regard, it has been reported that purified BTV VP6, upon incubation with dsRNA in the presence of ATP, led to the unwinding of the dsRNA template (Stauber *et al.*, 1997). Thus, VP6 may be involved in the unwinding the dsRNA genome prior to the initiation of transcription or it may be involved in the encapsidation of viral RNA.

1.3.3.4 Nonstructural proteins

The NS1 protein of orbiviruses is synthesized abundantly in virus-infected cells and is readily assembled as tubular structures within the cytoplasm. These tubules are biochemically and morphologically distinct from the microtubules and neurofilaments present in normal cells (Huismans and Els, 1979). The tubular structures are formed by helically coiled ribbons of NS1 dimers, but the biophysical character of the tubules differ between BTV and AHSV. In contrast to BTV tubules that have a diameter of 52 nm and lengths of up to 1000 nm (Hewat *et al.*, 1992b), the AHSV tubules have a diameter of 23 nm and vary in length up to 4 μm (Maree and Huismans, 1997). Moreover, whereas BTV tubules exhibit a defined ladder-like appearance, AHSV tubules appear to have a fine reticular “cross-weave” appearance. The NS1 protein of both BTV (Monastyrskaya *et al.*, 1994) and AHSV (Maree and Huismans, 1997) is rich in cysteine residues and contains several hydrophobic and hydrophilic regions spaced throughout the protein, which suggests that it has a highly ordered disulphide-bonded structure. It has been reported that cysteine residues at positions 240 and 337, as well as the N- and C-termini of BTV NS1 are important for tubule formation (Monastyrskaya *et al.*,

1994). Their early and abundant synthesis, together with the association of tubules with the intermediate filament components of the cytoskelet of the cell (Eaton *et al.*, 1987), and the association of virions and inner core particles with tubules in the cytoplasm of infected cells (Eaton *et al.*, 1988), suggest that NS1 may be involved in virus replication and/or virus translocation (Eaton *et al.*, 1990). Although the function of NS1 tubules in virus replication is unclear, a recent study, however, indicated that inhibition of NS1 synthesis, by making use of an intracellularly expressed single chain antibody to the NS1 protein, not only resulted in a reduction in virus-induced cytopathic effect, but there was a 10-fold increase in the amount of virus released and a shift from the lytic release of virus to budding from the plasma membrane. Based on the results, Owens *et al.* (2004) hypothesized that NS1 may be a determinant of pathogenesis in vertebrate hosts and that its mechanism of action is through augmentation of virus-cell association, which ultimately leads to lysis of the infected cell.

The NS2 protein is also synthesized at high levels early in orbivirus-infected cells and is the predominant component of viral inclusion bodies (VIBs) (Brookes *et al.*, 1993; Hyatt and Eaton, 1988). Early in infection, the VIBs appear as granular material scattered throughout the cell, which then coalesce to form a prominent inclusion with a perinuclear location. As the infection progresses, the VIBs increase both in size and number (Eaton *et al.*, 1990). In addition to NS2, newly synthesized viral transcripts, all four subcore proteins, as well as assembled cores and subcores have been identified within the VIBs. These results have led to the suggestion that VIBs are the sites of orbivirus replication (Hyatt and Eaton, 1988; Kar *et al.*, 2007). Expression of BTV (Thomas *et al.*, 1990) and AHSV (Uitenweerde *et al.*, 1995) NS2 by baculovirus recombinants in *S. frugiperda* cells resulted in the formation of inclusion bodies that were indistinguishable from the VIBs found in virus-infected cells, indicating that VIBs are formed by NS2. The full-length NS2 protein appears to be required for the formation of virus inclusion bodies (Thomas *et al.*, 1990; Kar *et al.*, 2007). NS2 is also the only virus-specific protein that is phosphorylated (Huismans *et al.*, 1987b; Devaney *et al.*, 1988). Although the functional significance of the modification is not known, it has nevertheless been reported that phosphorylation of NS2 down-regulates its ssRNA-binding ability (Theron *et al.*, 1994) and that phosphorylation of BTV NS2 is important for VIB formation (Modrof *et al.*, 2005). Moreover, the NS2 protein of AHSV has been reported to exist as a 7S multimer, which binds ssRNA (Uitenweerde *et al.*, 1995). Based on its high affinity for ssRNA, but not for dsRNA, it has been suggested that NS2 may have a role in the recruitment and packaging of viral mRNA for replication (Huismans *et al.*, 1987b). In support

of such a role, BTV RNA has been reported to be preferentially bound via N-terminal residues of the NS2 protein (Theron and Nel, 1997; Lymperopoulus *et al.*, 2003; Markotter *et al.*, 2004). Chemical and enzymatic structure probing of regions bound preferentially by NS2 has shown that NS2 binds BTV transcripts at different hairpin loops that are distributed throughout the coding and non-coding regions of the different genome segments (Lymperopoulus *et al.*, 2003; 2006). Although the ssRNA-binding activity may explain how BTV mRNAs are selected from the pool of cellular RNA, it remains unknown how only a single copy of each genome segment is packaged into the newly formed virus particles. BTV NS2 has been reported to demonstrate phosphohydrolase activity and could bind and hydrolyse ATP and GTP to their corresponding nucleotide monophosphates (Horscroft and Roy, 2000; Taraporewala *et al.*, 2001). Although the significance of this finding is not clear, it has been proposed that this enzymatic activity of NS2 may play a role in providing energy for the assortment, movement, packaging or condensation of bound ssRNA (Horscroft and Roy, 2000).

In contrast to NS1 and NS2, the two closely related nonstructural proteins NS3 and NS3A are synthesized in low abundance in orbivirus-infected cells (French *et al.*, 1989; Van Staden *et al.*, 1995). Biochemical and immunological analyses have indicated that NS3A is synthesized from a second downstream in-frame AUG translation initiation codon (Wu *et al.*, 1992). Analysis of the encoded amino acid sequence of the segment 10 gene has revealed the presence of two conserved hydrophobic regions that may serve as transmembrane domains (Van Staden and Huismans, 1991; Van Niekerk *et al.*, 2001; Beaton *et al.*, 2002). A single glycosylation site is present in BTV NS3 (Wu *et al.*, 1992; Bansal *et al.*, 1998), but absent in NS3 of AHSV (Van Staden and Huismans, 1991) and thus does not seem to be essential for the function of the protein. Notably, BTV NS3 and NS3A have been reported to facilitate the release of baculovirus-expressed virus-like particles in *S. frugiperda* cells (Hyatt *et al.*, 1993) and in BTV-infected cells the NS3 protein has been observed to co-localize with BTV particles within disrupted regions of the plasma membrane (Hyatt *et al.*, 1989). These results suggest that the NS3 proteins may be involved in the release of BTV from infected cells. Similarly, the AHSV NS3 protein has also been reported to be localized to sites of AHSV release (Stoltz *et al.*, 1996). Moreover, the NS3 protein of AHSV exhibits cytotoxicity when expressed in *S. frugiperda* cells (Van Staden *et al.*, 1995). The cytotoxicity of NS3 was shown to require both hydrophobic domains, suggesting that NS3 might function as a viroporin to facilitate virus release (Van Niekerk *et al.*, 2001). It has recently been reported that BTV NS3,

but not NS3A, interacts with the calpactin light chain (p11) of the cellular annexin II complex, which has been implicated in membrane-related events along the endocytic and regulated secretory pathways (Wirblich *et al.*, 2006). In addition, NS3 of both BTV and AHSV has also been reported to be capable of interacting with Tsg101, a cellular protein implicated in the intracellular trafficking and release of enveloped viruses (Wirblich *et al.*, 2006). Subsequent knockdown of Tsg101 with siRNA was shown to inhibit release of virus from mammalian cells, suggesting that it may play a role in virus release.

1.4 ORBIVIRUS REPLICATION AND MORPHOGENESIS

Although there are considerable differences in several steps of the replicative process of members of the *Reoviridae* family, the overall strategy appears to be the same. The major events in orbivirus replication are: (i) adsorption and penetration, (ii) uncoating and formation of replicative complexes, (iii) formation of virus tubules and viral inclusion bodies, and (iv) movement of the virus to and release from the cell surface. The following model for orbivirus replication, indicated schematically in Fig. 1.2, is based on that of BTV, as described by Gould and Hyatt (1994) and Roy (2001).

BTV rapidly adsorps to susceptible mammalian cells, with maximal adsorption occurring within 20 min (Huismans *et al.*, 1983). Although the cellular receptors to which BTV binds have not yet been determined, it has been reported that the binding and internalization of BTV is mediated by the outer capsid protein VP2 (Huismans and Van Dijk, 1990; Hassan and Roy, 1999). Following adsorption, the virus is transported to the cytoplasm of the cell via receptor-mediated endocytosis, which involves formation of clathrin-coated vesicles within the cell that subsequently fuse to form endosomes. Within the endosome, the outer capsid proteins (VP2 and VP5) are removed, presumably due to the acidic conditions within the endosome. The transcriptionally active core particles are subsequently released into the cytoplasm (Huismans *et al.*, 1987c). It has been proposed that VP5 may facilitate release of the core particles, since removal of VP2 from the virions results in exposure of the helical membrane-destabilizing domains of VP5 (Hassan *et al.*, 2001). Soon after the initiation of transcription, proteins produced by translation of viral mRNA condense with the viral ssRNA around the parental cores to form granular VIBs (Eaton *et al.*, 1990; Hyatt *et al.*, 1992). The newly synthesized viral mRNA transcripts that are released in the cytoplasm are capped and

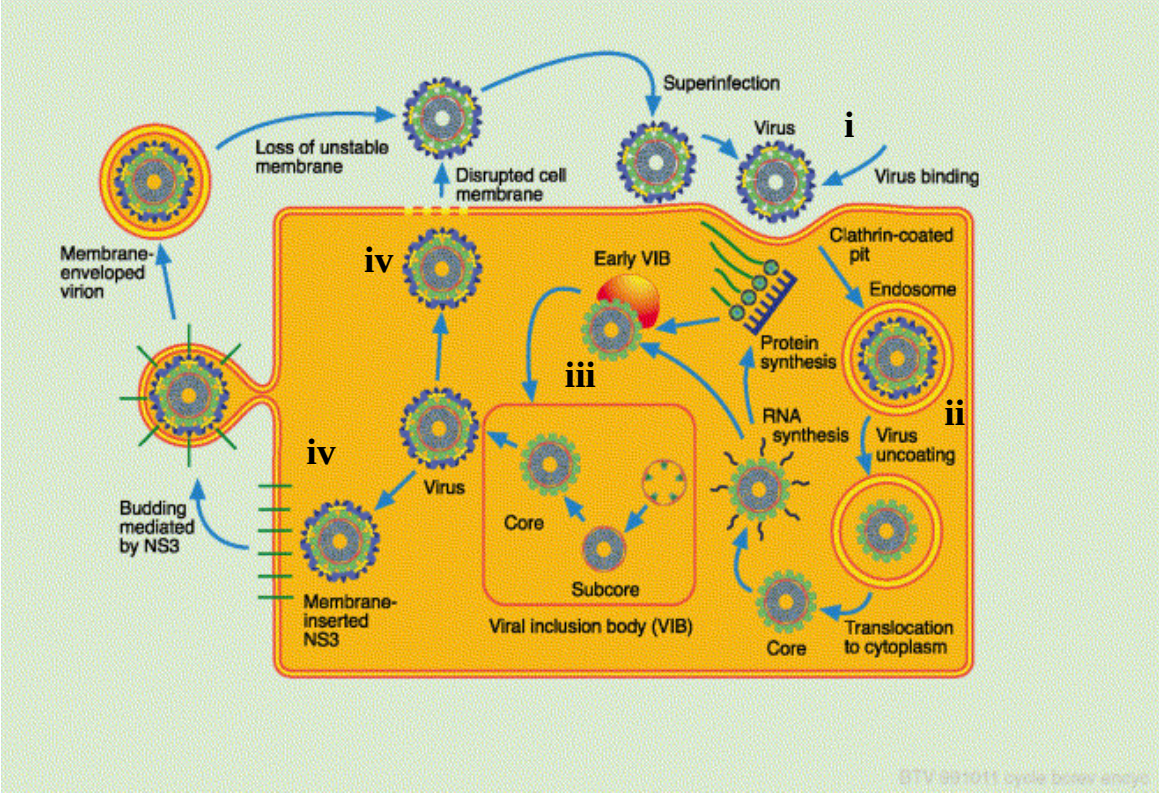

Fig. 1.2 Schematic diagram representing the replication cycle of bluetongue virus, the prototype orbivirus (Mertens, 2004). The major events in orbivirus replication are: (i) adsorption and penetration, (ii) uncoating and formation of replicative complexes, (iii) formation of virus tubules and virus inclusion bodies, and (iv) movement of the virus to and release from the cell surface. The adsorption of the virus involves a receptor of unknown nature in the cell membrane of susceptible host cells. The virus enters the cell via endocytosis after which clathrin-coated vesicles, containing the virions, form and are drawn to the cell nucleus. The outer capsid proteins are removed to yield core particles in the cell cytoplasm. Transcription of the virion RNA occurs and the proteins generated by translation of the viral mRNA condense with the viral ssRNA around the parental cores to form VIBs. Structural proteins are translated and condense at the VIB periphery to form cores and subcores. The outer capsid proteins are added after which the virions are released from the cells via lysis, budding or extrusion from the cells.

methylated, and program the synthesis of viral proteins in the cytoplasm. The mRNA also serves as templates for viral dsRNA genome synthesis (Mertens and Diprose, 2004), but the mechanism by which viral mRNAs are selected and encapsidated prior to replication is not yet known.

The VIBs, which consist mainly of the ssRNA-binding phosphoprotein NS2 (Thomas *et al.*, 1990; Uitenweerde *et al.*, 1995), grow in size and complexity during the infection cycle (Eaton *et al.*, 1990). The VIBs contain viral transcripts, assembled subcores and cores, as well as different subcore proteins (VP1, VP4, VP6 and VP3). The surface core protein VP7 requires VP3 to be recruited to the VIBs and may indicate that partially assembled core structures in which VP3 and VP7 are already interacting, are the building blocks of core formation (Kar *et al.*, 2004; 2007). Once stable cores have been assembled, the two outer capsid proteins VP2 and VP5 are acquired at the periphery of the VIBs by interaction with the core surface, both proteins being attached to the VP7 layer of the core. However, little is known of the mechanism whereby VP2 and VP5 are added to the developing virus particle. Nevertheless, once VP2 and VP5 have been attached, the viral particles are no longer transcriptionally active and are available for release from the infected cell. Although the NS1-rich virus tubules are not observed within the VIBs, they form part of the insoluble phase of the cell at an early stage of infection (Huismans and Els, 1979) and have recently been reported to be a determinant of pathogenesis in the vertebrate host by leading to lysis of infected cells (Owens *et al.*, 2004).

Investigations regarding virus release from mammalian cells have demonstrated a strong correlation between the presence of NS3 and NS3A, and virus release (Hyatt *et al.*, 1989; Stoltz *et al.*, 1996). In addition, virions have been reported to leave infected cells in two ways. Early after infection, when the host cell metabolism is not completely inhibited and the integrity of the host plasma membrane is maintained, progeny virions have been observed to bud through the plasma membrane and thus acquire a transient envelope (Gould and Hyatt, 1994). Alternatively, during the latter stages of infection, when the integrity of the plasma membrane is not maintained, egress of virions can be accomplished as non-enveloped virions by extrusion through the locally disrupted plasma membrane surface (Hyatt *et al.*, 1989).

1.5 RNA INTERFERENCE (RNAi)

For more than a decade, targeted inhibition of mammalian gene expression has been achieved primarily by approaches such as homologous recombination, antisense oligonucleotides, ribozymes and intrabodies (Rosen and Gretch, 1999; Nahreini *et al.*, 2004; Robishaw *et al.*, 2004; Visintin *et al.*, 2004; Owens *et al.*, 2004). However, in the past five years, RNA interference (RNAi) has emerged as the primary means by which specific genes in mammalian systems can be suppressed or silenced. RNAi is a form of post-transcriptional gene silencing that results in the sequence-specific degradation of mRNA by homologous dsRNA molecules. This RNA-silencing mechanism, which was first described in *Caenorhabditis elegans* (Fire *et al.*, 1998), displays many similarities with post-transcriptional gene silencing (PTGS) in plants (Napoli *et al.*, 1990; Kooter *et al.*, 1999) and the process of quelling in *Neurospora crassa* (Cogoni *et al.*, 1996). RNAi appears to be an evolutionary conserved gene silencing system and has also been demonstrated in insects, protozoa and animals (Kennerdell and Carthew, 1998; Ngo *et al.*, 1998; Wianny and Zernicka-Goetz, 2000). It is thought that RNAi and related RNA silencing mechanisms act as a natural defense system against virus infection (Keene *et al.*, 2004; Wilkins *et al.*, 2005) and mobilization of transposons (Blumenstiel and Hartl, 2005). In addition to these functions, RNAi may also play an important role in regulating cellular gene expression (Szweykowska-Kulinska *et al.*, 2003; Bernstein *et al.*, 2003). Because of its apparent universal applicability and high specificity, RNAi technology has become a powerful tool for reverse genetic studies in organisms where generating loss-of-function phenotypes by the direct manipulation of target genes have proven difficult or impossible. Moreover, many publications have described the inhibition of viruses belonging to several different viral families by targeting and silencing diverse viral genes that are essential for virus replication (Gitlin and Andino, 2003; Tan and Yin, 2004; Colbère and Garapin, 2005; Stram and Kuzntzova, 2006).

1.5.1 Mechanism of RNAi

Biochemical and genetic analyses have provided a mechanistic understanding of RNAi-induced gene silencing. The recognition and processing of dsRNA, followed by the subsequent cleavage of target homologous mRNA occurs through a highly conserved multi-step mechanism that involves three main stages: (i) the recognition and processing of dsRNA into siRNA, (ii) the assembly of RISC, and (iii) the sequence-specific cleavage of target

single-stranded (ss) RNA (Meister and Tuschl, 2004; Tomari and Zamore, 2005). A model for gene silencing induced by dsRNA is indicated in Fig. 1.3.

1.5.1.1 Processing of dsRNA

Long dsRNAs are recognized and processed into siRNAs by a dsRNA-specific RNase III family endonuclease, called Dicer (Hammond *et al.*, 2000; Zamore *et al.*, 2000; Bernstein *et al.*, 2001). Dicer is a 200-kDa multidomain protein, which has a N-terminal DexH/DEPH RNA helicase/ATPase domain, a PAZ (PIWI-Argonaute-Zwille) domain, two RNase III domains (RIIIa and RIIIb) and a C-terminal dsRNA-binding domain (dsRBD) (Zhang *et al.*, 2002; Provost *et al.*, 2002). Whereas the dsRBD and RNase III domains are involved in dsRNA-binding and cleavage, respectively, the PAZ domain is a RNA-binding domain that specifically recognizes the terminus of the base-paired helix of siRNA duplexes, including the 2-nt 3' overhang. The presence of the helicase/ATPase domain may be related to the observation that siRNA formation by *Drosophila melangoster* Dicer is greatly stimulated by the addition of ATP (Zamore *et al.*, 2000). However, no such effect is observed for mammalian Dicer and it was shown that human Dicer generates siRNAs from dsRNA efficiently in the presence of Mg^{2+} and the absence of ATP (Zhang *et al.*, 2002). Consequently, the exact function of ATP during processing remains to be elucidated.

Based on results obtained from mutagenesis of the human Dicer enzyme, Zhang *et al*. (2004) proposed a model for dsRNA cleavage by Dicer enzymes. It was proposed that Dicer functions through intramolecular dimerization of the RIIIa and RIIIb domains, assisted by the flanking RNA-binding domains dsRBD and PAZ, to form a single catalytic center that contains two RNA cleavage sites. Cleavage of dsRNA results in products with 2-nt 3' overhangs by cleaving two nearby phosphodiester bonds on opposite RNA strands. It is thought that whereas RIIIa cleaves the 3' hydroxyl-bearing RNA strand, RIIIb cleaves the 5' phosphate-bearing RNA strand (Zhang *et al.*, 2004). Processing of dsRNA by Dicer thus yields RNA duplexes that are typically 21-nt in length, have 5' phosphate and 3' hydroxyl groups and 2-nt overhangs at the 3'-termini. However, the length of the siRNAs produced in different organisms varies between 21 to 28 nt. This may be due to structural differences of the various Dicer orthologs, as well as reflect on differences in the geometric spacing between the active sites of dsRNA-bound Dicer dimers during dsRNA processing (Zamore *et al.*, 2001; Hannon, 2002).

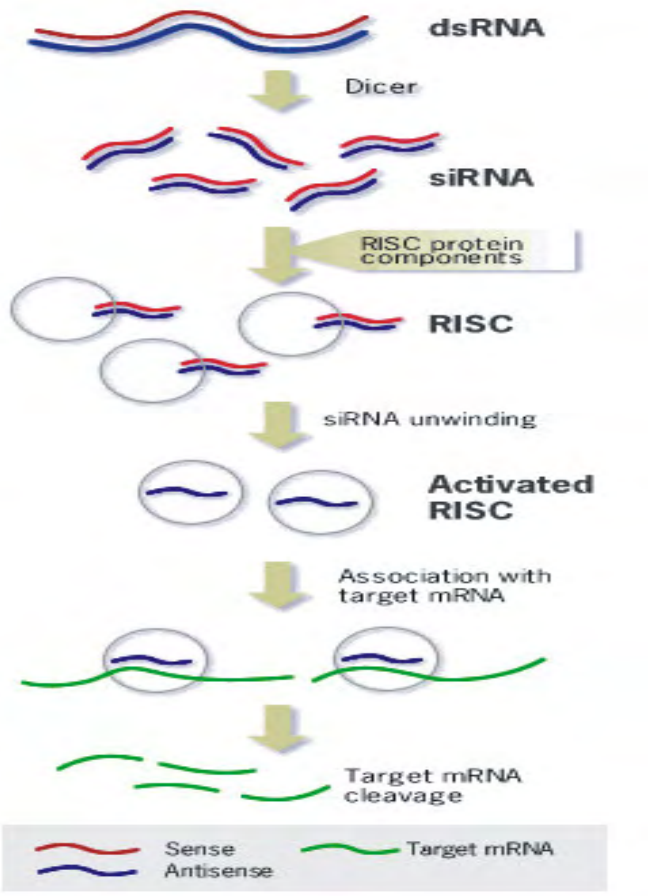

Fig. 1.3 Schematic diagram of RNAi-mediated gene silencing in mammals. The double-stranded RNAs are processed by Dicer to produce siRNAs. The siRNAs become associated with the RISC complex, after which the antisense strand guides the complex towards the cognate mRNA, resulting in endonucleolytic cleavage of the mRNA.

1.5.1.2 Assembly of RISC

Following cleavage of dsRNA by Dicer, the siRNA-containing ribonucleoprotein particles (RNPs) are assembled into a multi-component nuclease that guides the sequence-specific recognition of the target mRNA (Hammond *et al.*, 2000). This complex is referred to as the RNA-induced silencing complex (RISC). Several forms of RISC, differing in molecular weight (160-500 kDa) and composition, have been identified. These differences may be due to weak and/or transient association of proteins involved in the initial processing of dsRNA, as well as other factors of unknown function (Hammond *et al.*, 2001; Nykänen *et al.*, 2001; Jaronczyk *et al.*, 2005). However, every RISC contains a protein belonging to the Argonaute protein family, which is characterized by the presence of a PAZ domain and a C-terminal PIWI domain (Cerutti *et al.*, 2000; Carmell *et al.*, 2002). It is thought that interaction between the PAZ domain and 2-nt 3' overhangs of siRNA duplexes may allow for transfer of siRNAs from the RNP complexes into RISC. Moreover, solving of the crystal structures of an archaeal Argonaute protein (Song *et al.*, 2004) and PIWI domain in association with a siRNA-like duplex (Parker *et al.*, 2005) have provided insights regarding its role in the RISC assembly process. It was shown that the PIWI domain recognizes specifically the 5'-end of a siRNA and unwinds the first base-pair of the duplex, thus suggesting that binding of the siRNA to the PIWI domain might be the first step in siRNA duplex-unwinding in RISC (Parker *et al.*, 2005). Furthermore, it has also been shown that PIWI is a structural homolog for RNase H and since RNase H cleaves the RNA strand in RNA/DNA hybrids, it was proposed that Argonaute proteins may act similarly by cleaving target RNA in the RNA/siRNA hybrids (Song *et al.*, 2004).

The formation of RISC on siRNA duplexes requires ATP, but once formed, RISC can mediate robust sequence-specific cleavage of its target in the absence of ATP (Nykänen *et al.*, 2001; Bernstein *et al.*, 2001). The ATP is most likely required for energy-driven unwinding of the siRNA duplex and/or other conformational changes (Tomari *et al.*, 2004; Pham *et al.*, 2004). It has also been reported that thermodynamic differences in the base-pairing of the two siRNA strands determine which siRNA strand is assembled into RISC (Khvorova *et al.*, 2003; Schwarz *et al.*, 2003). This strand bias is presumably caused by a rate-limiting unwinding step that occurs during transition from the siRNA duplex-containing RNP to the RISC complex, which allows the 5'-end of the strand positioned at the weakly paired end of the siRNA to enter RISC first (Khvorova *et al.*, 2003).

1.5.1.3 mRNA cleavage

Following assembly of the RNA silencing effector complexes, the single-stranded siRNA in RISC guides sequence-specific degradation of complementary target mRNAs (Martinez *et al.*, 2002; Martinez and Tuschl, 2004), and Mg^{2+} has been shown to be required for this reaction (Schwarz *et al.*, 2004). Based on the similarity of the PIWI domain with RNase H (Song *et al.*, 2004), it has been proposed that the Argonaute proteins may act as the catalytic subunit, termed Slicer. Subsequent biochemical and genetic studies have indicated that although all four human Argonaute proteins bind to siRNA, only Argonaute2-containing complexes were able to cleave mRNA substrates (Liu *et al.*, 2004). The nuclease activity of Argonaute2 appears to be highly specific, since it did not display activity in the absence of single-stranded siRNAs and did not exhibit significant activity in the presence of dsRNA (Liu *et al.*, 2004). The current model of Argonaute Slicer activity indicates that the siRNA guide interacts with the PAZ domain of the Argonaute protein, while the mRNA substrate enters a binding groove formed by the N-terminal, middle and PIWI domains. The 5'-end of the mRNA is predicted to lie between the PAZ domain and N-terminus of Argonaute, with the latter functioning as an mRNA grip. The mRNA is positioned so that the active site, located in the PIWI domain, is 10 nt from the 5'-end of the siRNA/mRNA double-stranded region, thus allowing for cleavage of the mRNA target between 11 and 12 nt from the 3'-end of the siRNA guide (Tomari and Zamore, 2005).

1.6 RNAi-BASED GENE SILENCING IN MAMMALIAN CELLS

Despite its utility in diverse organisms for silencing of homologous gene expression (Fire *et al.*, 1998; Valdes *et al.*, 2003; Kuttenkeuler and Boutrous, 2004), it has been difficult to detect potent and specific RNAi in commonly used mammalian cell culture systems by application of dsRNA longer than 30 bp. This was largely due to the fact that introduction of the dsRNA into the cytoplasm of mammalian cells triggered an interferon response, which results in a systemic nonspecific shutdown of protein synthesis and eventual apoptosis (Manche *et al.*, 1992; Stark *et al.*, 1998).

Predominant amongst responses triggered by the presence of dsRNA in the cell cytoplasm is activation of two complementary yet independent systems, *i.e.* the dsRNA-activated protein kinase R (PKR) system and the 2',5'-oligoadenylate synthetase (2',5'-AS) system (Stark *et al.*, 1998). PKR is activated by binding to dsRNA with a minimal length of 30 bp, but full

activation requires dsRNA with a length of 80 bp. Upon binding dsRNA in a sequence-independent manner, PKR dimerizes, autophosphorylates and subsequently phosphorylates the alpha subunit of eukaryotic translation initiation factor 2 (eIF2α) to render it inactive for further initiations of viral and cellular translation (Sledz *et al.*, 2003). In addition, PKR can also induce apoptosis by activation of apoptotic gene expression (Goodbourn *et al.*, 2000; Li *et al.*, 2003). The 2',5'-AS system is activated upon binding to dsRNA of at least 70 bp, which results in the production of several 2',5'-linked oligoadenylates. These bind and activate RNase L, resulting in the nonspecific degradation of cellular ssRNA and the onset of apoptosis (Floyd-Smith *et al.*, 1981; Carroll *et al.*, 1996).

The above-mentioned sequence-nonspecific effects, however, have been resolved when it was reported that in mammalian cells RNAi can be triggered by introducing synthetic siRNAs of 21 to 22 nt in length directly into the cytoplasm of mammalian cells (Caplen *et al.*, 2001; Elbashir *et al.*, 2001a). The exogenously added siRNAs avoided provoking an interferon response by virtue of their small size and appear to be incorporated directly into the RNAi pathway by mimicking the products of the Dicer enzyme, which catalyzes the initiation step of RNAi. This discovery opened the door to RNAi approaches in mammalian cells, albeit that the gene-specific silencing is transient. For efficient RNAi in mammalian cells, some critical factors have been identified that include, amongst other, the design, identification and delivery of effective siRNAs. These aspects will therefore be discussed in greater detail in the following sections.

1.6.1 Design of siRNAs

At present, it is not possible to predict with complete certainty the degree of gene silencing a particular siRNA will produce and the design of an effective siRNA is still an empirical process. However, based on the first successful mammalian RNAi experiments, a number of general guidelines and recommendations have been proposed that may increase the probability of producing an effective siRNA (Elbashir *et al.*, 2001b; 2001c; Caplen *et al.*, 2001). In addition, high-throughput screening of candidate siRNAs and analyses of effective and ineffective siRNAs have led to the development of different siRNA design algorithms (Reynolds *et al.*, 2004; Ui-Tei *et al.*, 2004; Amarzguioui and Prydz, 2004). These guidelines and algorithms are, however, only predictive and do not guarantee a gene silencing effect. Nevertheless, based on the results of these analyses, it has emerged that the two most

important factors influencing siRNA efficiency are the structural characteristics of the siRNA and the target site within the gene.

To achieve efficient siRNA-mediated gene silencing, it has been suggested to select 19-nt long sequences in the coding region flanked by AA at the 5'-end and TT at the 3'-end. Furthermore, a GC content of 30-70% was reported to be advantageous for the internal stability of the siRNA (Elbashir *et al.*, 2001b; 2001c; Elbashir *et al.*, 2002). It has also generally been recommended that a target site should be located at least 100-200 nt downstream from the AUG initiation codon and that target sites within 50-100 nt of the termination codon should be avoided. Moreover, the 5' and 3' untranslated regions (UTRs) should also be avoided, since associated regulatory proteins may compromise RNAi (Elbashir *et al.*, 2002; Mittal, 2004).

Initial reports have indicated that mismatches of 1 to 2 nt between the antisense strand of the siRNA and the target mRNA can abolish siRNA activity (Elbashir *et al.*, 2001a). However, it has subsequently emerged that the effect of mismatches depends on their nature and position with respect to the cleavage site. The presence of single mismatches within the middle of the guide siRNA are more inhibitory than mismatches located at the 5'- and 3'-ends (Harborth *et al.*, 2003; Czauderna *et al.*, 2003). Furthermore, mismatches close to the 5'-end of the antisense strand of the siRNA are more disruptive than those at the 3'-end, which may be due to the 5'-end serving as a ruler to define the position of mRNA cleavage (Amarzguioui *et al.*, 2003). Based on a better understanding of the strand selection mechanism of RISC and analysis of effective siRNAs, it has been reported that efective siRNAs have a reduced thermodynamic stability at the 5'-end of the antisense strand relative to the 3'-end within the RNA duplex (Khvorova *et al.*, 2003; Schwarz *et al.*, 2003). This asymmetry allows for the unwinding of dsRNA from the one end preferentially and ensures that only one strand enters RISC (Schwarz *et al.*, 2003). Consequently, it was suggested that siRNAs with a thermodynamically unstable 5' antisense strand should be designed in order to increase gene silencing efficiency and to reduce off-target effects.

Several siRNAs synthesized against different regions of the same target mRNA have been reported to silence gene expression to differing extents (Harborth *et al.*, 2001; Holen *et al.*, 2002; Bohula *et al.*, 2003; Vickers *et al.*, 2003; Stassen *et al.*, 2007), suggesting that accessibility of the target sequence on the mRNA should also be taken into account when

designing siRNAs for gene silencing. Several reports have suggested that the low effectivity of siRNAs may be ascribed to the non-accessibility of the targeted mRNA regions for cleavage, which may be caused either by higher order RNA structures (Bohula *et al.*, 2003; Kretschmer-Kazemi Far and Sczakiel, 2003) or by protein coverage (Elbashir *et al.*, 2001a; Holen *et al.*, 2002). Consequently, it has been advised that at least two different siRNA duplexes targeting the same mRNA should be tested independently for a reproducible phenotype (Elbashir *et al*., 2002; Mittal, 2004).

1.6.2 Synthesis of siRNAs

Initially, RNAi-based gene silencing experiments were performed with chemically synthesized siRNAs (Elbashir *et al.*, 2001a; Caplen *et al.*, 2001). For chemical synthesis, automated synthesizers are used to produce each of two homologous RNA oligonucleotides by sequentially joining nucleotide monomers according to the desired siRNA sequence. The RNA oligonucleotides are subsequently annealed *in vitro* and results in short dsRNA molecules with 2-nt 3' overhangs that contain 3' hydroxyl and 5' phosphate groups (Dykxhoorn *et al.*, 2003). Despite being able to obtain siRNAs of high purity, uniform composition and large amounts, chemical synthesis of siRNAs is expensive. Consequently, alternative methods have been developed for synthesizing siRNAs.

A cost-effective and rapid method for siRNA synthesis is based on *in vitro* transcription from short oligonucleotide DNA cassettes, containing a phage T7 RNA polymerase promoter sequence upstream of the siRNA strand template sequence to be transcribed (Donze and Picard, 2002; Kim *et al*., 2004). Following synthesis of the two siRNA strands in two separate reactions, they are annealed and purified. However, the siRNAs generated by this method frequently contain a GGG leader sequence, which is derived from the promoter, and a 5' phosphate group (Kim *et al.*, 2004). Consequently, the hybridized siRNA precursor is treated with a combination of DNase I and RNase T1 to remove residual DNA template and the single-stranded leader sequence of the siRNA, respectively. Alternatively, long dsRNA (100-200 bp) that has been prepared by *in vitro* transcription can be cleaved with either Dicer or RNase III to generate a pool of siRNAs suitable for gene silencing (Yang *et al.*, 2002; Myers *et al.*, 2003; Xuan *et al*., 2006). Thus, the large pool of random siRNAs that are generated by this approach virtually guarantees that one or more of the siRNAs in the pool will have siRNA gene silencing activity, and therefore abrogates the need to screen and identify

individual effective siRNAs. However, there may be several potential limitations to this approach. In addition to the presence of unprocessed or partially processed long dsRNA that can activate PKR and result in nonspecific translation inhibition, there is also the potential for increased off-target effects. Moreover, competition from less effective siRNAs in a pool may also reduce the overall efficacy compared to the use of a single very effective siRNA.

1.6.3 Delivery of siRNAs into mammalian cells

For siRNAs to initiate gene-silencing effects, they must be introduced into the cytoplasm of mammalian cells and chemical transfection or electroporation have been used for this purpose (Elbashir *et al.*, 2002; Weil *et al.*, 2002). The transfection efficiency and the level of cytotoxicity resulting from different siRNA delivery methods have been reported to depend on the particular cell type being used (Walters and Jelinek, 2002). Thus, it has been proposed that the method and conditions of siRNA delivery should be optimized individually for the cell types under investigation.

Whereas electroporation has been reported to be well suited for cells in suspension (Weil *et al.*, 2002; Randall *et al.*, 2003), chemical transfection is widely used for introducing siRNAs into adherent cells and the transfectant reagents are typically cationic lipids (Elbashir *et al.*, 2002). The efficiency and toxicity of the transfection is determined by the ratio of siRNA duplex to transfection reagent. An excess of either of the components may negatively affect the formation of RNA/carrier complexes or may result in the presence of either component in a non-complexed state, which may be toxic to the cells or decrease the uptake of siRNA (Walters and Jelinek, 2002). Transfection efficiency is typically optimized by titrating cell density, transfection time, the ratio of siRNA-to-transfection reagent and the cell passage number (Mocellin and Provenzano, 2004). To provide reproducible results, it has been recommended that gene silencing experiments should be conducted at constant cell culture densities, since too low cell densities during the transfection procedure can lead to an increase in cytotoxicity and cell densities that are too high may lead to low transfection efficiencies (Elbashir *et al.*, 2002; Walters and Jelinek, 2002). For chemical transfections, cells are typically plated 24 h prior to transfection at a density that results in confluency at the time of performing the experiment.

1.6.4 Validation and verification of the targeted gene silencing effect

Establishing RNAi as a means to silence expression of a target gene in mammalian cells also requires methods whereby the level of targeted mRNA and presence of the encoded protein can be monitored. For validation of the gene silencing effect, standard molecular biology techniques are frequently used. Methods for quantification of the target mRNA level include Northern blot hybridization, quantitative reverse transcriptase (RT)-PCR or real-time PCR, whereas immunodetection methods are used to quantitate the level of protein and can be performed on either whole cells (*e.g.* flow cytometry) or cell lysates (*e.g.* Western blot analysis, immunoprecipitation and enzyme-linked immunosorbent assays) (Elbashir *et al.*, 2002; Ho *et al.*, 2006; Cullen, 2006). In contrast to methods based on cell lysates, which provide information regarding the average silencing effect for a cell population, methods based on whole cells provide information about the nature of the silencing effect, *i.e.* the percentage of the cell population that shows the gene silencing phenotype and to what extent (Ho *et al.*, 2006).

Despite careful design and selection of siRNAs, the possibility of off-target silencing effects or cross-reaction with non-target transcripts of limited similarity cannot be excluded (Saxena *et al.*, 2003; Jackson *et al.*, 2003; Jackson and Linsley, 2004). However, not all off-target effects may be seen at the mRNA level and it has been reported that siRNAs may act like endogenously encoded microRNA (miRNA), which inhibit translation by hybridizing to complementary sequences in the 3' UTR of mRNAs (Doench *et al.*, 2003; Scacheri *et al.*, 2004). However, since miRNAs usually require several such target sites in the mRNA, translation inhibition is likely not a prominent off-target effect of siRNAs (Scacheri *et al.*, 2004). Therefore, since any gene silencing effect obtained via RNAi can be due to both intended and off-target effects, and to avoid drawing wrong conclusions from the RNAi experiment, a number of controls are typically included in the RNAi assay to verify its specificity. In addition to testing two or more different siRNAs that target the same mRNA for a reproducible phenotype (Elbashir *et al.*, 2002; Mittal, 2004), a negative control whereby the specificity of the siRNA can be determined must also be included. The negative control can be a siRNA with mismatches or no homology to the target gene, including siRNAs against genes that are not typically expressed in mammalian cells (Mocellin and Provenzaro, 2004; Sandy *et al.*, 2005; Cullen, 2006).

1.7 VECTOR-EXPRESSED RNAi EFFECTOR MOLECULES

In contrast to transient gene silencing mediated by siRNAs, the development of expression vectors, which allow for the production of short hairpin RNAs (shRNAs) that can be converted by Dicer into functional siRNAs, has made it possible to induce long-term gene silencing in mammalian cell cultures (Brummelkamp *et al.*, 2002a; Lee *et al.*, 2002; Paddison *et al.*, 2002). The most commonly used approach for vector-based RNAi involves the use of RNA polymerase III promoters, such as the mouse or human U6 or human H1 promoters, to express shRNA *in vivo*. Not only are these promoters active in all cell types, but they efficiently transcribe small RNA transcripts that are not capped at the 5'-end or polyadenylated at the 3'-end. In addition, transcription is initiated at the +1 position and transcription is terminated when it encounters a stretch of four or five thymidine residues (Paule and White, 2000).

For expression of an shRNA, an expression cassette, encoding in the following order, the top strand of the hairpin, the hairpin loop, the bottom strand of the hairpin and the terminator, is inserted immediately downstream of the promoter. In most cases, the shRNA-encoding DNA fragment is made of two chemically synthesized 50- to 70-nt long oligonucleotides that are annealed and then ligated into an appropriate vector (Sandy *et al.*, 2005; Wadhwa *et al.*, 2004). As an alternative to the use of shRNA-expressing plasmid DNA vectors, it is also possible to synthesize shRNA *in vivo* by constructing shRNA expression cassettes (SECs) (Castanotto *et al.*, 2002; Scherer *et al.*, 2004). The expression cassettes were generated in a two-step PCR, and the final product contained a U6 promoter, followed by the DNA sequences that allowed formation of the shRNA (as indicated above) after it has been transcribed, and the termination sequences. Although the SECs were reported to be difficult to transfect into cells, the shRNAs generated by this approach were highly specific and effective, and gene silencing was reported to be comparable to the use of 21-nt siRNA duplexes or an expression plasmid containing the same shRNA (Scherer *et al.*, 2004).

Although plasmid DNA-based constitutive expression of shRNAs have been reported to be effective in suppressing target gene expression, a major limitation of such unregulated RNAi approaches is that it cannot be used to study the function of essential genes. To overcome this limitation, a number of systems for inducible expression of shRNAs from polymerase III promoters have been developed. Tetracycline-inducible promoters H1 (Van de Wetering *et*

al., 2003) or U6 (Matsukura *et al.*, 2003) have been generated by replacement of a 19-bp sequence between the TATA box and the transcription start site with a tetracycline repressor-binding site (*tetO*). In transgenic cells expressing the repressor, transcription will thus be blocked, while addition of the inducer tetracycline or its derivative, doxycycline, results in dissociation of the repressor, allowing transcription to proceed. A similar strategy has been used to replace a 26-nt sequence between the TATA box and the transcription start site in the H1 promoter with a *lac* operator (*lacO*), thus resulting in IPTG-inducible shRNA expression in transgenic cells expressing the *lac* repressor (Higuchi *et al.*, 2004). In both these inducible systems, target gene expression re-emerges two to four days after removal of the inducer. It has been proposed that the delay in gene expression may be due to the relatively long half-life of the siRNAs that are derived from Dicer cleavage of the expressed shRNA (Matsukura *et al.*, 2003).

In addition to the use of plasmid DNA vectors, viral vectors such as adenoviruses, retroviruses and lentiviruses have also been developed for expression of shRNAs. These viral-based vectors have been used successfully to deliver shRNAs into cells that are difficult to transfect (*e.g.* primary cells) and have enabled the engineering of shRNA-expressing stable cell lines (Wadhwa *et al.*, 2004; Bantounas *et al.*, 2004). Although adenoviruses can infect a wide range of dividing and non-dividing cell types, they do not integrate into the host cell genome and therefore RNAi is transient (Xia *et al.*, 2002; Shen *et al.*, 2003; Hommel *et al.*, 2003). In contrast, both retroviral (Brummelkamp *et al.*, 2002b; Schuck *et al.*, 2004) and replication-deficient lentiviral (Rubinson *et al.*, 2003; Qin *et al.*, 2003) vectors have been used to integrate shRNA expression cassettes into the genome of target host cells, thus allowing for stable, long-term gene silencing. Although the viral vector-based systems are effective, their use, however, may be limited due to safety concerns and inherent difficulties associated with viral production and transduction. To overcome these obstacles, transposon-based RNAi delivery systems for mammalian cells have been developed (Heggestadt *et al.*, 2004; Yang *et al.*, 2005) that combines the gene silencing capabilities of RNA polymerase III-transcribed shRNAs with the advantages of transposon-based gene delivery. Not only was it shown that these systems displayed an enhanced frequency of genomic integration, but the shRNA expression cassette and drug resistance marker was stably integrated on a defined segment of DNA. Moreover, the levels of endogenous (lamin A/C) and exogenous (green fluorescent protein [GFP]) gene silencing were uniform within bulk drug-selected cells, thus eliminating the need to generate clonal isolates (Heggestadt *et al.*, 2004). The advantages and

disadvantages of vector-expressed RNAi effector molecules compared to the use of chemically synthesized siRNAs as a means to suppress gene expression are provided in Table 1.2.

1.8 AIMS OF THIS STUDY

RNA interference (RNAi), which is triggered by dsRNA and targets degradation of complementary mRNAs, has emerged as an important mechanism for sequence-specific suppression of gene expression at the post-transcriptional level. Practical applications of RNAi in mammalian cells were hampered because the long dsRNA used initially triggered apoptosis, making it impossible to consider effects of specific sequence targeting. With the initial demonstration that siRNA duplexes could be used to largely circumvent apoptosis pathways (Elbashir *et al*., 2001a; Caplen *et al*., 2001), there has been a widespread increase in interest in RNAi technologies for use in mammalian systems. Moreover, there has been substantial progress in approaches to introduce recombinant plasmid DNA vectors, which encode siRNA and shRNA, into cells (Brummelkamp *et al*., 2002a; Paddison *et al*., 2002; Wadhwa *et al*., 2004). Compared to the use of chemically synthesized siRNAs, the advantages of such approaches are that they are not only cheaper, but also the RNAi effector molecules are expressed constitutively and should therefore allow for long-term gene silencing.

Although numerous reports have demonstrated that RNAi can be used to inhibit virus propagation in cell culture (Bitko and Barik, 2001; Tan and Yin, 2004; Stram and Kuzntzova, 2006), few studies have explored the potential of RNAi approaches to viruses with a segmented dsRNA genome other than rotaviruses (Silvestri *et al.*, 2004; López *et al.*, 2005; Campagna *et al.*, 2005). More recently, however, siRNA-mediated gene silencing approaches relating to orbivirus gene expression have been explored (Wirblich *et al.*, 2006; Stassen *et al.*, 2007). The results of these studies have shown that due to the segmented nature of the AHSV genome, it was possible to silence expression of specific individual genes without affecting expression of the other viral genes (Stassen *et al*., 2007). Thus, this investigation focused on developing a shRNA-based approach whereby the NS1 gene of AHSV-6 could be silenced. This gene was specifically chosen as it is expressed abundantly in mammalian cells soon after virus infection (Huismans, 1979), and except for a possible role in pathogenesis (Owens *et al.*, 2004), the function of the NS1 protein is still not known.

Table 1.2 Advantages and disadvantages of different RNAi approaches (adapted from Wadhwa *et al.*, 2004)

RNAi Approach	Advantages	Disadvantages
Chemically synthesized siRNAs	• Direct and easy approach • siRNAs can be generated rapidly • Very effective, even in low concentrations	• Expensive to generate • Must be sized-purified • The methods of delivery include transfections with polymer or lipid reagents that are toxic to some cells, can induce the interferon response and are ineffective with primary cells • The other method of delivery involves electroporation, which causes changes to the physiology of cells • Excess siRNAs can saturate the RNAi processing machinery • Duration of suppression is limited
Plasmid DNA and viral vectors	• Inexpensive and economical to generate • No size-purification required • Some vectors can provide unlimited source of siRNAs for longer durations • Vectors with antibiotic resistance markers can compensate for low transfection efficiencies • Viral vectors facilitate the easy entry of siRNA into cells, tissue and animal models that are difficult to transfect • Some viral vectors (retroviral and lentiviral vectors) can integrate into the host cell's genome to provide transitive RNAi • Some viral vectors (adenoviral vectors) have high levels of RNA expression that are independent of the host cell cycle	• Difficult to design • Plasmid-based vectors must be very pure for delivery into cells with transfection reagents, which have a number of disadvantages as discussed above • Viral vectors (retroviral and lentiviral vectors) can cause insertional mutagenesis

Therefore, the aims of the investigation were as follows:

- To develop a quantitative reported-based si/shRNA screening system that may be used to identify RNAi effector molecules capable of silencing AHSV-6 NS1 gene expression

- To develop a plasmid DNA-based RNAi assay whereby expression of the AHSV-6 NS1 gene can be silenced by shRNAs in BHK-21 cell culture

CHAPTER 2

EXPRESSION OF AN AHSV-6 NS1-eGFP CHIMERIC GENE IN MAMMALIAN (BHK-21) CELLS AND ITS USE TOWARDS ESTABLISHING A SCREENING SYSTEM FOR SELECTION OF EFFECTIVE RNAi EFFECTOR MOLECULES

2.1 INTRODUCTION

African horse sickness virus (AHSV), a member of the *Orbivirus* genus within the *Reoviridae* family, encodes four nonstructural proteins (NS1, NS2, NS3/3A) of which the function in virus replication is not fully understood. Of these, NS1 is the most abundant viral protein synthesized in infected cells and forms large numbers of intracellular tubular structures (Huismans and Els, 1979). It can be envisaged that an understanding of the biological role of NS1 may be obtained by observing phenotypic consequences resulting from its alteration or inactivation. Unfortunately, these types of studies have been precluded by the lack of a reverse genetics system for AHSV. However, the advent of RNA interference (RNAi) as a means to selectively silence gene expression may provide an investigative tool that can greatly facilitate studies aimed at generating loss-of-function phenotypes (Arias *et al*., 2004; López *et al*., 2005; Forzan *et al*., 2007).

RNA interference (RNAi) is a conserved gene silencing mechanism that recognizes double stranded (ds) RNA as a signal to trigger the sequence-specific degradation of homologous mRNA (Fire *et al*., 1998; Tuschl *et al.*, 1999). As a result of biochemical and genetic studies in several experimental systems, the mechanisms underlying RNAi have begun to unfold. These suggest the existence of conserved machinery for dsRNA-induced gene silencing, which proceeds via a multistep mechanism. Initially, long dsRNA molecules are recognized and cleaved into 21-23 nt small interfering RNA duplexes (siRNAs) by the action of an endogenous dsRNA-specific endonuclease, Dicer, a member of the RNAse III family. Subsequently, the siRNAs are incorporated into the RNA-induced silencing complex (RISC), which identifies substrates through their homology to siRNAs and target these cognate mRNAs for destruction (Meister and Tuschl, 2004; Tomari and Zamore, 2005).

Despite RNAi having become a powerful and widely used approach for the analysis of gene function in a variety of organisms, there were initially several impediments to the use of this approach in mammalian cells. Most mammalian cells harbour a potent antiviral response that is triggered by the presence of dsRNA viral replication intermediates. Key components of this response are the dsRNA-activated protein kinase R (PKR), which results in a generalized inhibition of translation, and 2’,5’-oligoadenylate synthetase (2’,5’-AS), the product of which is an essential co-factor for the nonspecific ribonuclease RNase L (Stark *et al*., 1998; Sledz *et al*., 2003). The ultimate outcome of this set of responses is cell death via apoptosis. This

impediment, however, was resolved when it was shown that short synthetic 21-nt siRNAs with 2-nt 3'overhangs allowed for sequence-specific gene silencing, yet avoided the nonselective cytotoxic effects of long dsRNAs in mammalian cells (Elbashir *et al*., 2001a; Caplen *et al*., 2001). Subsequent to this discovery, RNAi has led to a revolution in molecular virology. Not only has RNAi emerged as a powerful genetic approach to study the function of virus genes (López *et al*., 2005; Campagna *et al*., 2005; Wirblich *et al*., 2006; Stassen *et al*., 2007), but it is also increasingly being used as an antiviral therapy. Consequently, RNAi has been used to inhibit the replication of numerous mammalian viruses from diverse virus families both *in vitro* and *in vivo* (Gitlin and Andino, 2003; Tan and Yin, 2004; Colbère-Garapin *et al*., 2005; Stram and Kuzntzova, 2006).

Despite the excitement, it should be kept in mind that RNAi is still a relatively young field and understanding of the basic underlying biology remains incomplete. For example, despite the availability of a number of guidelines and recommendations (Caplen *et al*., 2001; Elbashir *et al*., 2002; Mittal, 2004), as well as design algorithms and programs (Ui-Tei *et al*., 2004; Amarzguioui and Prydz, 2004; Reynolds *et al*., 2004), it is still not possible to predict with complete certainty the degree of gene silencing a particular siRNA will produce. Consequently, it is generally recommended that the silencing capability of several (at least two) candidate siRNAs be evaluated (Elbashir *et al*., 2002; Mittal, 2004). To facilitate screening of the candidate RNAi effector molecules, a number of different assay methods have been used, which are aimed at detecting either the target protein levels or the target mRNA levels (Caplen *et al*., 2001; Elbashir *et al*., 2002; Sandy *et al*., 2005; Cullen, 2006). Due to its simplicity and rapidity, detection of protein knock-down has become the preferred approach for screening purposes (Sandy *et al*., 2005). Frequently, the coding sequence of the target gene has been cloned in-frame with either enzymatic (*e.g.* luciferase) or fluorescent (*e.g.* green fluorescent protein [GFP]) reporters and expressed as fusion proteins (Wu *et al*., 2004; Yang *et al*., 2005; Werk *et al*., 2005). Upon transcription, such constructs produce a chimeric mRNA and consequently, upon efficient gene silencing, no assayable reporter product is produced. Of these different reporters, a GFP variant that was codon-optimized for higher expression in mammalian cells has been used widely to evaluate the efficiency of different siRNAs for gene silencing. Not only does this eGFP protein contain chromophore mutations that make the protein 35-times brighter, but fluorescence from eGFP does not require additional cofactors or substrates (Zhang *et al*., 1996) and can be monitored non-

invasively by fluorescent microscopy and quantitatively by fluorometry (Caplen *et al.*, 2001; Werk *et al.*, 2005; Stassen *et al.*, 2007).

Towards developing RNAi assays whereby expression of the AHSV-6 NS1 gene can be silenced in BHK-21 mammalian cell culture, the aims of this part of the study were to construct recombinant mammalian vectors that express an eGFP reporter protein, the AHSV-6 NS1 protein and a NS1-eGFP chimeric protein. For this purpose, the mammalian expression vector pCMV-Script®, which has been designed to allow protein expression in a wide variety of mammalian systems, was selected for use. In addition, the NS1-eGFP chimeric gene was also evaluated as a reporter system whereby potentially effective RNAi effector molecules could be identified. For this purpose, a well characterized chemically synthesized siRNA that targets the eGFP gene was selected for use.

2.2 MATERIALS AND METHODS

2.2.1 Bacterial strains and plasmids

The *E. coli* strains were routinely cultured at 37°C with shaking at 200 rpm in LB broth (1% [w/v] tryptone, 1% [w/v] NaCl, 0.5% [w/v] yeast extract; pH 7.4) (Sambrook *et al.*, 1989), and maintained at 4°C on LB agar or at -70°C as glycerol cultures. For plasmid selection and maintenance in *E. coli*, the culture medium was supplemented with 100 µg/ml for ampicillin and 50 µg/ml for kanamycin (Roche Diagnostics). Recombinant plasmid pBS-NS1-6.2, containing a full-length cDNA copy of AHSV-6 genome segment 5, was previously constructed and characterized by F.F. Maree, Department of Genetics, University of Pretoria (Maree and Huismans, 1997). A recombinant pGEM®-T Easy construct containing the enhanced green fluorescent protein (eGFP) gene was obtained from L. Stassen, Department of Microbiology and Plant Pathology, University of Pretoria. The pGEM®-T Easy cloning system was obtained from Promega and the pCMV-Script® mammalian expression vector was obtained from Stratagene.

2.2.2 Cell culture

Baby hamster kidney-21 (BHK-21) cells were propagated and maintained as monolayers in 75 cm^2 tissue culture flasks, and cultured in Minimum Essential Medium (MEM) Eagles base (Highveld Biological) supplemented with 2.5% (v/v) foetal bovine serum (FBS) and antibiotics (pencillin, streptomycin and fungizone). The flasks were incubated at 37°C in a

humidified incubator with a constant supply of 5% CO_2. For subculturing of confluent monolayers, attached cells were removed from the surface of a 75 cm^2 tissue culture flask by adding a small volume of a Trypsin/Versene solution (Highveld Biological) to the cells. The flask was gently rocked to remove the cells, after which 5 ml of complete MEM medium was added, and the cell clumps were dispersed by repeated suspension with a 10-ml syringe. The BHK-21 cells were diluted by adding 20 ml of complete MEM medium to the cells and then subcultured to 75 cm^2 tissue culture flasks (20 ml/flask). The tissue culture flasks were incubated at 37°C in a CO_2 incubator until the monolayers were 100% confluent.

2.2.3 DNA amplification

2.2.3.1 Oligonucleotides

Oligonucleotides used in the construction of a NS1-eGFP chimeric gene were designed based on the published AHSV-6 NS1 gene sequence (Maree and Huismans, 1997; GenBank accession no. U73658) and on the nucleotide sequence determined for the eGFP gene (Burger, 2006). The oligonucleotides were designed using the DNAMAN v.4.13 (Lynnon Biosoft) software program. To facilitate subsequent cloning procedures, unique restriction endonuclease recognition sites were incorporated at the 5'-terminus of the respective oligonucleotides. The oligonucleotides, indicated in Table 2.1, were synthesized by Inqaba Biotechnical Industries.

2.2.3.2 Polymerase chain reaction (PCR)

Each of the PCR reaction mixtures (100 µl) contained template DNA (50 ng), 100 pmol of each of the sense and antisense oligonucleotides, 1 × PCR buffer (75 mM Tris-HCl [pH8.8], 16 mM $(NH_4)_2SO_2$, 0.1% [v/v] Tween-20), 1.5 mM $MgCl_2$, 250 µM of each deoxynucleotide triphosphate (dNTP) and 0.25 U of ***Taq*** DNA polymerase (Southern Cross Biotechnology). The PCR reaction mixtures were placed in a Perkin-Elmer GeneAmp® 2700 thermal cycler. Following incubation at 94°C for 3 min, the samples were subjected to 35 cycles of denaturation at 94°C for 1 min, annealing at 55°C for 1 min and extension at 72°C for 1.5 min. After the last cycle, a final extension step was performed at 72°C for 4 min to complete synthesis of all DNA strands. For control purposes, reaction mixtures containing all reagents except template DNA were included. Aliquots of the PCR reaction mixtures were analyzed by electrophoresis on a 0.8% (w/v) agarose gel in the presence of an appropriate DNA molecular weight marker.

2.2.4 Agarose gel electrophoresis

DNA was analyzed on horizontal 0.8% (w/v) agarose slab gels supplemented with 0.5 µg/ml of ethidium bromide (Sambrook *et al*., 1989). The agarose gels were electrophoresed at 100 V in 1 × TAE buffer (40 mM Tris-HCl, 20 mM NaOAc, 1 mM EDTA; pH 8.5) and the DNA was then visualized on a UV transilluminator. Where appropriate, DNA fragments were sized according to their migration in the gel as compared to that of standard DNA molecular weight markers, namely phage λ DNA digested with both *Eco*RI and *Hind*III (Roche Diagnostics) and GeneRuler™ 100-bp DNA Ladder Plus (Fermentas AB).

2.2.5 Purification of DNA fragments from agarose gels

DNA fragments were purified from agarose gel slices, as described by Boyle and Lew (1995). The DNA fragments were excised from the agarose gel with a scalpel blade, mixed with 400 µl of a 6 M NaI solution, and the agarose was melted by incubation at 55°C for 5-10 min. Following complete dissolution of the agarose, 10 µ1 of a silica suspension was added to the sample, vortexed for 10 s and then incubated on ice for 30 min. The silica-bound DNA was pelleted by centrifugation at 15 000 rpm for 1 min and the pellet was washed four times with 500 µ1 of ice-cold NEW Wash solution (50 mM NaCl, 10 mM Tris-HCl [pH 7.5], 2.5 mM EDTA, 50% [v/v] ethanol). The DNA was eluted from the silica matrix at 55°C for 3 min in a final volume of 14 µ1 of 1 × TE buffer (10 mM Tris-HCl, 1 mM EDTA; pH 8). Following brief centrifugation to pellet the residual silica, an aliquot of the recovered supernatant was analyzed by electrophoresis on a 0.8% (w/v) agarose gel to assess the purity and concentration of the DNA.

2.2.6 Cloning of DNA fragments into plasmid vectors

2.2.6.1 Ligation reactions

For cloning of PCR amplicons, the pGEM®-T Easy vector system (Promega) was used according to the manufacturer's instructions. The ligation reaction mixture contained 50 ng of pGEM®-T Easy vector DNA, 150 ng of purified amplicon, 5 µ1 of a 2 × Rapid Ligation Buffer, 1 µ1 of T4 DNA ligase (3 U/µl) and UHQ water to a final volume of 10 µ1. Ligation of specific DNA fragments and restricted pCMV-Script® vector DNA was performed in a 10-µ1 reaction volume containing 1 × DNA ligase buffer (66 mM Tris-HCl, 5 mM $MgCl_2$, 1 mM DTT, 1 mM ATP; pH 7.5) and 1 U of T4 DNA ligase (Roche Diagnostics). The ratio of insert

to vector was typically in excess of 3:1. All of the ligation reactions were incubated overnight at 16°C.

2.2.6.2 Preparation of competent *E. coli* DH5α cells

Competent *E. coli* DH5α cells were prepared and transformed, as described by Sambrook *et al.* (1989). An overnight culture was prepared by inoculating a single colony of a freshly streaked *E. coli* DH5α cell culture into 1 ml of LB broth. Following incubation overnight at 37°C, the culture was inoculated into 100 ml of LB broth and grown to an OD_{600} of 0.4 to 0.5. The flask was then placed on ice for 30 min to inhibit further growth. The cells from 20 ml of the culture were harvested by centrifugation at 4 000 rpm for 10 min at 4°C in an Eppendorf model 5804R centrifuge. The cell pellet was suspended in 10 ml of ice-cold 0.1 M $CaCl_2$, incubated on ice for 30 min, pelleted as before and gently resuspended in 1 ml of the $CaCl_2$ solution. The cells were incubated on ice for at least 1 h before use.

2.2.6.3 Transformation of the competent *E. coli* DH5α cells

The competent cells were transformed using the heat-shock method (Sambrook *et al.*, 1989). The competent *E. coli* DH5α cells (100 µl) and ligation reaction mixture (5 µl) was mixed in a pre-cooled microfuge tube and incubated on ice for 30 min. The cells were heat-shocked at 42ºC for 90 s and immediately placed on ice for 2 min. Subsequently, 900 µl of pre-warmed (37°C) LB broth was added and the cells incubated at 37°C for 1 h. Aliquots (200 µl) of the transformation mixtures were plated onto LB agar containing the appropriate antibiotic. In instances where DNA fragments were cloned into pGEM®-T Easy vector DNA, the cells were plated together with 10 µl of IPTG (100 mM stock solution) and 50 µl of X-gal (2% [w/v] stock solution) to allow identification of recombinant transformants based on insertional inactivation of the *lacZ'* marker gene. The agar plates were incubated overnight at 37°C. A positive control (10 ng of pUC18 plasmid DNA) and negative control (competent cells only) were included to determine the competency of the *E. coli* DH5α cells and to test for contamination, respectively.

2.2.6.4 Plasmid DNA extraction

Plasmid DNA was isolated from selected transformants using the alkaline lysis method, as described by Sambrook *et al.* (1989). Single colonies were each inoculated into 20 ml of LB

broth supplemented with the appropriate antibiotic and incubated overnight at 37°C with shaking. The cells from 1.5 ml of the overnight culture were collected by centrifugation at 15 000 rpm for 1 min. The bacterial cell pellets were suspended in 100 µl of Solution 1 (50 mM glucose, 25 mM Tris-HCl, 10 mM EDTA; pH 8) and incubated for 5 min at room temperature and 1 min on ice. The cells were lysed, following addition of 200 µl of freshly-prepared Solution 2 (1% [w/v] SDS, 0.2 M NaOH). After incubation on ice for 5 min, 150 µl of ice-cold Solution 3 (3 M NaOAc; pH 4.8) was added and incubation was continued on ice for a further 10 min. The insoluble aggregate was collected by centrifugation at 15 000 rpm for 5 min, after which the plasmid DNA was precipitated from the recovered supernatants by addition of 2 volumes of 100% ethanol and incubation at -20°C for 1 h. The precipitated plasmid DNA was collected by centrifugation at 15 000 rpm for 20 min, washed once with 70% ethanol, vacuum-dried and then suspended in 40 µl of 1 × TE buffer (10 mM Tris-HCl, 1 mM EDTA; pH 8). To remove contaminating RNA, the plasmid DNA was incubated with 1 µl of RNAse A (10 mg/ml) at 37ºC for 30 min.

2.2.6.5 Restriction endonuclease digestions

Restriction endonuclease digestions were performed in microfuge tubes in a final volume of 15 µl and contained 1 U of enzyme per µg of plasmid DNA in the appropriate concentration of salt, using the 10× buffer supplied by the manufacturer. The reaction mixtures were incubated at 37°C for 90 min. For digestions involving two enzymes of which the salt concentrations differed for optimal activity, the plasmid DNA was first digested with the enzyme requiring the lowest salt concentration. The salt concentration was then adjusted and the second enzyme added. All restriction enzymes were supplied by Roche Diagnostics or Fermentas AB. The digestion products were analyzed on a 0.8% (w/v) agarose gel in the presence of an appropriate DNA molecular weight marker.

2.2.7 Nucleotide sequencing and sequence analysis

Nucleotide sequencing of cloned insert DNA was performed with the ABI-PRISM® BigDye™ Terminator v.3.1 Cycle Sequencing Ready Reaction kit (Perkin-Elmer Applied Biosystems) according to the instructions of the manufacturer. In addition to the T3 and T7 sequencing oligonucleotides, NS1- and eGFP-specific internal oligonucleotides were also used in the sequencing reactions (Table 2.1 and Fig. 2.1). Each sequencing reaction contained 200-500 ng of purified template DNA, 3.2 pmol of sequencing oligonucleotide, 2 µl of

Table 2.1 Oligonucleotides used in PCR and nucleotide sequencing

Oligonucleotide	Nucleotide sequence (5'-3')
PCR amplification*	
eGFP-FSal	5'-CAC**gtcgac***ATG*GTGAGCAAGG-3'; *Sal*I site incorporated
eGFP-RKpn	5'-CAC**ggtacc***TTA*CTTGTACAGCTCGTCC-3'; *Kpn*I site incorporated
NS1-FBam	5'-CAC**ggatcc***ATG*GATAGGTTCTTG-3'; *Bam*HI site incorporated
NS1-RSal	5'-CAC**gtcgac**GACATTATGCATGAAATC-3'; *Sal*I site incorporated
Nucleotide sequencing	
T7	5'-GTAATACGACTCACTATAGGGC-3'
T3	5'-AATTAACCCTCACTAAAGGG-3'
Int-NS1F1	5'-CTTAGCCGATGGGGTCAATT-3'
Int-NS1F2	5'-GACAGCAAGGTTGGGACATCT-3'
Int-eGFPR	5'-TCGGGGTAGCGGCTGAAGCAC-3'

*In oligonucleotide sequences, the restriction endonuclease sites are indicated in bold lower case letters, while nucleotides specifying the start (ATG) and stop (TTA) codons are indicated in italics.

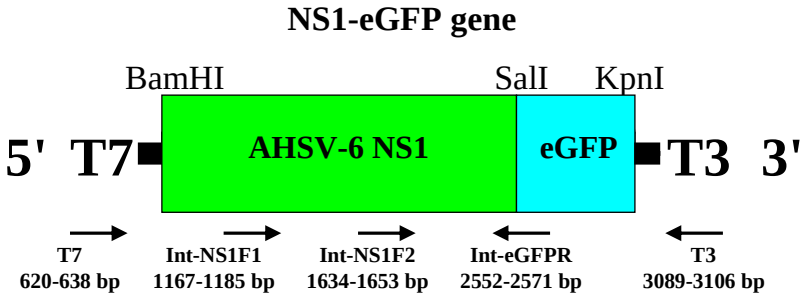

Fig. 2.1 Schematic representation of the oligonucleotide annealing positions and direction of sequencing of the AHSV-6 NS1-eGFP chimeric gene cloned into the pCMV-Script® vector. The annealing position of the oligonucleotides corresponds to its position relative to the first nucleotide of the NS1 initiation codon. The T7 and T3 oligonucleotides anneal to flanking DNA in the pCMV-Script® vector.

Terminator Ready Reaction mix, 2 µl of 5 × Sequencing buffer and UHQ water to a final volume of 10 µl. Cycle sequencing reactions were performed in a GeneAmp® 2700 thermal cycler (Perkin-Elmer) with 25 of the following cycles: denaturation at 96°C for 10 s, annealing at 50°C for 15 s and elongation at 60°C for 4 min. The extension products were subsequently precipitated by addition of 2 µl of 3 M NaOAc (pH 4.6) and 50 µl of 95% ethanol. The tubes were vortexed briefly, incubated at room temperature for 15 min in the dark, centrifuged at 15 000 rpm for 30 min and the supernatants carefully aspirated. The pellets were rinsed with 250 µl of 70% ethanol, vacuum-dried and then stored at -20°C until electrophoresis. Prior to electrophoresis, the purified extension products were suspended in 3 µ1 of sequencing loading buffer, denatured by heating to 90°C for 2 min and loaded onto an ABI PRISM™ Model 377 DNA sequencer. The nucleotide sequences obtained were edited and analyzed with the BioEdit sequence Alignment Editor v.5.0.9 (Hall, 1999) and DNAMAN v.4.13 (Lynnon Biosoft) software programs.

2.2.8 Construction of recombinant pCMV-Script® mammalian expression vectors

All molecular cloning techniques employed in construction of the respective recombinant mammalian expression vectors were performed according to the procedures described in the preceding sections. All plasmid constructs were verified by restriction endonuclease digestions and by nucleotide sequencing.

- **pCMV-NS1**

To construct the recombinant mammalian expression vector pCMV-NS1, the *ca*. 1.7-kb AHSV-6 NS1 gene was excised from plasmid pBS-NS1-6.2 by digestion with *Bam*HI and then cloned into *Bam*HI-digested pCMV-Script®. The transcriptional orientation of the cloned NS1 gene relative to the CMV promoter was confirmed by restriction mapping with *Hind*III.

- **pCMV-eGFP**

To construct the recombinant mammalian expression vector pCMV-eGFP, the *ca*. 720-bp eGFP gene was excised from plasmid pGEM-eGFP by digestion with both *Bam*HI and *Eco*RI, and cloned directionally into pCMV-Script® that had been prepared in an identical manner.

- **pCMV-NS1-eGFP**

Towards construction of the recombinant mammalian expression vector pCMV-NS1-eGFP, a truncated NS1 gene that lacked a TAG stop codon was PCR-amplified using plasmid pBS-NS1-6.2 as template DNA, together with oligonucleotides NS1-FBam and NS1-RSal (Table 2.1). The amplicon was cloned into pGEM®-T Easy to generate pGEM-NS1chm. The insert DNA was subsequently recovered by digestion with both *Bam*HI and *Sal*I, and cloned into the identical sites of pCMV-Script® to yield pCMV-NS1chm. Oligonucleotides eGFP-FSal and eGFP-RKpn (Table 2.1) were used with plasmid pGEM-eGFP as template DNA to PCR-amplify the eGFP gene, which was cloned into pGEM®-T Easy to generate pGEM-eGFPchm. The insert DNA was recovered by digestion with both *Sal*I and *Kpn*I, and cloned into identically digested pCMV-NS1chm to complete construction of pCMV-NS1-eGFP. The cloning strategy employed in the construction of pCMV-NS1-eGFP is indicated in Fig. 2.2.

2.2.9 Plasmid isolation of recombinant mammalian expression vectors

2.2.9.1 Large-scale plasmid DNA extraction

Large-scale plasmid DNA extractions were performed according to procedures described by Sambrook *et al.* (1989) with the following modifications. Five ml of an overnight culture was inoculated into 500 ml of LB broth supplemented with kanamycin, and incubated overnight at 37°C. The cells were collected by centrifugation at 5 000 rpm for 15 min in a HS-4 rotor using a Sorvall RC-5B centrifuge (Du Pont Instruments). The cell pellet was suspended in 40 ml of Solution 1 (50 mM glucose, 25 mM Tris-HCl, 10 mM EDTA; pH 8) and incubated on ice for 30 min. The cells were lysed by addition of 80 ml of Solution 2 (1% [w/v] SDS, 0.2 M NaOH) and following incubation on ice for 5 min, 60 ml of Solution 3 (3 M NaOAc; pH 4.8) was added. After incubation on ice for 1 h, the insoluble aggregate was removed by centrifugation at 10 000 rpm for 15 min. The plasmid DNA-containing supernatant was recovered, filtered through Whatman filter paper and then precipitated by addition of 2.5 volumes of 96% ethanol and incubation overnight at -20°C. The precipitated plasmid DNA was collected by centrifugation at 10 000 rpm for 15 min and subsequently suspended in 60 ml of UHQ water. High-molecular-weight RNA was precipitated by addition of 25 ml of ice-cold 7.5 M NH_4OAc and incubation on ice for at least 30 min. Following centrifugation at 10 000 rpm for 10 min, the plasmid DNA was recovered from the supernatant by ethanol precipitation, as described above. The DNA pellet was washed with 70% ethanol, vacuum-dried and resuspended in 200 µl of 1 × TE buffer.

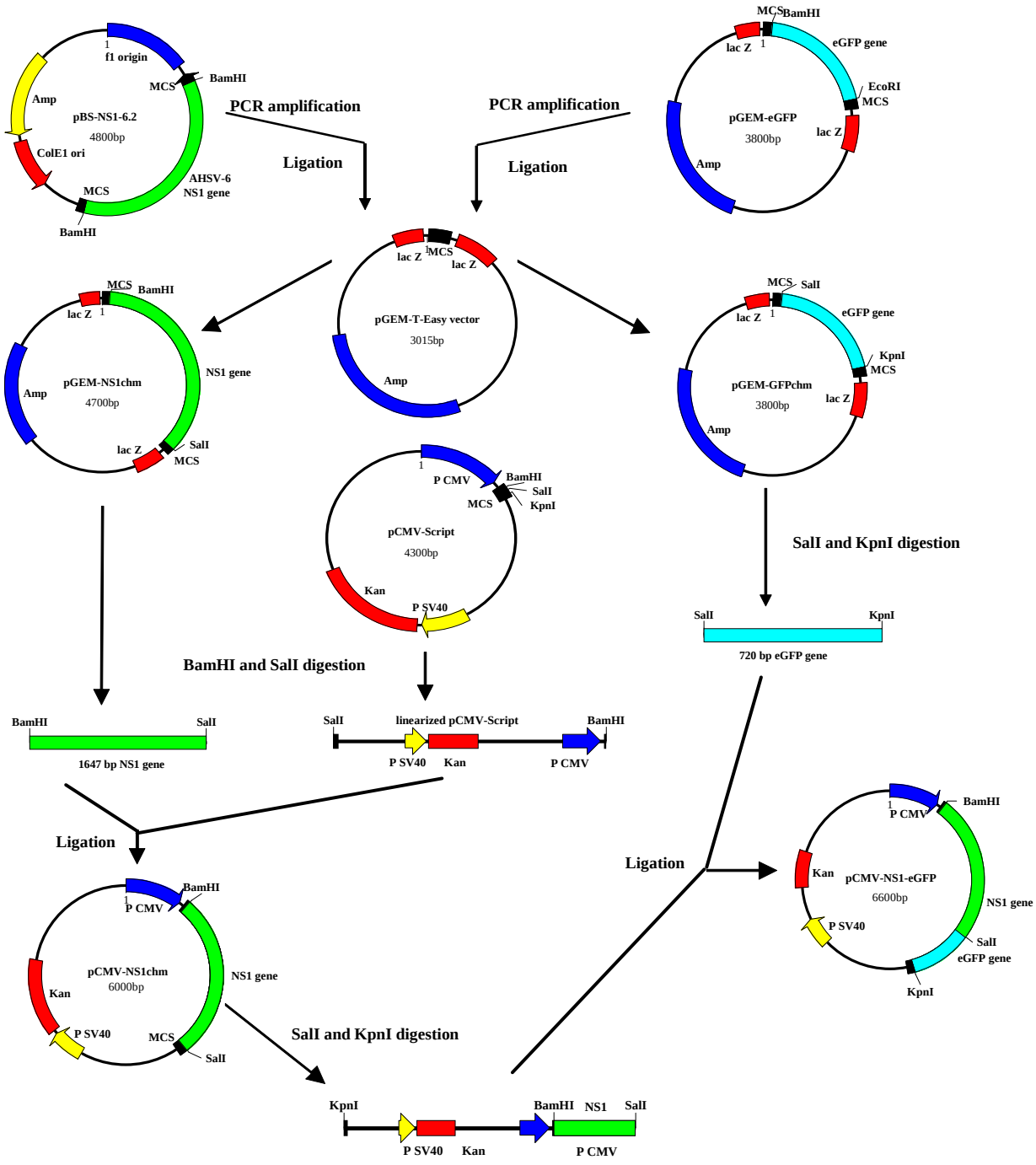

Fig. 2.2 Schematic diagram indicating the strategy used for the construction and cloning of the AHSV-6 NS1-eGFP chimeric gene into the pCMV-Script® mammalian expression vector. Abbreviations: **Amp**, ampicillin resistance gene; **MCS**, multiple cloning site; **Ori**, origin of replication; **P CMV**, CMV promoter; and **P SV40**, SV40 promoter.

2.2.9.2 Cesium chloride (CsCl)-ethidium bromide density gradient centrifugation

The volume of the large-scale plasmid DNA solution was adjusted to 3 ml with 1 × TE and 3.234 g of CsCl was added to the solution. After the CsCl was dissolved, 240 µ1 of ethidium bromide (10 mg/ml) was added and the solution was poured into a 5-ml polyallomer centrifuge tube (Beckman). The gradient was centrifuged at 38 000 rpm for 40 h at 20°C in a Beckman SW 55Ti swing-bucket rotor using a Sorvall UltraPro80 centrifuge (Du Pont Instruments). The tubes were then viewed under UV light and the plasmid DNA-containing lower band was removed by inserting the needle of a syringe into the tube beneath the lower band. The plasmid DNA solution was removed, transferred to a 50-ml Greiner tube and diluted with 3 volumes of 1 × TE buffer. The ethidium bromide was removed from the solution by repeated extraction with an equal volume of water-saturated *n*-butanol. The lower aqueous phase was then transferred to a 15-ml Greiner tube and the volume was adjusted to 1 ml with 1 × TE. Plasmid DNA was subsequently precipitated by addition of 2 volumes of 96% ethanol at 4°C for 1 h or overnight. The precipitated DNA was recovered by centrifugation at 10 000 rpm for 20 min, washed with 70% ethanol and vacuum-dried before being suspended in 100 µl of 1 × TE buffer. The concentration of the purified plasmid DNA was determined spectrophometrically with a Nanodrop instrument (Thermo Scientific) according to the manufacturer's instructions.

2.2.10 Expression of eGFP and NS1-eGFP proteins in BHK-21 cells

2.2.10.1 Transfection of BHK-21 cells

BHK-21 cells were transfected with purified recombinant pCMV-Script® plasmid DNA by means of lipofection with Lipofectamine™ 2000 (Invitrogen) according to the manufacturer's instructions. The BHK-21 cells were seeded in 24-well tissue culture dishes to reach 80% confluency within 24 h of incubation at 37°C in the presence of 5% CO_2. For each transfection, 800 ng of purified plasmid DNA and 2 µ1 of Lipofectamine™ 2000 reagent were each diluted separately in 50 µ1 of MEM medium that lacked serum and antibiotics. The two solutions were incubated for 5 min at room temperature, mixed and then incubated at room temperature for a further 20 min to allow formation of DNA-lipofectamine complexes. The cell monolayers were prepared for transfection by rinsing the cells three times with 500 µ1 of MEM medium lacking serum and antibiotics. After addition of 400 µl of MEM medium supplemented with 2.5% (v/v) FBS, but lacking antibiotics, the cells were overlayed with the

DNA-lipofectamine complexes and the tissue culture dishes were incubated at 37°C for 24 h in a CO_2 incubator. Untransfected BHK-21 cells and cells transfected with parental pCMV-Script® plasmid DNA were included as controls. The cell monolayers were subsequently examined by fluorescence microscopy, as described below, as well as by SDS-PAGE and Western blot analysis.

2.2.10.2 SDS-PAGE

Transfected BHK-21 cells were harvested by trypsinization, collected by centrifugation at 3 000 rpm for 10 min and washed once in 1 × phosphate-buffered saline (PBS: 137 mM NaCl, 2.7 mM KCl, 4.3 mM Na_2HPO_4. $2H_2O$, 1.4 mM KH_2PO_4; pH 7.4). The cells were suspended in 20 µ1 of 1 × PBS and an equal volume of 2 × protein solvent buffer (PSB: 125 mM Tris-HCl [pH 6.8], 4% [w/v] SDS, 20% [v/v] glycerol, 10% [v/v] 2-mercaptoethanol, 0.002% [w/v] bromophenol-blue) was added to each sample. The samples were heated for 10 min in boiling water prior to SDS-PAGE.

Protein samples were analyzed by electrophoresis in a discontinuous gel system, as described by Laemmli (1970). A 5% (w/v) acrylamide stacking gel and 12% (w/v) acrylamide separating gel was used of which the acrylamide:bisacrylamide ratio was 30:0.8. The stacking gel was polymerized in buffer containing 0.125 mM Tris-HCl (pH 6.8), 0.1% (w/v) SDS, 0.08% (w/v) ammonium persulphate and 10 µ1 of TEMED. The separating gel was polymerized similarly, except that the buffer comprised of 0.375 M Tris-HCl (pH 8.8) and 0.1% (w/v) SDS. The protein samples were loaded onto the SDS-polyacrylamide gel and electrophoresed in a Hoefer Mighty Small™ electrophoresis unit at 120 V for 2-3 h in 1 × TGS electrophoresis buffer (25 mM Tris-HCl [pH 8.3], 0.192 M glycine, 0.1% [w/v] SDS). Following electrophoresis, the gels were stained with 0.125% (w/v) Coomassie brilliant blue (prepared in 50% [v/v] methanol and 10% [v/v] acetic acid) and the proteins were visualized by destaining the gels in a solution containing 10% (v/v) methanol and 10% (v/v) glacial acetic acid. The sizes of the resolved proteins were estimated by comparison to reference marker proteins (Rainbow™ protein molecular weight marker; Amersham-Pharmacia Biotech AB).

2.2.10.3 Western blot analysis

For Western blot analysis, proteins resolved by SDS-PAGE were electroblotted from an unstained SDS-polyacrylamide gel onto a Hybond™-C^+ nitrocellulose membrane (Amersham-Pharmacia Biotech AB), as described by Sambrook *et al.* (1989). The gel, two sheets of filter paper and nitrocellulose membrane, cut to the same size of the gel, were equilibrated for 30 min in transfer buffer (25 mM Tris, 186 mM glycine). The proteins were electroblotted onto the membrane at 28 V and 120 mA for 2 h in a Mighty Small™ Transphor wet blotting apparatus (Hoefer) filled with transfer buffer. Following transfer, the membrane was rinsed once in 1 × PBS for 5 min and then incubated at room temperature for 30 min or overnight at 4°C in blocking solution (1% [w/v] fat-free milk powder in 1 × PBS) to block non-specific binding sites. The membrane was subsequently transferred to blocking solution containing the primary antibody, which comprised a polyclonal anti-eGFP antibody (Sigma-Aldrich) diluted 1:2000, and incubated at room temperature for 2 h with gentle agitation. The unbound primary antibodies were removed by washing the membrane three times for 5 min each in wash buffer (0.05% [v/v] Tween-20 in 1 × PBS). The secondary antibody, horseradish peroxidase-conjugated Protein A (Sigma-Aldrich), diluted 1:1000 in 1 × PBS, was added to the membrane and incubated at room temperature for 1 h. The membrane was washed three times for 5 min each in wash buffer and once for 5 min in 1 × PBS. To detect immuno-reactive proteins calorimetrically, the membrane was immersed in a freshly prepared peroxidase enzyme substrate solution (60 mg 4-chloro-1-naphtol in 20 ml of ice-cold methanol and 100 ml of 1 × PBS containing 60 µl of H_2O_2) until the bands became visible. The colour reaction was then stopped by rinsing the membrane with distilled water and air-dried.

2.2.11 RNA interference (RNAi) assays in BHK-21 cells

2.2.11.1 Small interfering RNAs (siRNAs)

A chemically synthesized siRNA directed against eGFP mRNA, which has been reported to inhibit eGFP expression by 90% (Caplen *et al.*, 2001), was obtained from Qiagen. As a control for the RNAi assays, a nonsilencing control siRNA was designed by scrambling the sequence of the eGFP-spesific siRNA. The sequences were as follow: eGFP-siRNA, sense 5'-GCAAGCUGACCCUGAAGUUCAU-3', antisense 5'-GCCGUUCGACUGGGACUUCAAG-3'; and scrambled-siRNA, sense 5'-

UUCUCCGAACGUGUCACGUTT-3', antisense 5'-TTAAGAGGCUUGCACAGUGCA-3'. The siRNAs were supplied as lyophilized, desalted duplexes and were suspended in the provided RNAse-free buffer (100 mM KOAc, 30 mM HEPES-KOH, 2 mM MgOAc; pH 7.4) at a concentration of 20 µM. To disrupt aggregates that may have formed during lyophilization, the suspensions were incubated at 90°C for 1 min and then at 37°C for 1 h. The siRNAs were dispensed in aliquots and stored at -20°C until needed.

2.2.11.2 Co-transfection of BHK-21 cells with siRNA and recombinant pCMV-Script® expression vectors

The siRNA-mediated RNAi assays were performed according to procedures described by Gitlin *et al*. (2002) and Yu *et al*. (2002). The day before transfection, BHK-21 cells were trypsinized, diluted in fresh MEM medium and seeded in 24-well tissue culture dishes to reach 60% confluency within 24 h of incubation at 37°C in the presence of 5% CO_2. Recombinant mammalian expression vectors pCMV-eGFP and pCMV-NS1-eGFP were subsequently co-transfected together with the siRNA into the BHK-21 cells using Lipofectamine™ 2000 (Invitrogen). For this purpose, 800 ng of purified recombinant plasmid DNA and 2 µ1 of the Lipofectamine™ 2000 reagent were each diluted in 50 µ1 of MEM medium lacking serum and antibiotics, incubated at room temperature for 5 min and then mixed to allow the formation of DNA-lipofectamine complexes. Separately, 20 pmol of the siRNA and 1 µl of the Lipofectamine™ 2000 reagent were each diluted in 50 µl of serum- and antibiotic-free MEM medium and, following incubation at room temperature for 5 min, were mixed to allow the formation of RNA-lipofectamine complexes. After incubation at room temperature for 20 min, the two solutions were mixed and then overlayed on the BHK-21 cell monolayers, which had been prepared for transfection as described above. Following the addition of 300 µl of MEM medium supplemented with 2.5% (v/v) FBS, but lacking antibiotics, the tissue culture dishes were incubated at 37°C for 24 h in a CO_2 incubator. Untransfected BHK-21 cells and cells transfected with the recombinant pCMV-Script® vectors were included as controls in the RNAi assay.

2.2.11.3 Analysis and quantification of eGFP and NS1-eGFP expression in siRNA-treated BHK-21 cells

BHK-21 cell monolayers were observed at 24 h post-transfection for eGFP and NS1-eGFP protein expression on a Zeiss Axiovert 200 fluorescent microscope fitted with the no. 10 Zeiss filter set (excitation at 450-490 nm; emission at 515-560 nm). The images were captured for

separate microscope fields with a Nikon DMX 1200 digital camera. For fluorometry, the BHK-21 cell monolayers were rinsed once with 1 × PBS and trypsinized by addition of 30 µl of Trypsin/Versene. After incubation at 37°C for 1 min, the cells were collected by centrifugation at 3 000 rpm for 10 min, rinsed with 1 × PBS and suspended in 1 ml of 1 × PBS. The relative fluorescence was determined with a BioRad Versafluor™ fluorometer (excitation at 485-495 nm; emission at 515-525 nm).

2.3 RESULTS

2.3.1 Construction of recombinant pCMV-Script® mammalian expression vectors containing the AHSV-6 NS1, eGFP and NS1-eGFP chimeric genes

2.3.1.1 Construction of plasmid pCMV-NS1

A cDNA copy of the 1.7-kb NS1 gene of AHSV-6 had been cloned previously into the *Bam*HI site of plasmid pBS and the recombinant plasmid was designated pBS-NS1-6.2 (Maree and Huismans, 1997). The NS1 gene was subsequently excised from plasmid pBS-NS1-6.2 and cloned into the *Bam*HI site of the pCMV-Script® mammalian expression vector. Following transformation of competent *E. coli* DH5α cells, the plasmid DNA extracted from randomly selected kanamycin-resistant transformants was analyzed by agarose gel electrophoresis. Plasmid DNAs migrating slower than parental pCMV-Script® vector DNA on agarose gels were selected and analyzed for the presence of a cloned insert DNA by digestion with *Bam*HI. In contrast to non-recombinant plasmid DNA, which was linearized (Fig 2.3B, lane 5), digestion of the recombinant plasmid DNA excised a 1.7-kb DNA fragment (Fig. 2.3B, lane 7), indicating that the NS1 gene had been cloned successfully. A clone that displayed the correct transcriptional orientation was selected following restriction enzyme digestion with *Hind*III. The enzyme cuts once within the multiple cloning site of the vector (*ca*. 40 bp from the 3'-end of the NS1 gene) and *ca*. 500 bp from the 5'-end of the cloned NS1 gene, thus resulting in the excision of a DNA fragment of *ca*. 1.2 kb (Fig. 2.3B, lane 8). One such clone was selected, designated pCMV-NS1, and the integrity of the cloned insert DNA was verified by sequencing both strands of the cloned insert DNA prior to it being used in further experiments.

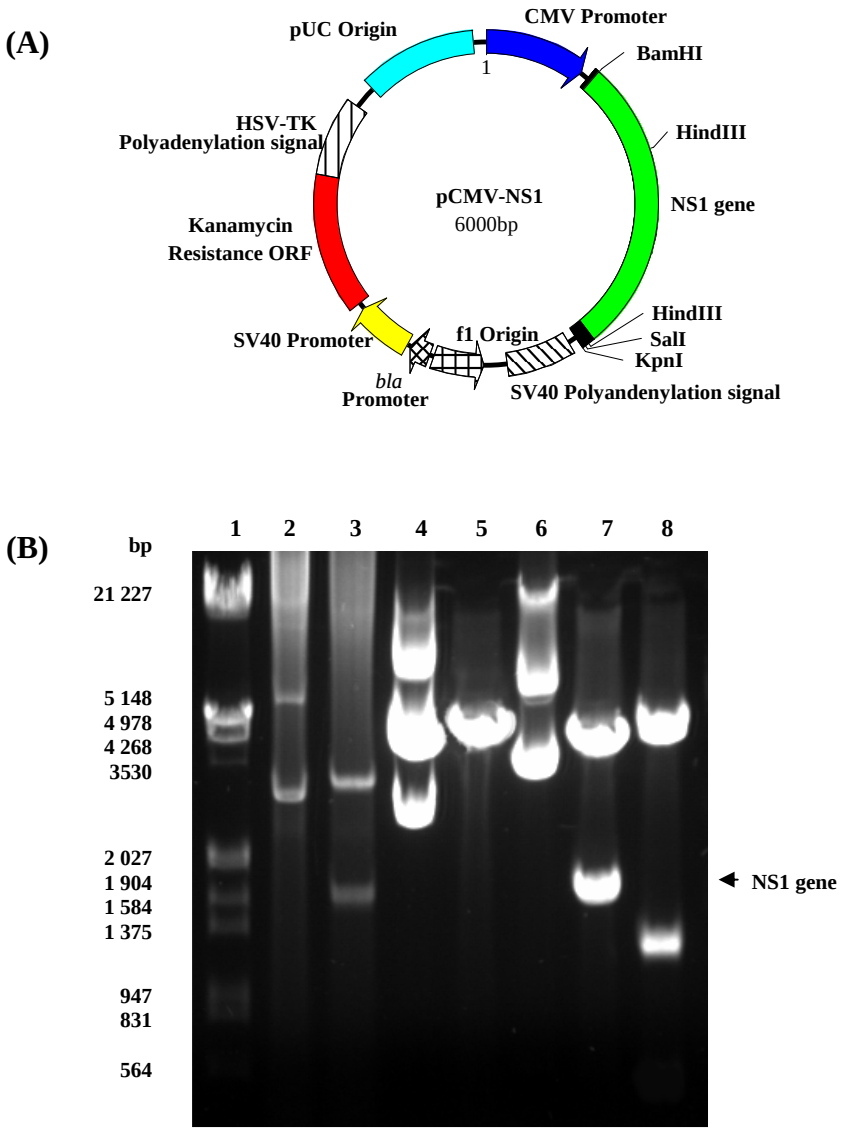

Fig. 2.3 Schematic diagram of the recombinant pCMV-NS1 construct (A) and agarose gel electrophoretic analysis of the recombinant plasmid pCMV-NS1 (B). Lanes: 1; DNA molecular weight marker; 2, uncut plasmid pBS-NS1-6.2; 3, *Bam*HI-digested plasmid pBS-NS1-6.2; 4, uncut parental pCMV-Script® vector; 5, *Bam*HI-digested pCMV-Script® vector; 6, uncut recombinant plasmid pCMV-NS1; 7, B*am*HI-digested recombinant plasmid pCMV-NS1; 8, *Hind*III-digested recombinant plasmid pCMV-NS1. The sizes of the molecular weight marker, phage λ DNA digested with both *Eco*RI and *Hind*III, are indicated to the left of the figure.

2.3.1.2 Construction of plasmid pCMV-eGFP

To enable cloning of the eGFP gene into the pCMV-Script® mammalian expression vector, the gene was recovered from pGEM-eGFP by digestion with both *Bam*HI and *Eco*RI and then cloned into identically prepared pCMV-Script® vector DNA. Using a screening strategy similar to that described above, the derived recombinant plasmids were subsequently digested with both *Bam*HI and *Eco*RI and resulted in the excision of a 720-bp eGFP-specific insert DNA (Fig. 2.4B, lane 7). A recombinant clone, designated pCMV-eGFP, was selected and the integrity of the cloned insert DNA was verified by nucleotide sequencing.

2.3.1.3 Construction of plasmid pCMV-NS1-eGFP

It has previously been reported that the eGFP reporter gene provides a simple and impartial model for assessing the efficacy of gene silencing by analysis at the protein level visually and quantitatively by fluorometry (Werk *et al*., 2005; Stassen *et al*., 2007). Consequently, a NS1-eGFP chimeric gene was constructed that could be used to facilitate screening of different candidate RNAi effector molecules for their efficiency to silence NS1 gene expression in mammalian cell culture. The chimeric gene was constructed by fusing the eGFP reporter gene in-frame to the 3'-end of the NS1 gene, thereby ensuring that transcription of the full-length NS1 gene would need to have occurred in order to obtain a fluorescently tagged protein. For this purpose, the NS1 gene was PCR-amplified by making use of a 3'-end specific oligonucleotide that had been designed to delete the TAG stop codon and 3' non-coding region of the NS1 gene. In addition, both this NS1-specific oligonucleotide and the 5'-end specific oligonucleotide used in PCR amplification of the eGFP gene were designed to contain a unique *Sal*I restriction enzyme recognition site. Following restriction enzyme digestion of the respective amplicons, they could therefore be ligated to yield the desired NS1-eGFP chimeric gene (Fig. 2.5A).

Towards constructing the NS1-eGFP chimeric gene, the AHSV-6 NS1 and eGFP genes were PCR-amplified with recombinant plasmids pBS-NS1-6.2 and pGEM-eGFP as template DNA, respectively, together with the appropriate oligonucleotides, as described under Materials and Methods (Section 2.2.8). The amplicons, *ca*. 1.7 kb for NS1 and *ca*. 720 bp for eGFP, were each cloned into pGEM®-T Easy vector DNA. Following transformation of competent *E. coli* DH5α cells, recombinant transformants with a Gal^- phenotype were selected on X-gal containing selective agar medium and then cultured overnight in LB broth supplemented with

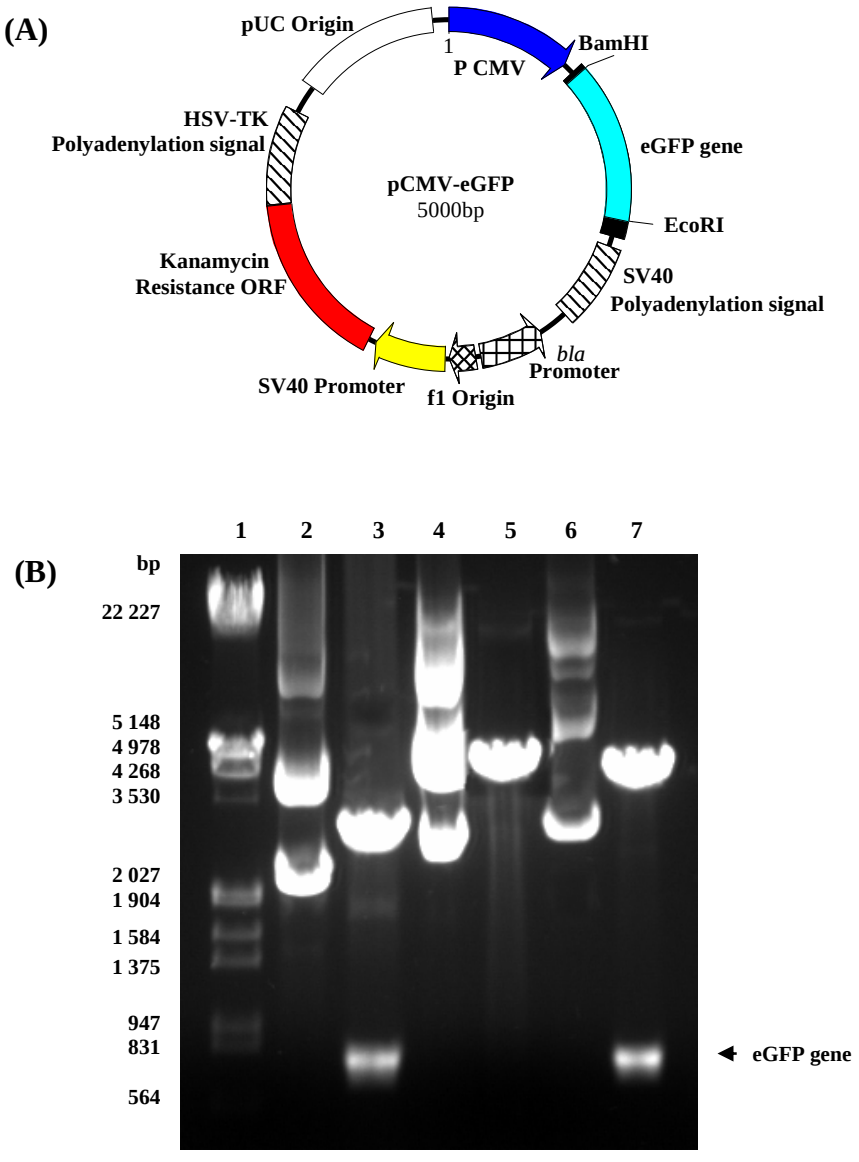

Fig. 2.4 Schematic diagram of the recombinant pCMV-eGFP construct (A) and agarose gel electrophoretic analysis of the recombinant plasmid pCMV-eGFP (B). Lanes: 1, DNA molecular weight marker; 2, uncut pGEM-eGFP plasmid; 3, *Bam*HI- and *Eco*RI-digested pGEM-eGFP plasmid; 4, uncut parental pCMV-Script® vector; 5, *Bam*HI- and *Eco*RI-digested parental pCMV-Script® vector; 6, uncut recombinant plasmid pCMV-eGFP; 7, *Bam*HI- and E*co*RI-digested recombinant plasmid pCMV-eGFP. The sizes of the molecular weight marker, phage λ DNA digested with both *Eco*RI and H*ind*III, are indicated to the left of the figure.

ampicillin. The derived recombinant constructs, designated pGEM-NS1chm and pGEM-eGFPchm, respectively, were analyzed for the presence of a cloned insert DNA by using restriction enzymes of which the recognition sites had been incorporated during design of the oligonucleotides. Digestion of the recombinant plasmid DNA resulted in the excision of the cloned NS1 and eGFP insert DNAs (Fig 2.5B, lanes 3 and 9, respectively) and the integrity of cloned insert DNA was verified by nucleotide sequencing.

Having confirmed deletion of the stop codon and the 3' non-coding region, the NS1chm gene was recloned from pGEM-NS1chm into the *Bam*HI and *Sal*I sites of the mammalian expression vector pCMV-Script® to generate pCMV-NS1chm. Subsequently, the eGFPchm gene was excised from pGEM-eGFPchm by digestion with both *Sal*I and *Kpn*I, and cloned into identically prepared pCMV-NS1chm to yield pCMV-NS1-eGFP. The recombinant plasmid was characterized by restriction enzyme digestion. To verify the presence of the cloned NS1chm insert DNA, plasmid pCMV-NS1chm was digested with both *Bam*HI and *Sal*I, and yielded expected DNA fragments corresponding in size to the pCMV-Script® vector DNA (*ca* 4.3 kb) and NS1chm insert DNA (*ca.* 1.7 kb) (Fig. 2.5B, lane 7). The recombinant plasmid pCMV-NS1-eGFP was subsequently characterized by digestion with *Bam*HI and *Kpn*I, and resulted in the excision of a 2.4-kb DNA fragment corresponding in size to the NS1-eGFP chimeric gene (Fig. 2.5B, lane 11).

As a final confirmation regarding the integrity of the constructed NS1-eGFP gene, the nucleotide sequence of the full-length chimeric gene was determined. Analysis of the nucleotide sequence and deduced amino acid sequence indicated that the stop codon was deleted from the NS1 gene and replaced by six nucleotides specifying the *Sal*I restriction enzyme site that allowed for in-frame fusion of the NS1 and eGFP genes. No other sequence differences were noted between the NS1-eGFP gene sequence and those of the NS1 and eGFP genes. The sequence analysis also confirmed that the reading frame of the NS1-eGFP chimeric protein was maintained.

2.3.2 Expression of the eGFP and NS1-eGFP proteins in BHK-21 cells

To determine whether the eGFP and chimeric NS1-eGFP genes are expressed in BHK-21 cells, purified parental pCMV-Script® and recombinant pCMV-eGFP and pCMV-NS1-eGFP mammalian expression vectors were transfected into BHK-21 cell monolayers by means of

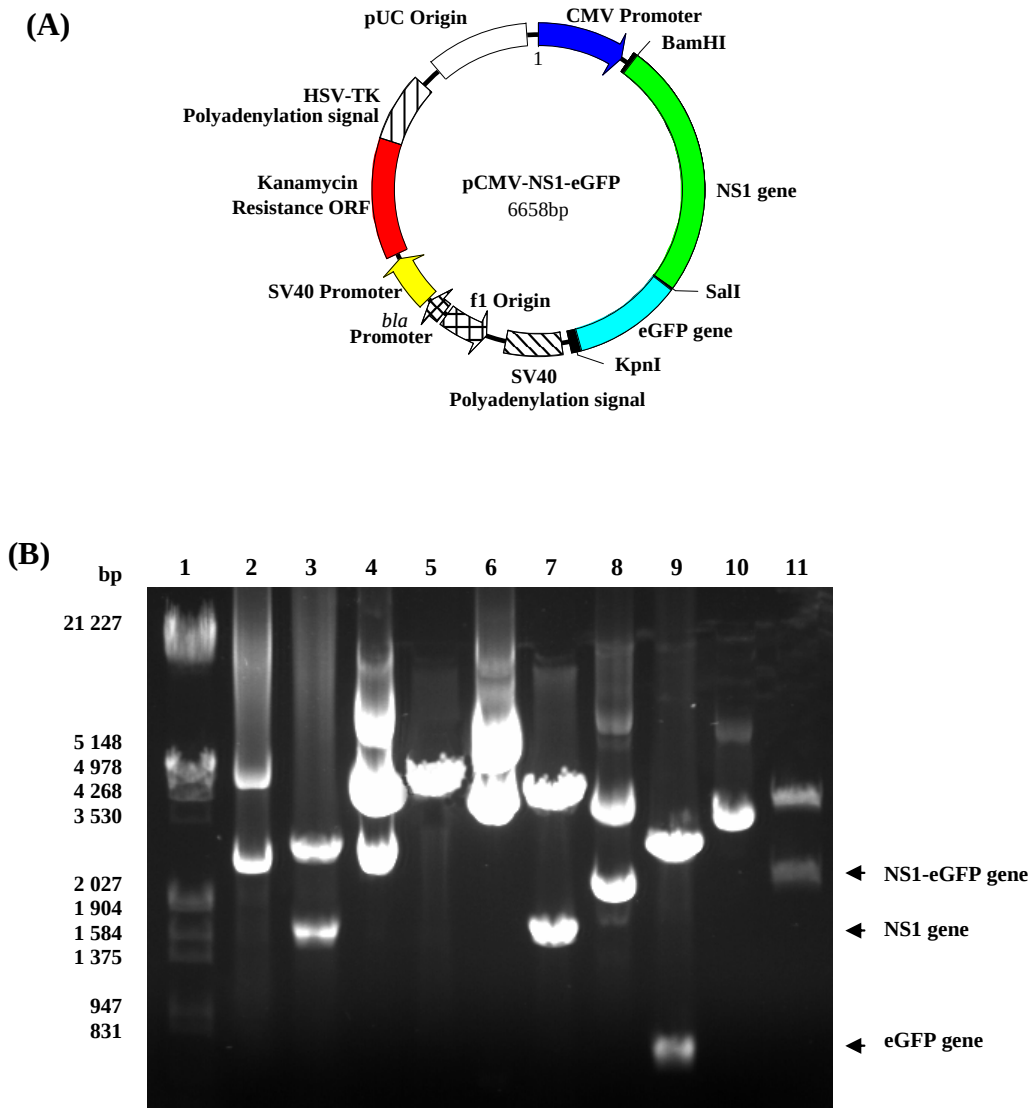

Fig. 2.5 Schematic diagram of the recombinant pCMV-NS1-eGFP construct (A) and agarose gel electrophoretic analysis of the recombinant pCMV-NS1-eGFP plasmids (B). Lanes: 1, DNA molecular weight marker; 2, uncut plasmid pGEM-NS1chm; 3, *Bam*HI- and *Sal*I-digested plasmid pGEM-NS1chm; 4, uncut parental pCMV-Script® vector; 5, *Bam*HI- and *Sal*I-digested parental pCMV-Script® vector; 6, uncut plasmid pCMV-NS1chm; 7, *Bam*HI- and *Sal*I-digested parental plasmid pCMV-NS1chm; 8, uncut pGEM-eGFPchm vector; 9, *Sal*I- and *Kpn*I-digested plasmid pGEM-eGFPchm; 10, uncut recombinant plasmid pCMV-NS1-eGFP; 11, *Bam*HI- and *Kpn*I-digested recombinant plasmid pCMV-NS1-eGFP. The sizes of the molecular weight marker, phage λ DNA digested with both *Eco*RI and H*ind*III, are indicated to the left of the figure.

lipofection. At 24 h post-transfection, the cell monolayers were examined by fluorescence microscopy. The results (Fig. 2.6) indicated that BHK-21 cells transfected with pCMV-eGFP and pCMV-NS1-eGFP fluoresced brightly. In contrast, no fluorescence was observed in the untransfected cells or cells transfected with the parental pCMV-Script® vector. To confirm expression of the eGFP and NS1-eGFP proteins, whole-cell lysates of the transfected cell monolayers were prepared and subjected to SDS-PAGE and Western blot analysis. However, analysis of the Coomassie blue-stained gel did not indicate the presence of uniquely expressed proteins in the lysates prepared from BHK-21 cells transfected with the recombinant expression vectors when compared to that of untransfected cells. Moreover, Western blot analysis performed with a polyclonal anti-eGFP antibody yielded several non-specific immuno-reactive protein bands (results not shown).

The inability to detect the expressed eGFP and NS1-eGFP proteins in the above assays may have been due to low levels of transient gene expression. Transient gene expression often results in low expression levels, since only a fraction of the plasmid DNA transfected into the cells is transported to the cell nucleus where transcription occurs (Yin *et al.*, 2007). Despite these results, the fluorescence observed in the transfected cells provides strong evidence for successful expression of the respective proteins in the BHK-21 cells. Moreover, the recombinant pCMV-Script® plasmids served as sources for the construction of recombinant baculoviruses, which were subsequently shown by Western blot analysis to express the eGFP and NS1-eGFP genes in *S. frugiperda* cells (Chapter 3, Fig. 3.7).

2.3.3 Silencing of eGFP and NS1-eGFP expression by eGFP-specific siRNA in BHK-21 cells

To evaluate the usefulness of the NS1-eGFP chimeric gene as a reporter whereby effective RNAi effector molecules can be identified, an siRNA directed against the eGFP reporter gene was selected for use. As a control, scrambled-siRNA that is non-homologous to the targeted gene, was included in the assay. In the RNAi assay, the pCMV-eGFP and pCMV-NS1-eGFP plasmids were co-transfected into BHK-21 cells with either the eGFP-specific siRNA or the control scrambled-siRNA, as described under the Materials and Methods (Section 2.2.11). The BHK-21 cell monolayers were analyzed at 24 h post-transfection by fluorescence microscopy and the eGFP fluorescence was quantified by fluorometry.

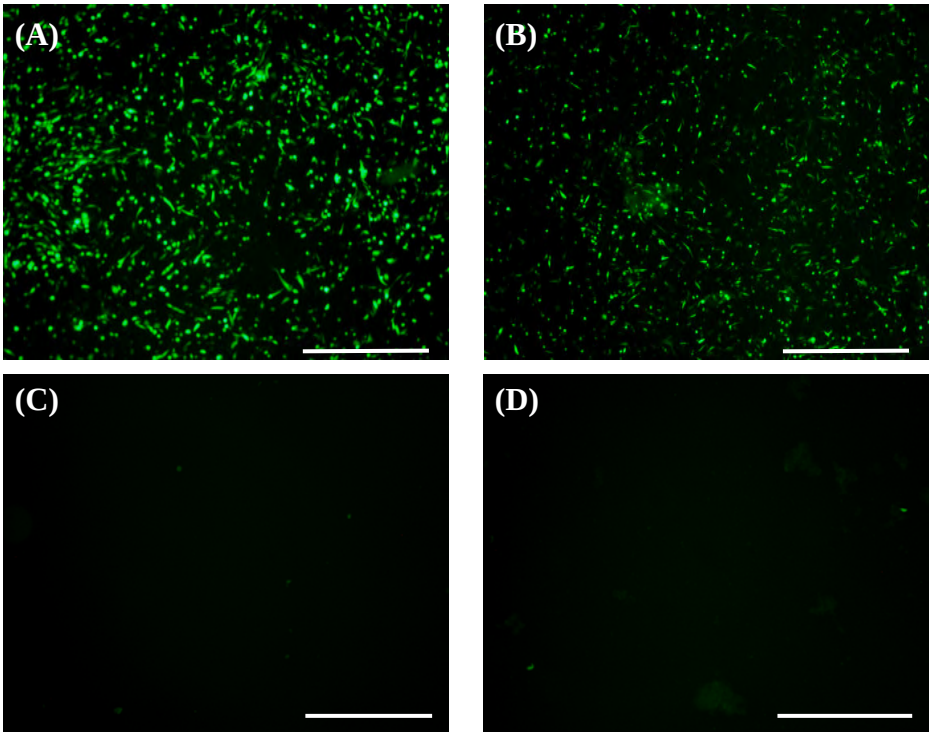

Fig. 2.6 Fluorescent micrographs of eGFP and NS1-eGFP proteins expressed in BHK-21 cells. BHK-21 cell monolayers were transfected with pCMV-eGFP (A) and pCMV-NS1-eGFP (B), and then analyzed for protein expression at 24 h post-transfection with a Zeiss Axiovert fluorescent microscope. Untransfected cells (C) and cells transfected with parental pCMV-Script vector DNA (D) were included as controls. Bar = 500 µm.

Examination of the BHK-21 cell monolayers by fluorescence microscopy (Fig. 2.7) indicated that in contrast to BHK-21 cells transfected with pCMV-eGFP or pCMV-NS1-eGFP, both of which fluoresced extensively, the fluorescence observed in cells co-transfected with these plasmids and eGFP-siRNA was diminished. Notably, eGFP and NS1-eGFP expression in cells co-transfected with control scrambled-siRNA was comparable to that observed in cells transfected with pCMV-eGFP and pCMV-NS1-eGFP, respectively. Quantitative analysis of eGFP expression by fluorometry (Fig. 2.8) indicated that the eGFP-siRNA inhibited eGFP expression by *ca*. 87%, while expression of NS1-eGFP was inhibited by *ca*. 55% in cells co-transfected with eGFP-siRNA. The results obtained in this section not only indicated that eGFP and NS1-eGFP expression could be suppressed by a gene-specific siRNA in BHK-21 cells, but also that the reporter system provided an easy gene knock-down readout that can be used to identify potentially effective RNAi effector molecules.

2.3 DISCUSSION

Numerous studies published in the last few years have demonstrated the effectiveness of chemically synthesized siRNA molecules to suppress gene expression in various types of mammalian cells (Elbashir *et al*., 2001b; Caplen *et al*., 2001; Dorsett and Tuschl, 2004; Kaykas and Moon, 2004). Although the molecular mechanisms underlying siRNA-mediated gene silencing is not completely understood, it is generally believed that siRNA induces degradation of target mRNA in a sequence-specific manner, leading to post-transcriptional silencing of gene expression. As such, siRNA-mediated gene silencing has emerged as a powerful genetic approach whereby gene function in mammalian cells can be analyzed (Arias *et al*., 2004; Forzan *et al*., 2007).

Experimental evidence has shown that only a limited number of siRNAs is capable of inducing highly effective target gene silencing in a sequence-specific manner (Khvorova *et al*., 2003; Reynolds *et al*., 2004). Moreover, the efficiency of siRNAs is dependent on the specificity of the target sequence within a gene and can only be determined experimentally based on the inhibition of the target gene expression. Since determination of the precise level of gene silencing for each siRNA is a demanding process, and the assays need to be adapted for each newly targeted gene, reporter-based assays have been developed to accelerate the identification of effective siRNAs (Wu *et al*., 2004; Werk *et al*., 2005; Stassen *et al*., 2007). In these systems, plasmids that carry the target gene fused to a reporter gene, are co-

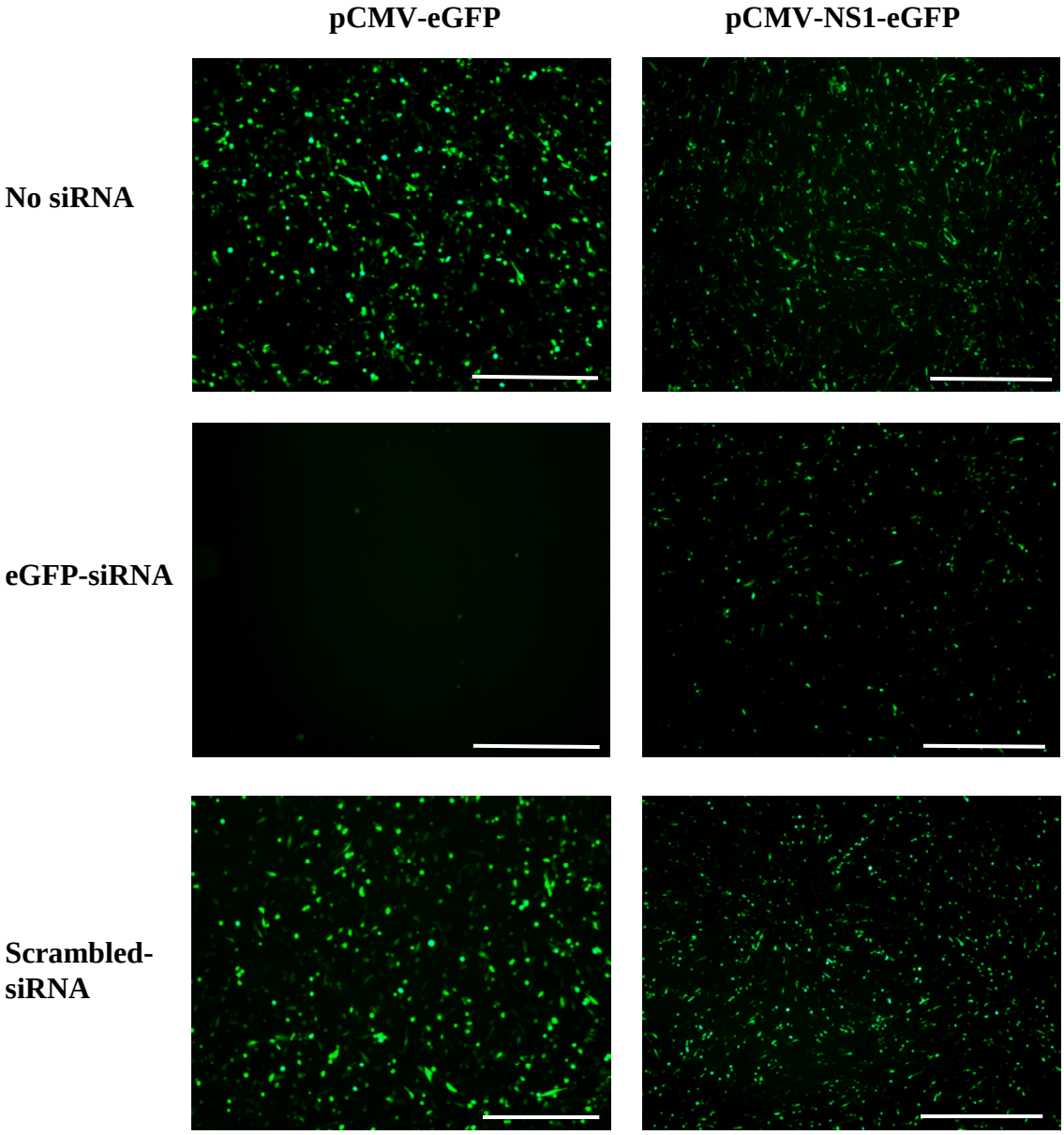

Fig. 2.7 Short interfering RNA (siRNA)-mediated suppression of eGFP and NS1-eGFP protein expression in BHK-21 cells. The BHK-21 cells were co-transfected with either pCMV-eGFP or pCMV-NS1-eGFP, together with the eGFP-specific siRNA (eGFP-siRNA) or control scrambled-siRNA. At 24 h post-transfection, the cells were examined with a Zeiss Axiovert fluorescent microscope and representative fields were photographed. Bar = 500 µm.

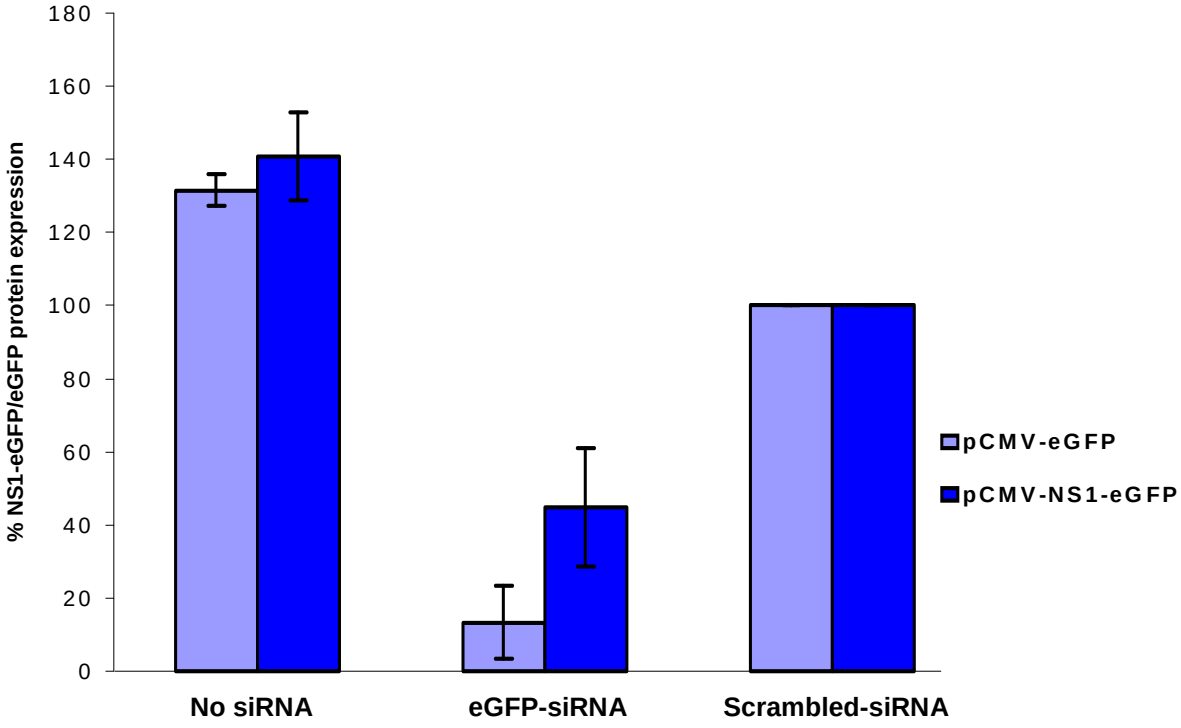

Fig. 2.8 Suppression of eGFP and NS1-eGFP expression by an eGFP-specific siRNA in BHK-21 cells. BHK-21 cells were co-transfected with either pCMV-eGFP or pCMV-NS1-eGFP, together with the eGFP-siRNA or scrambled siRNA. BHK-21 cells, co-transfected with either pCMV-eGFP or pCMV-NS1-eGFP and the scrambled siRNA, were used as control. At 24 h post-transfection, the cells were processed for analysis of eGFP reporter protein expression by fluorometry. The values are expressed as percentages of the value for cells transfected with the control scrambled-siRNA and represent the mean ± standard deviation (SD) from three independent experiments.

transfected into cells together with the target-specific siRNA. Consequently, in this part of the investigation, an AHSV-6 NS1-eGFP chimeric gene was constructed and the performance and accuracy of the reporter-based siRNA validation system were evaluated.

To investigate, recombinant pCMV-Script® mammalian expression vectors containing the NS1, eGFP and chimeric NS1-eGFP genes were constructed, and expression of the eGFP and NS1-eGFP proteins in transfected BHK-21 cells was evidenced by brightly fluorescing cells. Expression of these proteins could not be confirmed by Western blot analysis, possibly due to the low levels of expression associated with transient gene expression in mammalian cells. Transient gene expression involves gene expression from non-integrated plasmid DNA and because only a fraction of the DNA delivered to the cells is transported to the cell nucleus for transcription, expression levels may be similar or less than cellular expression levels (Yin *et al.*, 2007). Due to the strategy used to construct the NS1-eGFP chimeric gene, eGFP nevertheless proved to be a sensitive reporter for NS1-eGFP protein expression in transfected BHK-21 cells.

The performance and accuracy of the AHSV-6 NS1-eGFP reporter-based siRNA validation system was subsequently evaluated using a well characterized RNAi targeting sequence, eGFP-siRNA. Previous studies have shown that eGFP-siRNA exhibited a potent silencing effect on eGFP protein expression (90%) (Caplen *et al.*, 2001). Following co-transfection of BHK-21 cells with the recombinant pCMV-Script® mammalian expression vectors and eGFP-siRNA, analysis of the results indicated that eGFP and NS1-eGFP protein expression was suppressed by 87% and 55%, respectively. The high inhibition effect on eGFP expression is in agreement with the high level of eGFP protein inhibition reported previously in mouse fibroplasts, HeLa and HEK-293 cell cultures (Caplen *et al.*, 2001). The difference in eGFP-siRNA-mediated silencing of eGFP and NS1-eGFP protein suggests that the secondary structure of the target site may play a role in determining silencing efficiency. It can be hypothesized that the siRNA may have been less effective because of changes in the secondary structures normally formed in the full-length eGFP transcripts compared to those formed in the NS1-eGFP chimeric transcripts. This is in agreement with several other studies that have suggested that the secondary structures of mRNA might interfere with the target site accessibility for the RNA-induced silencing complex (RISC) (Harborth *et al.*, 2003; Holen *et al.*, 2002; Kretschmer-Kazami Far and Sczakiel, 2003; Heale *et al.*, 2005).

In conclusion, in this part of the investigation, a quantitative reporter-based siRNA validation system was established, and it was also demonstrated that this system could reliably report the gene silencing efficiency of a given siRNA. The reporter-based system was subsequently used to screen for effective NS1-directed shRNAs, the details of which are provided in Chapter 4.

CHAPTER 3

EXPRESSION OF AHSV-6 NS1 AND NS1-eGFP PROTEINS IN THE BAC-TO-BAC™ BACULOVIRUS EXPRESSION SYSTEM

3.1 INTRODUCTION

In the previous Chapter it was reported that expression of an eGFP reporter gene and an AHSV-6 NS1-eGFP chimeric gene, by making use of the pCMV-Script® mammalian expression vector, yielded very low levels of heterologous protein expression in BHK-21 cells that could not be detected by Western blot analysis. Thus, to allow for characterization of the NS1-eGFP chimeric protein prior to its use in the si/shRNA-mediated gene silencing assays, both the eGFP and NS1-eGFP proteins were expressed by making use of the baculovirus expression system. This expression system has been frequently used for the expression of biologically active heterologous proteins in *Spodoptera frugiperda* insect cells (O'Reilly *et al*., 1992; Possee, 1997).

The baculovirus expression system relies on *in vivo* recombination to replace a baculovirus allele, usually the dispensable polyhedrin or p10 genes of *Autographa californica* nuclear polyhedrosis virus (AcNPV), with a heterologous gene. The gene of interest is cloned into an appropriate transfer vector that contains flanking viral sequences to provide the homologous sequences for recombination (O'Reilly *et al*., 1992; Ciccarone *et al*., 1997). However, the percentage of recombinant viruses obtained by this approach has been reported to constitute 0.1 to 1% of the progeny viruses (Kitts *et al*., 1990; Kitts and Possee, 1993) and multiple rounds of plaque purification are required to obtain pure stocks of the recombinant virus (O'Reilly *et al*., 1992). In an alternative approach whereby recombinant baculoviruses can be generated rapidly and efficiently, recombinant baculovirus shuttle vectors (bacmids) are engineered in *E. coli* by site-specific transposition of the expression cassette from a donor plasmid, which contains the gene of interest and baculovirus promoter (Luckow *et al*., 1993). The mini-Tn7 element of the donor plasmid transposes to the mini-*att*Tn7 attachment site on the bacmid DNA when the Tn7 transposition functions are provided *in trans* by a helper plasmid (Luckow *et al*., 1993). Using this approach, there is no need to isolate a single recombinant by plaque assays, since recombinant bacmids are selected for in *E. coli*. As a result, recombinant viral DNA is transfected into the insect cells thereby allowing for stocks of the recombinant baculovirus to be obtained within seven to ten days (Luckow *et al*., 1993).

The expression of individual AHSV proteins in *S. frugiperda* cells by appropriately constructed baculovirus recombinants has made significant contributions to understanding the structure-function relationships of several viral proteins, including the nonstructural proteins

NS1 (Maree and Huismans, 1997), NS2 (Uitenweerde *et al.*, 1995) and NS3 (Van Staden *et al.*, 1998; Van Niekerk *et al.*, 2001), as well as the structural proteins VP2 (Bentley *et al.*, 2000), VP6 (De Waal and Huismans, 2005) and VP7 (Basak *et al.*, 1996). Moreover, co-expression of AHSV VP3 and VP7 in insect cells by means of recombinant baculoviruses has been reported to result in their spontaneous intracellular assembly into core-like particles (CLPs) that structurally resemble authentic AHSV core particles (Maree *et al.*, 1998). In addition, the baculovirus expression system has also been used for the synthesis of BTV virus-like particles (VLPs), which were formed by co-expression of the outer capsid proteins VP2 and VP5 along with the core proteins VP3 and VP7. Due to the presence of many essential epitopes, the VLPs were reported to induce broad and strong immune responses and have thus received attention as potential vaccine candidates (Roy *et al.*, 1992; Roy *et al.*, 1993; Roy and Sutton, 1998). More recently, the ability to co-express different viral genes using baculovirus recombinants has been exploited to facilitate investigations regarding the BTV assembly process, as well as the minimal requirements for inner and outer capsid assembly (Nason *et al.*, 2004; Kar *et al.*, 2004; 2005).

Based on the successful expression of different AHSV proteins in the baculovirus/insect cell expression system and the fact that the AHSV-6 NS1 and chimeric NS1-eGFP proteins were expressed poorly in BHK-21 cells (Chapter 2), the aim of this part of the investigation was to express the AHSV-6 NS1 and NS1-eGFP proteins in *S. frugiperda* cells using the Bac-to-Bac™ baculovirus system. The expressed proteins were subsequently characterized immunologically and by electron microscopy to ensure the integrity of the expressed recombinant proteins.

3.2 MATERIALS AND METHODS

3.2.1 Bacterial strains and plasmids

The *E. coli* strains were routinely cultured at 37°C with shaking at 200 rpm in LB broth (1% [w/v] tryptone, 1% [w/v] NaCl, 0.5% [w/v] yeast extract; pH 7.4) (Sambrook *et al.*, 1989), and maintained at 4°C on LB agar or at -70°C as glycerol cultures. For plasmid selection and maintenance in *E. coli*, the following concentrations of antibiotics were used: 100 µg/ml for ampicillin, 12 µg/ml for tetracycline, 50 µg/ml for kanamycin and 7 µg/ml for gentamicin. All antibiotics were obtained from Roche Diagnostics. Recombinant pCMV-Script® mammalian expression vectors harboring an AHSV-6 NS1 gene and NS1-eGFP chimeric gene,

respectively, had been constructed previously (Chapter 2) and were used as sources for donor plasmid construction. The pFastBac1™ bacmid donor plasmid was obtained from Invitrogen.

3.2.2 Cells and viruses

A baculovirus recombinant expressing eGFP, designated Bac-eGFP, was obtained from L. Stassen, Department of Microbiology and Plant Pathology, University of Pretoria. Cells and viruses were propagated according to the procedures described by Summers and Smith (1987). *Spodoptera frugiperda* (Sf-9) insect cells were propagated as monolayer or as suspension cultures at 27°C in Grace's insect medium (Highveld Biological) supplemented with 10% (v/v) foetal calf serum (FCS) and antibiotics (0.12 mg/ml penicillin G, 0.12 mg/ml streptomycin sulphate, 0.0325 µg/ml Fungizone) (Highveld Biological). The cell density was determined using a haemocytometer, while the viability of the cells was determined by staining the cells with trypan blue.

3.2.3 Construction of recombinant pFastBac1™ donor plasmids

All molecular cloning techniques employed in the construction of the bacmid donor plasmids were performed according to the procedures described in Chapter 2 (Sections 2.2.4-2.2.7). The recombinant plasmid constructs were verified by restriction endonuclease digestion and by nucleotide sequencing. The cloning strategies employed in the construction of the respective recombinant plasmids are depicted in Figs. 3.1 and 3.2.

- **pFB-NS1**

To construct the recombinant bacmid donor plasmid pFB-NS1, the *ca.* 1.7-kb AHSV-6 NS1 gene was excised from plasmid pCMV-NS1 by digestion with *Bam*HI, and then cloned into *Bam*HI-digested pFastBac1™. The transcriptional orientation of the cloned NS1 gene relative to the polyhedrin promoter was confirmed by restriction mapping with *Hind*III.

- **pFB-NS1-eGFP**

To construct the recombinant bacmid donor plasmid pFB-NS1-eGFP, the *ca.* 2.4-kb NS1-eGFP chimeric gene was recovered from plasmid pCMV-NS1-eGFP by digestion with both *Bam*HI and *Kpn*I, and then cloned directionally into pFastBac1™ that had been prepared in an identical manner.

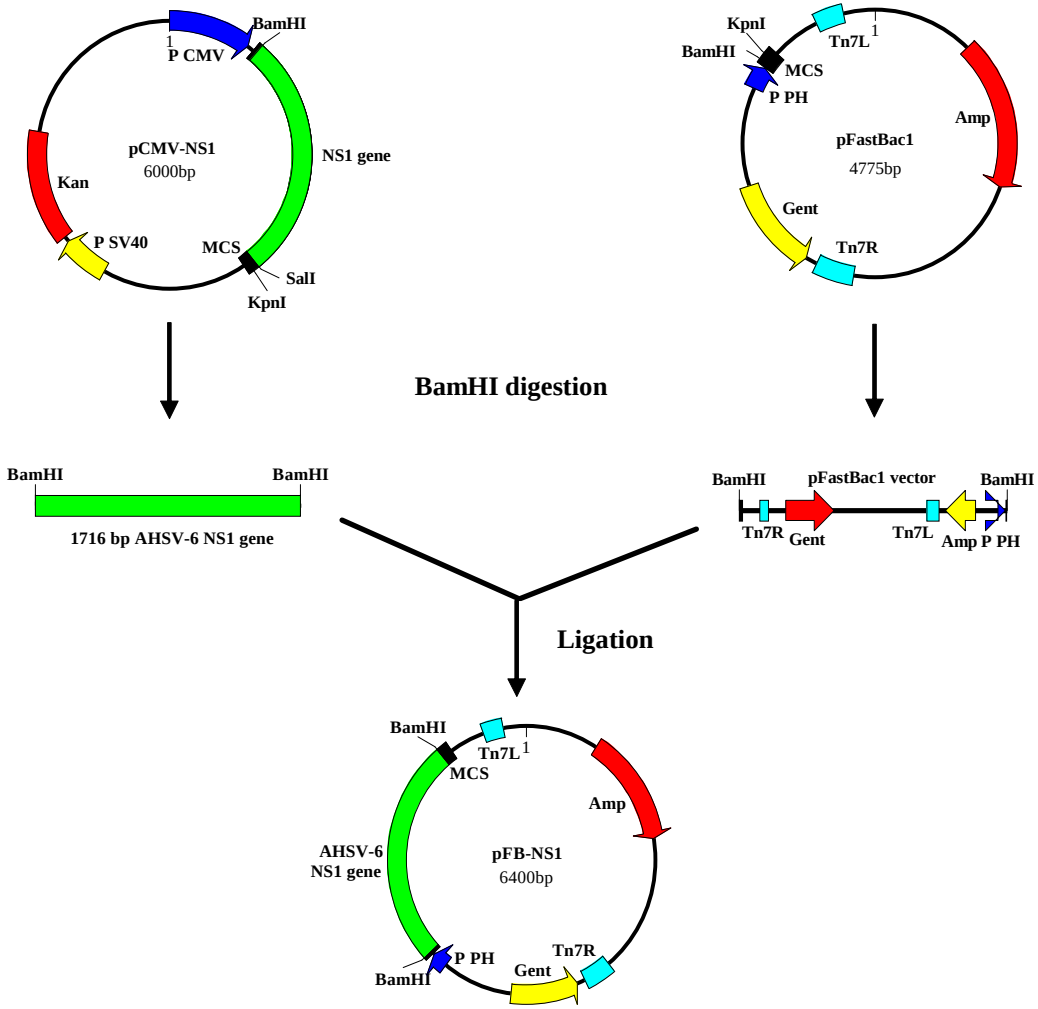

Fig. 3.1 Schematic diagram indicating the cloning strategy for cloning of the AHSV-6 NS1 gene into the pFastBac1™ donor plasmid. Abbreviations: **P CMV**, CMV promoter; **Kan**, kanamycin resistance gene; **P SV40**, SV40 promoter; **MCS**, multiple cloning site; **Tn7L** and **Tn7R**, mini-Tn7 elements for site-specific transposition; **P PH**, polyhedrin promoter; **Amp,** ampicillin resistance gene; **Gent**, gentamicin resistance gene.

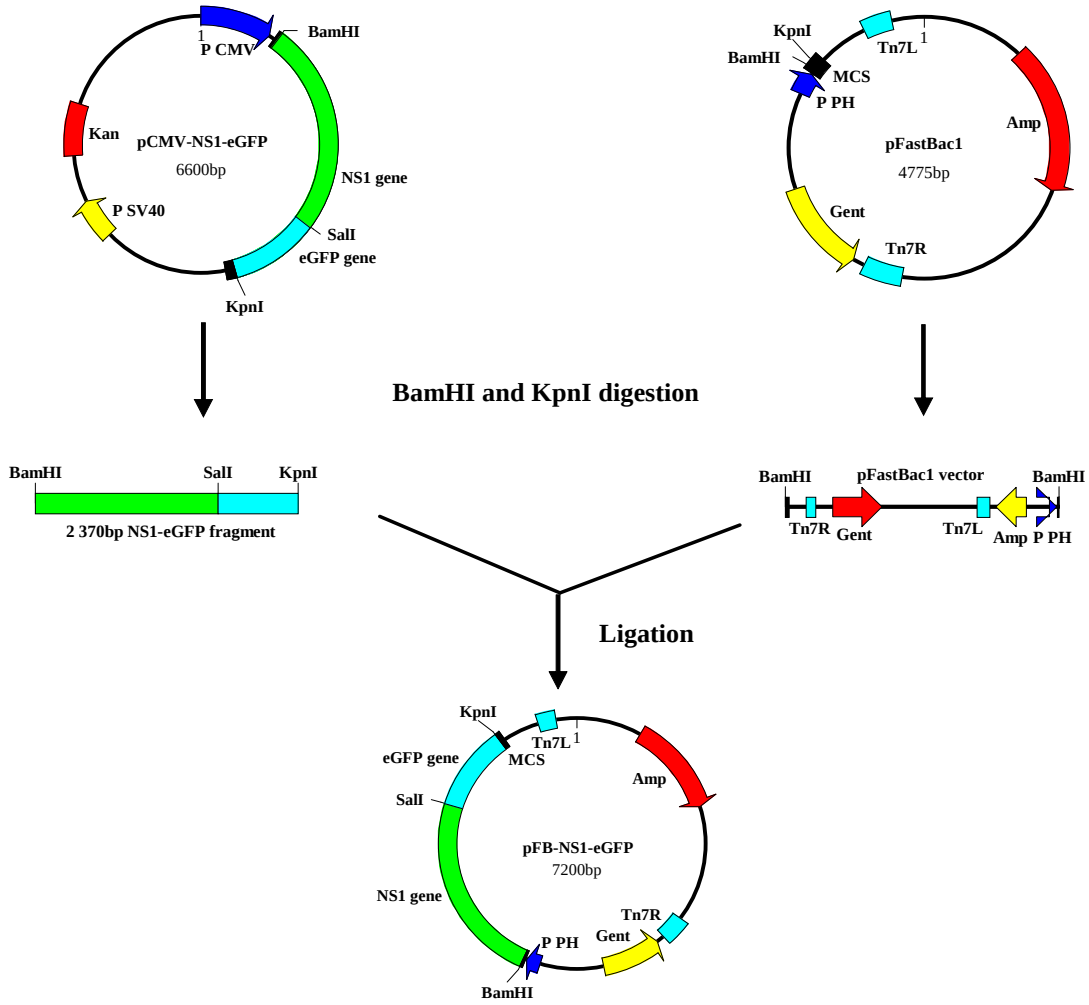

Fig. 3.2 Schematic diagram indicating the cloning strategy for cloning of the NS1-eGFP chimeric gene into the pFastBac1™ donor plasmid. Abbreviations: **P CMV**, CMV promoter; **Kan**, kanamycin resistance gene; **P SV40**, SV40 promoter; **MCS**, multiple cloning site; **Tn7L** and **Tn7R**, mini-Tn7 elements for site-specific transposition; **P PH**, polyhedrin promoter; **Amp**, ampicillin resistance gene; **Gent**, gentamicin resistance gene.

3.2.4 Construction and characterization of recombinant bacmids

3.2.4.1 Preparation and transformation of competent *E. coli* DH10Bac™ cells

Competent *E. coli* DH10Bac™ cells (Invitrogen), containing the bacmid genome and helper plasmid, were prepared as described previously (Chapter 2, Section 2.2.6.2), except that an overnight culture was prepared by inoculating a single colony of a freshly streaked *E. coli* DH10Bac™ culture into 1 ml of LB broth supplemented with antibiotics (12.5 µg/ml tetracycline, 50 µg/ml kanamycin). For transformation, 100 ng of the recombinant bacmid donor plasmid DNA was added to 100 µl of competent *E. coli* DH10Bac™ cells and incubated on ice for 30 min. After a heat shock at 42ºC for 45 s, the cells were cooled on ice for 2 min. Subsequently, 900 µl of pre-warmed SOC broth (2% [w/v] tryptone, 0.5% [w/v] yeast extract, 10 mM NaCl, 2.5 mM KCl, 10 mM $MgCl_2$, 20 mM glucose; pH 7) was added and the cells were incubated at 37ºC for 4 h to allow the cells to recover, to express the antibiotic resistance genes and to allow for transposition to occur. Aliquots (200 µl) of the transformation mixture were plated onto LB agar supplemented with antibiotics (50 µg/ml kanamycin, 12.5 µg/ml tetracycline, 7 µg/ml gentamycin) in the presence of 10 µl of 100 mM IPTG and 50 µl of 2% (w/v) X-gal. The agar plates were incubated at 37°C for at least 24 h. Transformants displaying a white colony phenotype were selected and restreaked onto fresh agar medium, as above, to verify the phenotype. A positive control (10 ng of pUC18 plasmid DNA) and negative control (competent cells only) were included to determine the competency of the *E. coli* DH10Bac™ cells and to test for contamination, respectively.

3.2.4.2 Extraction of recombinant bacmid DNA

The high-molecular-weight recombinant bacmid DNA was isolated by the rapid alkaline lysis method modified for the isolation of large plasmid DNA (Invitrogen). Colonies confirmed as having a white phenotype were inoculated into 20 ml of LB broth containing antibiotics (50 µg/ml kanamycin, 12.5 µg/ml tetracycline, 7 µg/ml gentamycin) and cultured overnight at 37ºC. The cells from 1 ml of each culture were collected by centrifugation at 15 000 rpm for 1 min. The supernatant was decanted and the cell pellet suspended in 300 µl of ice-cold Solution I (15 mM Tris-HCl [pH 8.0], 10 mM EDTA, 100 µg/ml RNase A), followed by the addition of 300 µl of Solution II (0.2 N NaOH, 1% SDS). After incubation at room temperature for 5 min, 300 µl of Solution III (3 M KOAc; pH 5.5) was added and the tubes were incubated on ice for 10 min. The proteins and *E. coli* genomic DNA were removed by centrifugation at 15 000 rpm for 10 min. The bacmid DNA was precipitated from the

recovered supernatants by the addition of 800 µl of isopropanol and then incubated on ice for 10 min. The precipitated bacmid DNA was collected by centrifugation at 15 000 rpm for 15 min, rinsed with 70% ethanol and air-dried for 10 min at room temperature prior to suspension in 40 µl of 1 × TE buffer. An aliquot of the bacmid DNA was analyzed by electrophoresis on a 0.5% (w/v) agarose gel at 70 V for 45 min in 1 × TAE buffer.

3.2.4.3 Analysis of recombinant bacmid DNA

To confirm successful transposition of the NS1 and chimeric NS1-eGFP genes into the bacmid DNA, PCR analysis of the extracted bacmid DNA was performed. For this purpose, the universal pUC/M13 forward (5'-GTTTTCCCAGTCACGAC-3') and reverse (5'-CAGGAAACAGCTATGAC-3') oligonucleotides were used, which anneal at sites flanking the mini-*att*Tn7 site. Each of the PCR reaction mixtures (100 µl) contained 50 ng of bacmid DNA as template, 25 pmol of each the forward and reverse oligonucleotides, 1 × PCR buffer (75 mM Tris-HCl [pH 8.8], 16 mM $(NH_4)_2SO_4$, 0.1% [v/v] Tween-20), 1.5 mM $MgCl_2$, 250 µM of each deoxynucleotide triphosphate (dNTP) and 0.25 U of *Taq* DNA polymerase (Southern Cross Biotechnology). Reaction mixtures from which template DNA was omitted were also included for control purposes. The PCR was performed in a GeneAmp® 2700 thermal cycler (Applied Biosystems). Following an initial denaturation at 94°C for 3 min, the reaction mixtures were subjected to 30 cycles of denaturation at 94°C for 1 min, annealing at 55°C for 1 min and extension at 72°C for 5 min. Aliquots of the reaction mixtures were analyzed on a 0.8% (w/v) agarose gel in the presence of an appropriate DNA molecular weight marker.

3.2.5 Transfection of *S. frugiperda* cells

The recombinant bacmid DNA was transfected into *S. frugiperda* cells with Cellfectin™ transfection reagent (Invitrogen) according to the manufacturer's instructions. The cells were seeded in 35-mm-diameter wells (9×10^5 cells/well) in 2 ml of Grace's medium supplemented with serum and antibiotics, and allowed to attach at room temperature for 1 h. For each transfection, the Cellfectin™ reagent (6 µl) and bacmid DNA (1 µg) was diluted separately in 100 µ1 of Grace's medium lacking serum and antibiotics. The two solutions were then combined, mixed gently and incubated at room temperature for 30 min before addition of 800 µ1 of Grace's medium (lacking serum and antibiotics). Meanwhile, the attached *S. frugiperda* cells were washed twice with 2 ml of Grace's medium (lacking serum

and antibiotics) before being overlayed with 1 ml of the diluted DNA-lipid complexes. Following incubation at 27℃ for 5 h, the transfection mixtures were removed and replaced with 2 ml of Grace's medium supplemented with 10% (v/v) FCS and antibiotics. The tissue culture dishes were then incubated at 27℃ for 72 h. The baculovirus-containing supernatants were subsequently removed, centrifuged at 3 000 rpm for 4 min, filter-sterilized and stored at 4°C. Mock-transfected cells and cells transfected with wild-type bacmid DNA were included as controls whereby infection of the cells could be monitored.

3.2.6 Analyses of recombinant baculovirus-expressed proteins

S. frugiperda cells were seeded in 35-mm-diameter wells (9×10^5 cells/well) and subsequently infected with recombinant or wild-type baculoviruses using 250 µl of the prepared virus stocks. For control purposes, mock-infected cells were included in the analyses. The cell monolayers were incubated at 27°C for 72 h and then observed for expression of the eGFP reporter protein on a Zeiss Axiovert 200 fluorescent microscope fitted with the no. 10 Zeiss filter set (excitation at 450-490 mm; emission at 515-565 nm). The images were captured with a Nikon DXM 1200 digital camera. Subsequently, the cells were harvested from the surfaces of the wells by pipeting and the cell lysates were subjected to SDS-PAGE and Western blot analyses as described previously (Chapter 2, Sections 2.2.10.2 and 2.2.10.3).

3.2.7 Characterization of baculovirus-expressed AHSV NS1 and NS1-eGFP proteins

3.2.7.1 Purification of recombinant proteins

Monolayers of *S. frugiperda* cells (1×10^7 cells/75 cm^2 flask) were infected with recombinant baculoviruses expressing either the AHSV-6 NS1 or chimeric NS1-eGFP genes and incubated at 27°C for 72 h. The cells were harvested, collected by centrifugation at 3 000 rpm for 10 min and washed once with 10 ml of 1 × PBS. The cell pellets were each suspended in 1 ml of 1 × PBS, homogenized by 30 strokes with a Dounce homogenizer and centrifuged at 1 000 rpm for 3 min. Aliquots (500 µ1) of the cytoplasmic extracts were loaded onto a 50-70% linear sucrose gradient, prepared in 1 × PBS (Maree and Huismans, 1997). The gradients were centrifuged at 40 000 rpm for 3 h at 4°C in a Beckman SW55Ti rotor using a Sorvall® UltraPro80 centrifuge (Du Pont Instruments). Twelve fractions of 20 drops each (*ca*. 400 µl/fraction) were collected drop-wise from the bottom of the gradients. The remaining pellets were suspended in 15 µl of 1 × PBS. The proteins from each fraction were recovered by

diluting 200 µ1 of each fraction with 1.2 ml of 1 × PBS, followed by centrifugation at 5 000 rpm for 45 min at 4°C. The protein pellets were suspended in 15 µ1 of 1 × PBS and analyzed by SDS-PAGE.

3.2.7.2 Transmission electron microscopy

Sucrose gradient-purified protein samples containing the AHSV-6 NS1 or NS1-eGFP proteins were adsorbed onto carbon-coated grids for 1 min, and washed with 10 to 20 drops of 1 × PBS and sterile SABAX water, respectively. The samples were stained negatively with 2% (w/v) uranyl acetate for 30 s, after which the stained grids were rinsed as described above. The samples were viewed on a Phillips 301 transmission electron microscope.

3.3 RESULTS

3.3.1 Construction of recombinant bacmid donor plasmids containing the AHSV-6 NS1 and chimeric NS1-eGFP genes

To enable cloning of the AHSV-6 NS1 gene into the bacmid donor plasmid pFastBac1™, both the recombinant pCMV-NS1 plasmid and pFastBac1™ vector was digested with *Bam*HI. The excised NS1 gene and linearized vector DNA were purified from an agarose gel and ligated overnight. Similarly, the NS1-eGFP chimeric gene was excised from recombinant plasmid pCMV-NS1-eGFP by digestion with both *Bam*HI and *Kpn*I and then ligated into identically prepared pFastBac1™ vector DNA. Following transformation of competent *E. coli* DH5α cells, ampicillin-resistant transformants were cultured overnight and the extracted plasmid DNA was analyzed by agarose gel electrophoresis. Plasmid DNA migrating slower than the parental pFastBac1™ vector DNA on agarose gels were selected and analyzed for the presence of cloned insert DNA. Recombinant plasmids from which either a 1.7-kb NS1-specific (Fig. 3.3B, lane 7) or 2.4-kb NS1-eGFP-specific (Fig. 3.4B, lane 7) insert DNA was excised, were selected for further use and designated pFB-NS1 and pFB-NS1-eGFP, respectively. Moreover, the transcriptional orientation of the cloned NS1 gene in pFB-NS1 was confirmed by restriction enzyme mapping with *Hind*III, which cuts *ca*. 500 nt from the 5'-end of the NS1 gene and once in the multiple cloning site of the vector (Fig. 3.3B, lane 8).

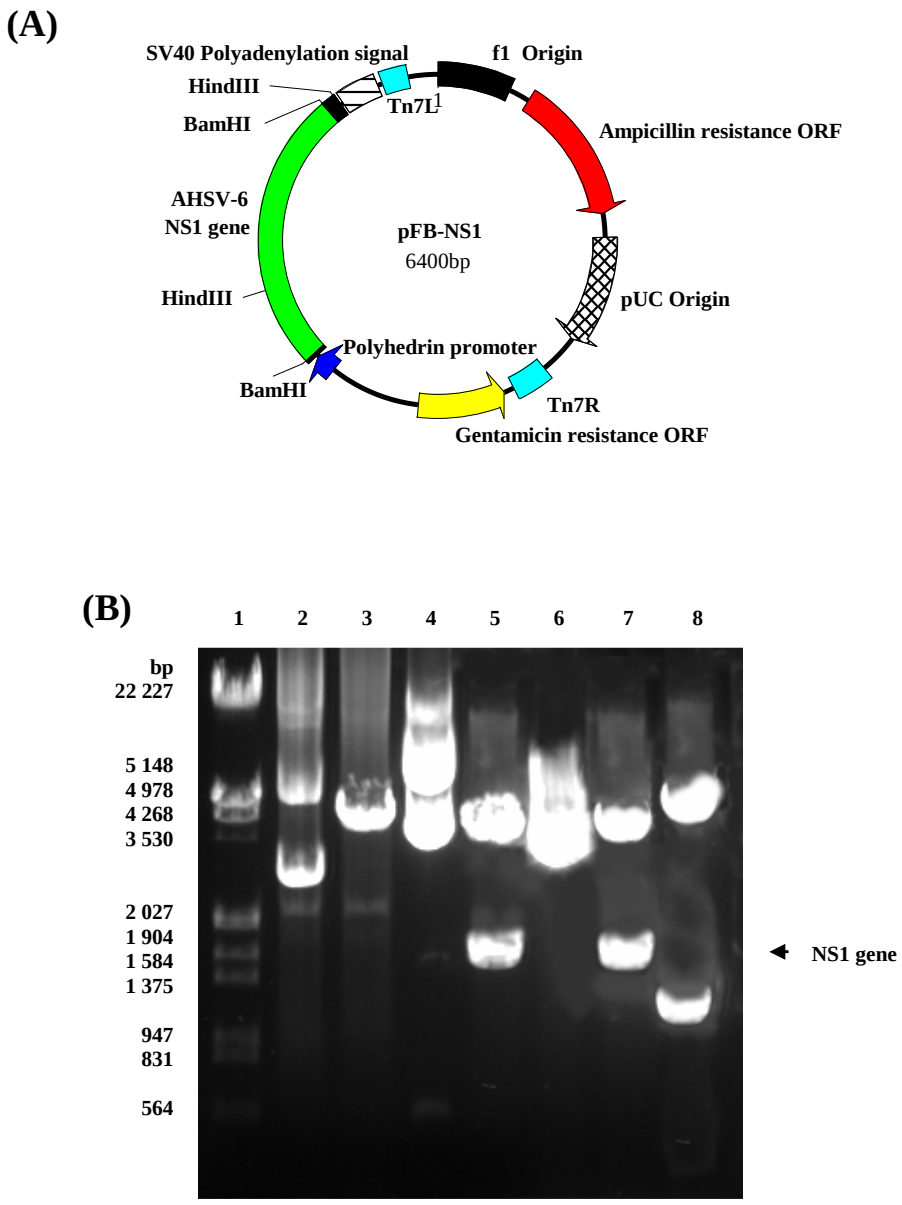

Fig. 3.3 Schematic diagram of the recombinant pFB-NS1 construct (A) and agarose gel electrophoretic analysis of the recombinant plasmid pFB-NS1 (B). Lanes: 1, DNA molecular weight marker; 2, uncut parental pFastBac1™ vector; 3, *Bam*HI-digested parental pFastBac1™ vector; 4, uncut recombinant plasmid pCMV-NS1; 5, *Bam*HI-digested recombinant plasmid pCMV-NS1; 6, uncut recombinant plasmid pFB-NS1; 7, *Bam*HI-digested recombinant plasmid pFB-NS1; 8, *Hind*III-digested recombinant plasmid pFB-NS1. The sizes of the molecular weight marker, phage λ DNA digested with both *Eco*RI and *Hind*III, are indicated to the left of the figure.

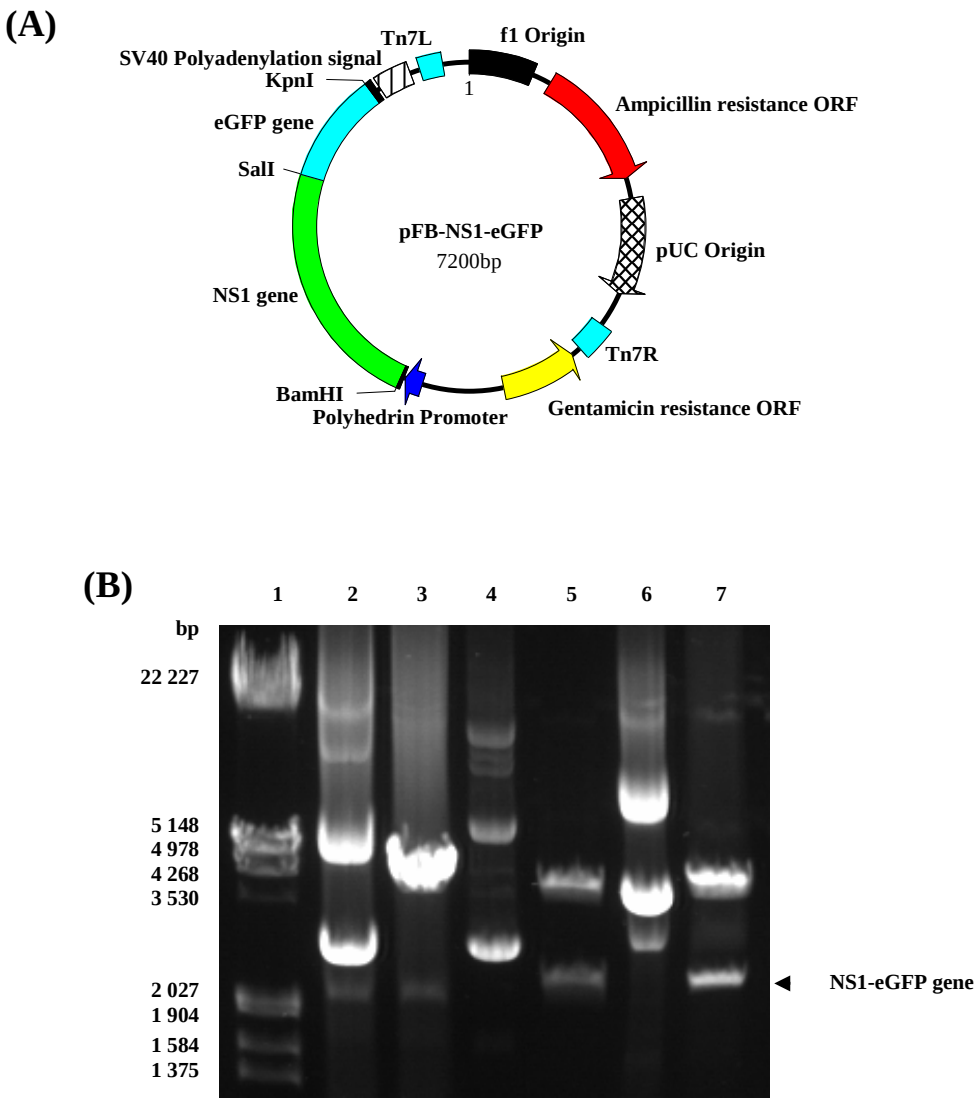

Fig. 3.4 Schematic diagram of the recombinant pFB-NS1-eGFP construct (A) and agarose gel electrophoretic analysis of the recombinant plasmid pFB-NS1-eGFP (B). Lanes: 1, DNA molecular weight marker; 2, uncut parental pFastBac1™ vector; 3, *Bam*HI- and *Kpn*I-digested parental pFastBac1™ vector; 4, uncut recombinant plasmid pCMV-NS1-eGFP; 5, *Bam*HI- and *Kpn*I-digested recombinant plasmid pCMV-NS1-eGFP; 6, uncut recombinant plasmid pFB-NS1-eGFP; 7, *Bam*HI- and *Kpn*I-digested recombinant plasmid pFB-NS1-eGFP. The sizes of the molecular weight marker, phage λ DNA digested with both *Eco*RI and *Hind*III, are indicated to the left of the figure.

3.3.2 Engineering of recombinant bacmids

Bacmid DNA contained in *E. coli* DH10Bac™ cells replicates as a large plasmid and confers resistance to kanamycin, as well as complements a *lacZ* deletion present on the *E. coli* genome to form colonies that are blue in the presence of X-gal and the inducer IPTG. During site-specific transposition of the recombinant donor plasmid, the mini-Tn7 cassette is inserted from the donor plasmid into the mini-*att*Tn7 attachment site on the bacmid DNA, thereby disrupting expression of the *lac*Zα peptide from the bacmid genome. Thus, colonies containing the recombinant bacmid display a white colony-phenotype that can be readily distinguished from blue colonies that harbour the unaltered bacmid DNA. The transposition functions are provided *in trans* by helper plasmid pMON1724 that encodes the transposase and confers resistance to tetracycline (Luckow *et al*., 1993).

To engineer recombinant bacmid DNA, competent *E. coli* DH10Bac™ cells were thus transformed with the recombinant donor plasmids pFB-NS1 and pFB-NS1-eGFP, and selected by plating the transformed cells onto a selective medium. The high-molecular-weight recombinant bacmid DNA was extracted from selected transformants and used as template DNA in PCR assays to confirm successful transposition of the respective genes into the bacmid DNA. The oligonucleotides used in these assays were the universal pUC/M13 forward and reverse oligonucleotides, which anneal to sequences flanking the mini-*att*Tn7 attachment site within the *lac*Zα gene of the bacmid DNA.

By making use of recombinant bacmid DNA transposed with either the pFB-NS1 or pFB-NS1-eGFP donor plasmid as templates for PCR, bands of *ca*. 4 kb and 4.7 kb were obtained, respectively (Fig. 3.5, lanes 4 and 5, respectively). These corresponded with the size of the NS1 gene (*ca*. 1.7 kb) or NS1-eGFP chimeric gene (*ca*. 2.4 kb), together with the size of the mini-Tn7 cassette (*ca*. 2 kb) and bacmid DNA flanking the mini-*att*Tn7 site (*ca*. 300 bp). In contrast, when wild-type bacmid DNA was used as template in the PCR reaction, an amplicon of *ca*. 300 bp was observed (Fig. 3.5, lane 3). No amplicons were observed in a control reaction from which template DNA was omitted. The recombinant bacmids were selected, designated Bac-NS1 and Bac-NS1-eGFP, respectively, and used in all subsequent experiments.

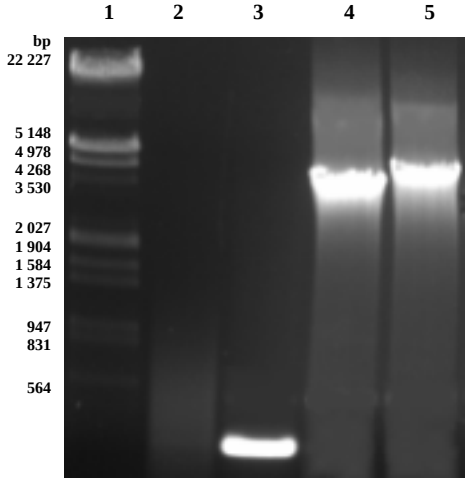

Fig. 3.5 Agarose gel electrophoretic analysis of the amplicons obtained, following PCR analysis using the universal pUC/M13 forward and reverse oligonucleotides, to verify the presence of the AHSV-6 NS1 and chimeric NS1-eGFP genes in recombinant bacmid DNA. Lanes: 1, DNA molecular weight marker; 2, control PCR reaction mixture in which template DNA was omitted; 3, amplicon obtained using wild-type bacmid DNA as template; 4, amplicon obtained using Bac-NS1 DNA as template; 5, amplicon obtained using Bac-NS1-eGFP as template. The sizes of the molecular weight marker, phage λ DNA digested with both *Eco*RI and *Hind*III, are indicated to the left of the figure.

3.3.3 Analyses of proteins synthesized in infected *S. frugiperda* cells

The recombinant bacmid DNA was isolated from *E. coli* DH10Bac™ cultures, transfected into *S. frugiperda* cells and the recombinant progeny viruses were then subjected to amplification in monolayer cultures. To investigate whether the eGFP, AHSV-6 NS1 and NS1-eGFP proteins were expressed in recombinant baculovirus-infected cells, monolayers of *S. frugiperda* cells were mock-infected and infected with either the wild-type or different baculovirus recombinants. Following incubation, the monolayers were examined by fluorescence microscopy, and whole-cell lysates were prepared and analyzed by SDS-PAGE and Western blot analysis. In addition, cytoplasmic extracts prepared from recombinant baculovirus-infected *S. frugiperda* cells were subjected to sucrose gradient centrifugation and the purified protein samples were analyzed by transmission electron microscopy (TEM).

3.3.3.1 Fluorescence microscopy of cell monolayers

Examination of the mock-infected and baculovirus-infected *S. frugiperda* cell monolayers by fluorescence microscopy (Fig. 3.6) indicated that cells infected with the Bac-eGFP and Bac-NS1-eGFP recombinants fluoresced brightly. As expected, no fluorescence was observed in control mock-infected cells or in cells infected with either the wild-type baculovirus or Bac-NS1 recombinant baculovirus. Since no background or autofluorescence were observed in these cell monolayers, it was therefore concluded that the fluorescence observed in cells infected with Bac-eGFP and Bac-NS1-eGFP was due to successful expression of the eGFP and NS1-eGFP proteins.

3.3.3.2 SDS-PAGE and Western blot analysis

Analysis of the Coomassie blue-stained gel (Fig. 3.7A) indicated the presence of different expressed proteins in the cell lysates prepared from *S. frugiperda* cells infected with the Bac-eGFP (lane 4), Bac-NS1-eGFP (lane 5) and Bac-NS1 (lane 6) baculovirus recombinants. The molecular mass of these proteins corresponded with the predicted molecular mass of the eGFP protein (27 kDa), the NS1-eGFP chimeric protein (90 kDa) and the NS1 protein of AHSV-6 (63 kDa). The identity of the expressed proteins was subsequently verified by subjecting an unstained SDS-polyacrylamide gel to Western blot analysis using a polyclonal anti-eGFP antibody (Fig. 3.7B). The anti-eGFP antibody reacted specifically with the 27-kDa eGFP protein and 90-kDa NS1-eGFP chimeric protein (lanes 4 and 5,

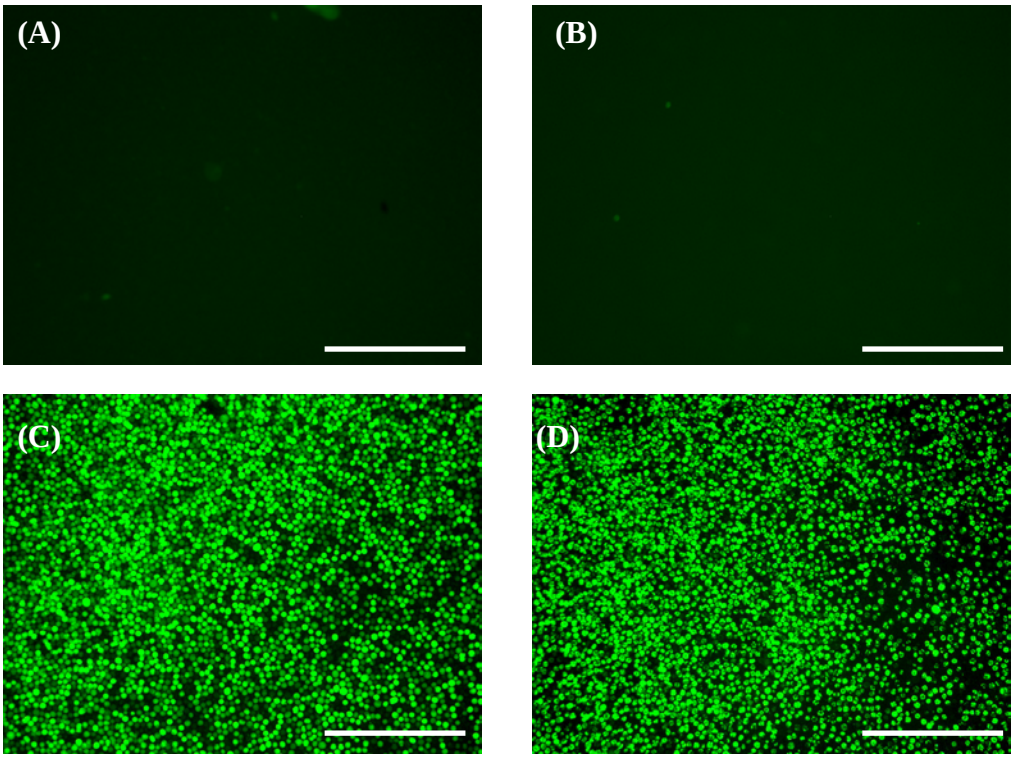

Fig. 3.6 Fluorescent micrographs of recombinant baculovirus-infected *S. frugiperda* cells. *S. frugiperda* cells were mock-infected (A) and infected with the wild-type baculovirus (B) or the recombinant baculoviruses Bac-eGFP (C) and Bac-NS1-eGFP (D). The cell monolayers were examined for recombinant protein expression at 24 h post-infection with a Zeiss Axiovert fluorescent microscope. Bar = 500 µm.

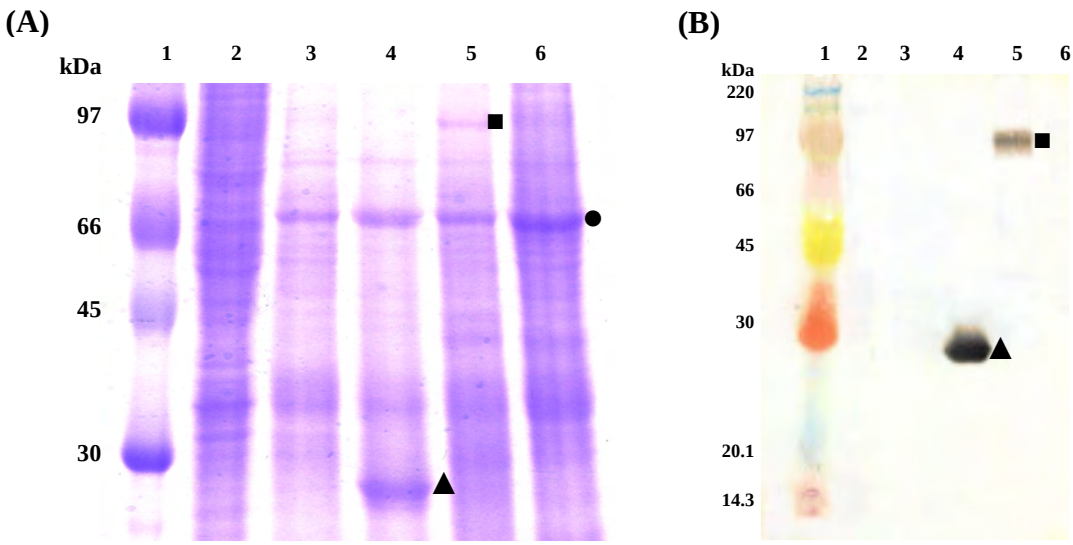

Fig. 3.7 SDS-PAGE analysis (A) and Western blot analysis with a polyclonal anti-eGFP antibody (B) of cell lysates prepared from recombinant baculovirus-infected *S. frugiperda* cells. Lanes: 1, Protein molecular weight marker; 2, mock-infected cells; 3, cells infected with wild-type baculovirus; 4, cells infected with Bac-eGFP; 5, cells infected with Bac-NS1-eGFP; 6, cells infected with Bac-NS1. The sizes of the Rainbow™ protein molecular weight marker (Amersham-Pharmacia Biotech AB) are indicated to the left of the figures. The eGFP protein is indicated by a triangle, while the NS1-eGFP and NS1 proteins are indicated by a square and a circle, respectively.

respectively). These results therefore confirmed successful expression of the respective proteins by means of the constructed baculovirus recombinants.

3.3.3.3 Transmission electron microscopy of purified proteins

One of the hallmarks of orbivirus infection is the production of large numbers of intracellular tubular structures that are composed of the NS1 protein only (Huismans and Els, 1979). It has also been reported previously that expression of the NS1 protein of BTV and AHSV in insect cells by means of recombinant baculoviruses results in the formation of tubules similar to those observed in virus-infected cells (Urakawa and Roy, 1989; Maree and Huismans, 1997). Thus, to investigate whether the in-frame addition of eGFP to the C-terminus of NS1 may affect its ability to form tubular structures, sucrose gradient-purified NS1 and chimeric NS1-eGFP proteins were negatively stained and examined by transmission electron microscopy (TEM).

To purify the NS1-rich tubular structures, cell extracts were prepared from recombinant baculovirus-infected *S. frugiperda* cells and subjected to sucrose gradient centrifugation. An aliquot of each fraction was analyzed by SDS-PAGE, the results of which indicated that the NS1 and NS1-eGFP proteins sedimented as a heterogenous peak (fractions 4 to 11). As similar heterogenous 200 to 400S complexes had been identified for baculovirus-expressed BTV NS1 (Urakawa and Roy, 1988) and AHSV NS1 (Maree and Huismans, 1997), these results thus suggested that the expressed AHSV-6 NS1 and NS1-eGFP proteins were present in a particulate or polymerized form in the infected cells (results not shown). Examination of the sucrose gradient-purified protein samples by TEM indicated that the expressed NS1 and NS1-eGFP proteins were able to form tubules that were morphologically similar (Fig. 3.8). These results therefore indicated that the C-terminal addition of eGFP did not affect the ability of the baculovirus-expressed AHSV-6 NS1 protein to form tubules.

3.4 DISCUSSION

The first manipulation of a baculovirus for the expression of non-baculoviral DNA was described 25 years ago (Smith *et al.*, 1983). Since then, the baculovirus expression system has become one of the most powerful and versatile eukaryotic expression systems for the production of high levels of properly post-translationally modified biologically active and

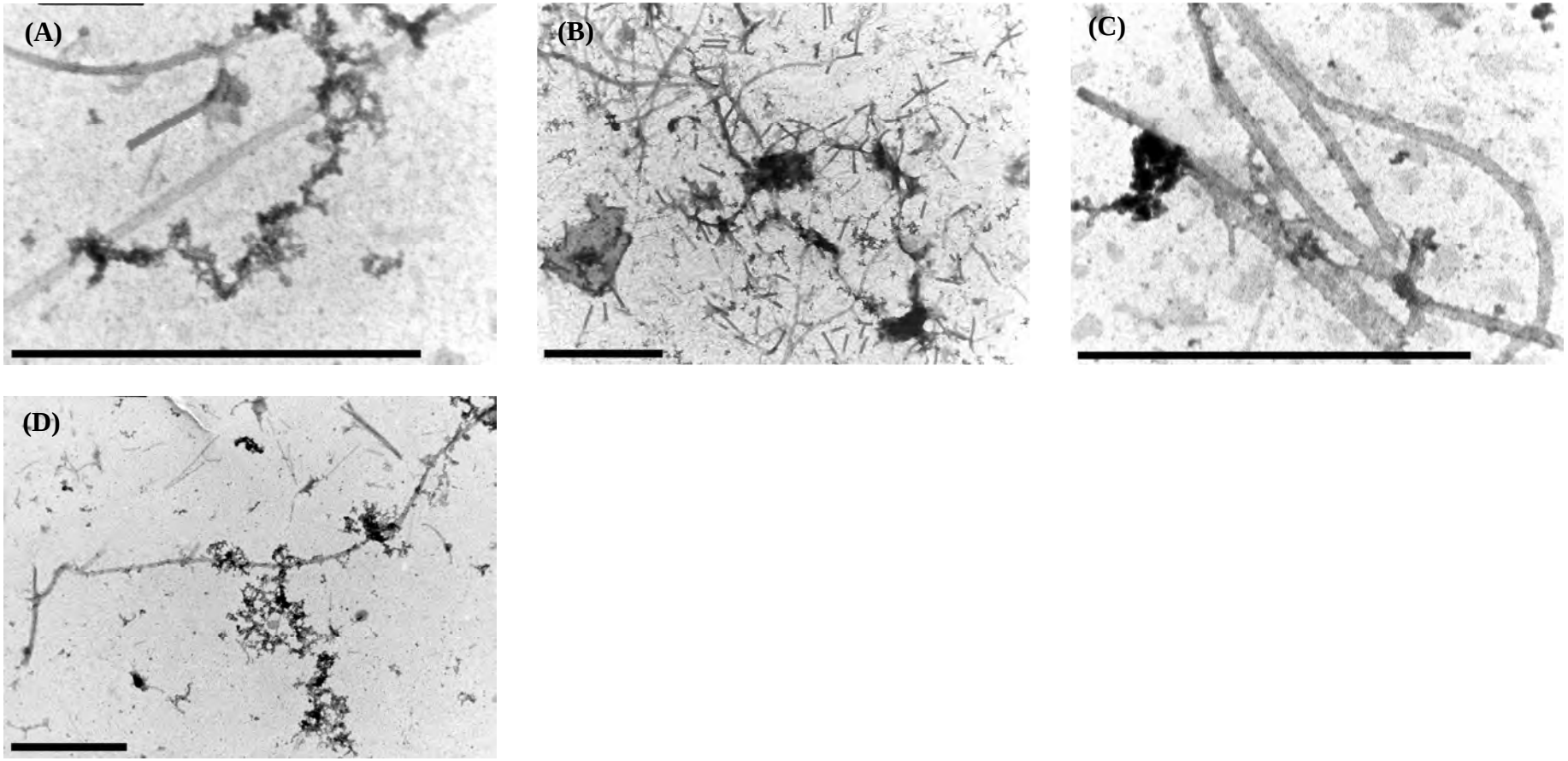

Fig. 3.8 Transmission electron micrographs of AHSV-6 NS1 tubules (A, B and C) and chimeric NS1-eGFP tubules (D) expressed in recombinant baculovirus-infected *S. frugiperda* cells. The respective proteins were purified by sucrose gradient centrifugation and negatively stained with uranyl acetate for transmission electron microscopy. Bar = 1 µm.

functional recombinant proteins (O'Reilly *et al.*, 1992; Hu, 2005; Yin *et al.*, 2007). The baculovirus expression system has greatly facilitated studies aimed at understanding the assembly of orbivirus structural proteins into core- and virus-like particles through co-expression of the respective proteins (Maree *et al.*, 1998; Kar *et al.*, 2004; 2005), as well as studies aimed at characterizing the individual AHSV proteins (Van Staden *et al.*, 1998; Uitenweerde *et al.*, 1995; De Waal and Huismans, 2005). Indeed, using the baculovirus expression system, the biochemical and biophysical properties of recombinant baculovirus-expressed AHSV-6 NS1 tubules have been reported (Maree and Huismans, 1997).

During the course of this investigation, an AHSV-6 NS1-eGFP chimeric gene was initially constructed in the pCMV-Script® mammalian expression vector and expression of the NS1-eGFP protein in transfected BHK-21 cells was evidenced by fluorescent cells (Chapter 2, Fig. 2.6). However, expression of the NS1-eGFP chimeric protein could not be confirmed by Western blot analysis, probably as a consequence of the low levels of transient gene expression, which is often the case when using mammalian expression systems (Yin *et al.*, 2007). In this part of the study, the efficiency and speed of the BAC-to-BAC® baculovirus system was exploited in order to produce sufficient levels of the NS1-eGFP protein to allow for its characterization. Thus, to characterize the NS1-eGFP chimeric protein, recombinant baculoviruses were generated that harboured a transposed copy of the NS1, eGFP and NS1-eGFP genes under transcriptional control of the strong polyhedrin promoter. The polyhedrin promoter directs high-level protein synthesis during the late stages of baculovirus infection and it has been reported that the expression of heterologous proteins can represent 20 to 50% of the total proteins of the infected host cell (Matsuura *et al.*, 1987). SDS-PAGE analysis of cell lysates prepared from recombinant baculovirus-infected *S. frugiperda* cells indicated the presence of a unique protein in each of the lysates that was absent from the cell lysates prepared from the control mock-infected and wild-type baculovirus-infected cells. The identity of the respective proteins was confirmed by Western blot analysis and the polyclonal eGFP antibody reacted specifically with the eGFP (27 kDa) and chimeric NS1-eGFP (90 kDa) proteins.

The ability of AHSV NS1 molecules to form tubules in both virus-infected BHK-21 cells (Huismans and Els, 1979) and in recombinant baculovirus-infected *S. frugiperda* cells (Maree and Huismans, 1997) is currently being exploited towards the development of a particulate immunogen delivery system by insertion of different immunogens at the C-terminus of the

AHSV NS1 protein (Prof. H. Huismans, Department of Genetics, University of Pretoria). Consequently, the chimeric AHSV-6 NS1-eGFP protein was investigated for its ability to assemble into tubules similar to those described for NS1 in baculovirus-infected *S. frugiperda* cells (Maree and Huismans, 1997). To investigate, cytoplasmic extracts of recombinant baculovirus-infected cells were prepared and purified by sucrose gradient centrifugation. Transmission electron microscopy studies by negative staining indicated that the addition of eGFP (239 amino acids in length) did not alter the formation of the tubules, as the observed NS1-eGFP chimeric tubules were morphologically similar to those made by the wild-type NS1 protein (Fig. 3.8). These results are also in agreement with those reported by Ghosh *et al*. (2002), who demonstrated that addition of GFP to the C-terminus of BTV-10 NS1 did not perturb the ability of the chimeric protein to form tubules. More recently, Larke *et al*. (2005) reported the use of BTV-10 NS1 tubules to present a multicomponent protein antigen that represents a series of epitopes of HIV. Despite the immunogen being 527 amino acids in length and thus comparable in size to the NS1 monomer (552 amino acids in length), the tubular structure was maintained albeit with a slight abrogation that may have been due to the large size of the antigen (Larke *et al*., 2005). The ability of AHSV-6 NS1 tubules to carry large proteins (*e.g.* eGFP), whilst maintaining the ability to form the tubular structure, may thus be a promising feature of the AHSV NS1 immunogen delivery system.

In conclusion, since the NS1-eGFP chimeric gene was constructed with the aim of using it in a quantitative reporter-based si/shRNA screening assay, it was therefore important to verify the integrity of the gene construct and expressed chimeric protein. In contrast to the mammalian expression system used previously (Chapter 2), expression of the NS1-eGFP chimeric gene in the baculovirus/insect cell expression system yielded sufficient amounts of the recombinant protein that greatly facilitated its characterization. The results from SDS-PAGE and Western blot analyses indicated the successful expression of a single polypeptide of the expected size, while TEM analysis confirmed that, despite the in-frame C-terminus addition of eGFP, the NS1-eGFP chimeric protein retained its ability to fold into a tubular structure. Overall, the results obtained therefore served to validate the use of the recombinant mammalian expression vector pCMV-NS1-eGFP, which harbours the identical chimeric gene expressed in this part of the investigation, as a reporter vector whereby different NS1-directed shRNAs could be screened for their ability to silence AHSV-6 NS1 gene expression.

CHAPTER 4

SHORT HAIRPIN RNA (shRNA)-MEDIATED SILENCING OF AHSV-6 NS1 GENE EXPRESSION IN BHK-21 CELLS

4.1 INTRODUCTION

African horse sickness virus (AHSV), a member of the *Orbivirus* genus in the family *Reoviridae*, causes an acute infectious but non-contagious disease of equids. Like other orbiviruses, the genome of AHSV consists of ten double-stranded (ds) RNA segments that encode seven structural proteins (VP1-VP7) and four nonstructural proteins (NS1, NS2 and NS3/NS3A) (Bremer *et al*., 1990; Grubman and Lewis, 1992; Roy *et al*., 1994). The nonstructural protein NS1 is synthesized abundantly and forms tubular structures, which are present in large numbers in peri- or juxtanuclear positions in infected cells (Eaton *et al*., 1988; Huismans and Els, 1979). The function of the NS1 tubules in orbivirus replication is not yet completely understood. It has been proposed that the tubules may be involved in translocation of virus particles from virus inclusion bodies (VIBs) to the cell plasma membrane prior to virus release or that they may prevent the core particle from assembling before the minor structural proteins (VP1, VP4, VP6) and/or genome segments have been incorporated (Eaton *et al*., 1990). More recently, however, it has been suggested that the NS1 protein of bluetongue virus (BTV) could be a major determinant of pathogenesis since it augments virus-cell association that leads to lysis of the infected cell (Owens *et al*., 2004).

RNA interference (RNAi) is a process of sequence-specific post-transcriptional gene silencing that is triggered by dsRNA homologous to the target transcript (Fire *et al*., 1998; Tuschl *et al*., 1999). RNAi is triggered in mammalian cells by exposing the cells to dsRNA either via exogenous delivery of chemically synthesized small interfering RNAs (siRNAs) or endogenous expression of short hairpin RNAs (shRNAs) (Elbashir *et al*., 2002; Amarzguioui *et al*., 2005). Due to its specificity, RNAi technology has been applied in studies to ascertain viral gene function (Déctor *et al*., 2002; Campagna *et al*., 2005; Wirblich *et al*., 2006) and as a means whereby virus infections can be controlled (McCown *et al*., 2003; Zhang *et al*., 2004; Chen *et al*., 2006; Huang *et al*., 2006; Lambeth *et al*., 2007). Due to the absence of a reverse genetics system for AHSV, the characterization of AHSV gene function has been limited to their expression and analyses in eukaryotic expression systems (Van Staden *et al*., 1995; Uitenweerde *et al*., 1995; Maree and Huismans, 1997; De Waal and Huismans, 2005). However, the segmented nature of the AHSV genome makes it particularly amenable to analysis by RNAi, since each of the ten dsRNA genome segments is transcribed into a single mRNA, each encoding a single protein (except NS3). Therefore, RNAi technology is ideally suited to silence expression of individual AHSV genes without affecting the expression of

others and thus may allow for characterization of the function of proteins encoded by the silenced genes in the context of the whole virus (Silvestri *et al*., 2004; Stassen *et al*., 2007).

Although RNAi can be triggered in mammalian cells by chemically (Elbashir *et al*., 2001a; Caplen *et al*., 2001) and enzymatically (Myers *et al*., 2003; Xuan *et al*., 2006) synthesized 21-23 nt long RNA duplexes, the silencing effect induced by exogenous delivery of these synthetic siRNAs is transient and reactivation of the target gene normally occurs after a few days. In addition, in order to obtain effective siRNAs it is necessary to design, synthesize and screen many different siRNAs, which is expensive due to the cost of chemical synthesis of RNA oligonucleotides (Elbashir *et al*., 2002; Mittal, 2004; Cullen, 2006). To overcome these limitations, RNA expression vectors have been developed to screen numerous candidate RNAi effector molecules cost-effectively (Brummelkamp *et al*., 2002a; Wadhwa *et al*., 2004; Amarzguioui *et al*., 2005). These vectors use RNA polymerase III promoters to direct the synthesis of shRNA molecules from a DNA template, which are subsequently processed intracellularly in mammalian cells into siRNA-like molecules. RNA polymerase III promoters, especially H1 and U6 from human and mouse origin, have been used frequently since they have a well-defined transcription start site and a simple termination signal consisting of four to five consecutive thymidine residues. Moreover, they can efficiently transcribe small RNA transcripts that lack both the 5' cap and 3' polyadenosine tail (Paule and White, 2000). Such shRNA-expressing plasmid DNA vectors have been used to inhibit virus gene expression (Brummelkamp *et al*., 2002a; Zhang *et al*., 2004; De Los Santos *et al*., 2005) and as a promising tool for *in vivo* antiviral therapy (Ge *et al*., 2004; Chen *et al*., 2004; Carmona *et al*., 2005; Chen *et al*., 2006).

In Chapter 2 it was shown that a chemically synthesized siRNA can silence eGFP and NS1-eGFP gene expression, indicating that RNAi is tractable in BHK-21 cells. Moreover, use of a NS1-eGFP reporter construct in those assays suggested that it may be used to facilitate screening of different RNAi effector molecules, both visually at the protein level by fluorescent microscopy and quantitatively by fluorometry. In this part of the study, the primary aim was to establish and evaluate a plasmid DNA vector-based RNAi assay for silencing of AHSV-6 NS1 gene expression in BHK-21 cells. For this purpose the shRNA delivery vector pSUPER (suppression of endogenous RNA), which directs the intracellular synthesis of siRNAs in mammalian cells (Brummelkamp *et al*., 2002a), was selected for use. Consequently, two recombinant pSUPER shRNA delivery vectors were constructed, each

targeting a distinct 19-nt sequence in the AHSV-6 NS1 gene. The levels of NS1 protein and transcripts in the presence of the recombinant vectors were subsequently analyzed.

4.2 MATERIALS AND METHODS

4.2.1 Bacterial strains and plasmids

The *E. coli* strains were routinely cultured at 37°C with shaking at 200 rpm in LB broth (1% [w/v] tryptone, 1% [w/v] NaCl, 0.5% yeast extract; pH 7.4) (Sambrook *et al.*, 1989), and maintained at 4°C on LB agar or at -70°C as glycerol cultures. For plasmid selection and maintenance in *E. coli*, the culture medium was supplemented with 100 µg/ml of ampicillin (Roche Diagnostics). Recombinant mammalian expression plasmids pCMV-eGFP, pCMV-NS1-eGFP and pCMV-NS1 were constructed and characterized previously (Chapter 2). Recombinant plasmids pSUPER-Uneg, which contains a control non-silencing oligonucleotide insert DNA, and pSUPER-eGFP, which contains an oligonucleotide insert DNA corresponding in sequence to that of eGFP-siRNA (Chapter 2), were obtained from M.A. Nieuwoudt (Department of Microbiology and Plant Pathology, University of Pretoria). The pSUPER shRNA delivery vector was obtained from OligoEngine.

4.2.2 Cells and viruses

Baby hamster kidney cells (BHK-21) were propagated and maintained as monolayers in 75 cm^2 tissue culture flasks, and cultured in Minimum Essential Medium (MEM) Eagles base (Highveld Biological) supplemented with 2.5% (v/v) foetal bovine serum (FBS) and antibiotics (penicillin, streptomycin and fungizone). The flasks were incubated at 37°C in a humidified incubator with a constant supply of 5% CO_2. African horse sickness virus serotype 6 (AHSV-6) was kindly provided by F. Wege (Department of Genetics, University of Pretoria). The virus was propagated in confluent BHK-21 monolayers using a low-passage stock virus as inoculum according to previously described procedures (Huismans, 1979).

4.2.3 Oligonucleotides for short hairpin RNA (shRNA) construction

Oligonucleotides whereby shRNAs could be expressed *in vivo* were designed based on the AHSV-6 NS1 gene sequence (GenBank accession no. U73658) and by making use of the design tools available at the siRNA Design Software website, which incorporates 12 different siRNA design tools (http://i.cs.hku.hk/~sirna/software/sirna.php). To verify their target

specificity, the oligonucleotide sequences were compared to entries of the GenBank database by making use of the BLASTN program (Altschul *et al.*, 1997), available on the National Center for Biotechnology Information web page (http://www.ncbi.nlm.nih.gov/). The accessibility of the target sites was also evaluated by RNA secondary structure analyses of the NS1 and chimeric NS1-eGFP mRNA, using MFOLD hybridization and folding software v.3.1 (Zuker, 2003). The results of these analyses are shown in (Figs. 4.1 and Fig 4.2, respectively). The forward and reverse oligonucleotides (each 64 nt in length) contained the 19-nt target sequence in both sense and antisense orientation, separated by a 9-nt loop sequence. Whereas the forward oligonucleotides were designed to contain a *Bgl*II restriction enzyme site at their 5'-end and a RNA polymerase H1 transcription termination sequence (five thymidine residues), the reverse oligonucleotides were designed to contain a *Hind*III restriction enzyme site at the 5'-end of the oligonucleotides. The oligonucleotides used in this study for shRNA construction are shown in Table 4.1 and were obtained from Qiagen.

4.2.4 Construction of recombinant pSUPER shRNA delivery vectors

4.2.4.1 Preparation of oligonucleotide insert DNA

The oligonucleotides were each dissolved in sterile nuclease-free water to a final concentration of 3 mg/ml and 1 µl of the forward and reverse oligonucleotides were subsequently mixed with 48 µl of annealing buffer (100 mM NaCl, 50 mM HEPES; pH 7.4). The suspension was incubated at 90°C for 4 min, followed by incubation at 70°C for 10 min and then cooled to room temperature. Since the respective oligonucleotides are synthesized lacking 5' phosphate groups, the 5'-ends of the annealed oligonucleotides were phosphorylated to enable their ligation with dephosphorylated vector DNA. The reaction mixture contained 500 ng of annealed oligonucleotides, 10 U of T4 Polynucleotide kinase (10 U/µl; Fermentas), 10 mM ATP, 1 × reaction buffer and UHQ water to a final volume of 20 µl. The reaction mixtures were incubated at 37°C for 30 min and then stored at -20°C until use.

4.2.4.2 Preparation of pSUPER vector DNA

To prepare the pSUPER vector for cloning, 3 µg of vector DNA was digested at 37°C first with 10 U of *Hind*III for 1 h, followed by digestion with 10 U of *Bgl*II for 2 h. The digested pSUPER vector DNA was subsequently dephosphorylated in a 40-µl reaction volume,

Table 4.1 Oligonucleotides* used for shRNA construction

NS1 oligonucleotide 1 (shNS1-1464)

Forward oligonucleotide:

5’ GATCCCCTGTCTTGGATGGAAGAGATTTCAAGAGAATCTCTTCCATCCAAGACA**TTTTTT**GGAAA 3’

Reverse oligonucleotide:

5’ *AGCTTT*TCCAAAAATGTCTTGGATGGAAGAGATTCTCTTGAAATCTCTTCCATCCAAGACAGGG 3’

Resulting duplex oligonucleotide:

5’ GATCCCCTGTCTTGGATGGAAGAGATTTCAAGAGAATCTCTTCCATCCAAGACA**TTTTTT**GGAAA 3’
3’ GGGACAGAACCTACCTTCTCTAAAGTT CTCTTAGAGAAGGTAGGTTCTGTAAAAACCT*TTTCGA* 5’

NS1 oligonucleotide 2 (shNS1-710)

Forward oligonucleotide:

5’ GATCCCCTGCGTAGAGCGGCACAGGATTCAAGAGATCCTGTGCCGCTCTACGCA**TTTTTT**GGAAA 3’

Reverse oligonucleotide:

5’ *AGCTTT*TCCAAAAATGCGTAGAGCGGCACAGGATCTCTTGAATCCTGTGCCGCTCTACGCAGGG 3’

Resulting duplex oligonucleotide:

5’ GATCCCCTGCGTAGAGCGGCACAGGATTCAAGAGATCCTGTGCCGCTCTACGCA**TTTTTT**GGAAA 3’
3’ GGGACGCATCTCGCCGTGTCCTAAGTT CTCTAGGACACGGCGAGATGCGTAAAAACCT*TTTCGA* 5’

Control non-silencing oligonucleotide (shUneg)

Forward oligonucleotide:

5’ GATCCCCAATTCTCCGAACGTGTCACGTTTCAAGAGAACGTGACACGTTCGGAGAATT**TTTTTT**GGAAA 3’

Reverse oligonucleotide:

5’ *AGCTTT*TCCAAAAAAATTCTCCGAACGTGTCACGTTCTCTTGAAACGTGACACGTTCGGAGAATTGGG 3’

Resulting duplex oligonucleotide:

5’ GATCCCCAATTCTCCGAACGTGTCACGTTTCAAGAGAACGTGACACGTTCGGAGAATT**TTTTTT**GGAAA 3’
3’ GGGTTAAGAGGCTTGCACAGTGCAAAGTT CTCTTGCACTGTGCAAGCCTCTTAAAAAAACCT*TTTCGA* 5’

eGFP oligonucleotide (sheGFP)

Forward oligonucleotide:

5’ GATCCCCGCAAGCUGACCCUGAAGUUCTTCAAGAGAAUGAACUUCAGGGUCAGCUUGC**TTTTTT**GGAAA 3’

Reverse oligonucleotide:

5’ *AGCTTT*TCCAAAAAGCAAGCUGACCCUGAAGUUCAUTCTCTTGAAAUGAACUUCAGGGUCAGCUUGCGGG 3’

Resulting duplex oligonucleotide:

5’ GATCCCCGCAAGCUGACCCUGAAGUUCAUTTCAAGAGAAUGAACUUCAGGGUCAGCUUGC**TTTTTT**GGAAA 3’
3’GGGCGUUCGACUGGGACUUCAAGUAAAGTTTCTUACUUGAAGUCCCAGUCGAACGAAAAACCT*TTTCGA* 5’

* The *Bgl*II restriction enzyme site is underlined, the *Hind*III restriction enzyme site is indicated in italics, the target NS1 and eGFP regions are highlighted in grey and the termination signal (five thymidine residues) is indicated in bold letters.

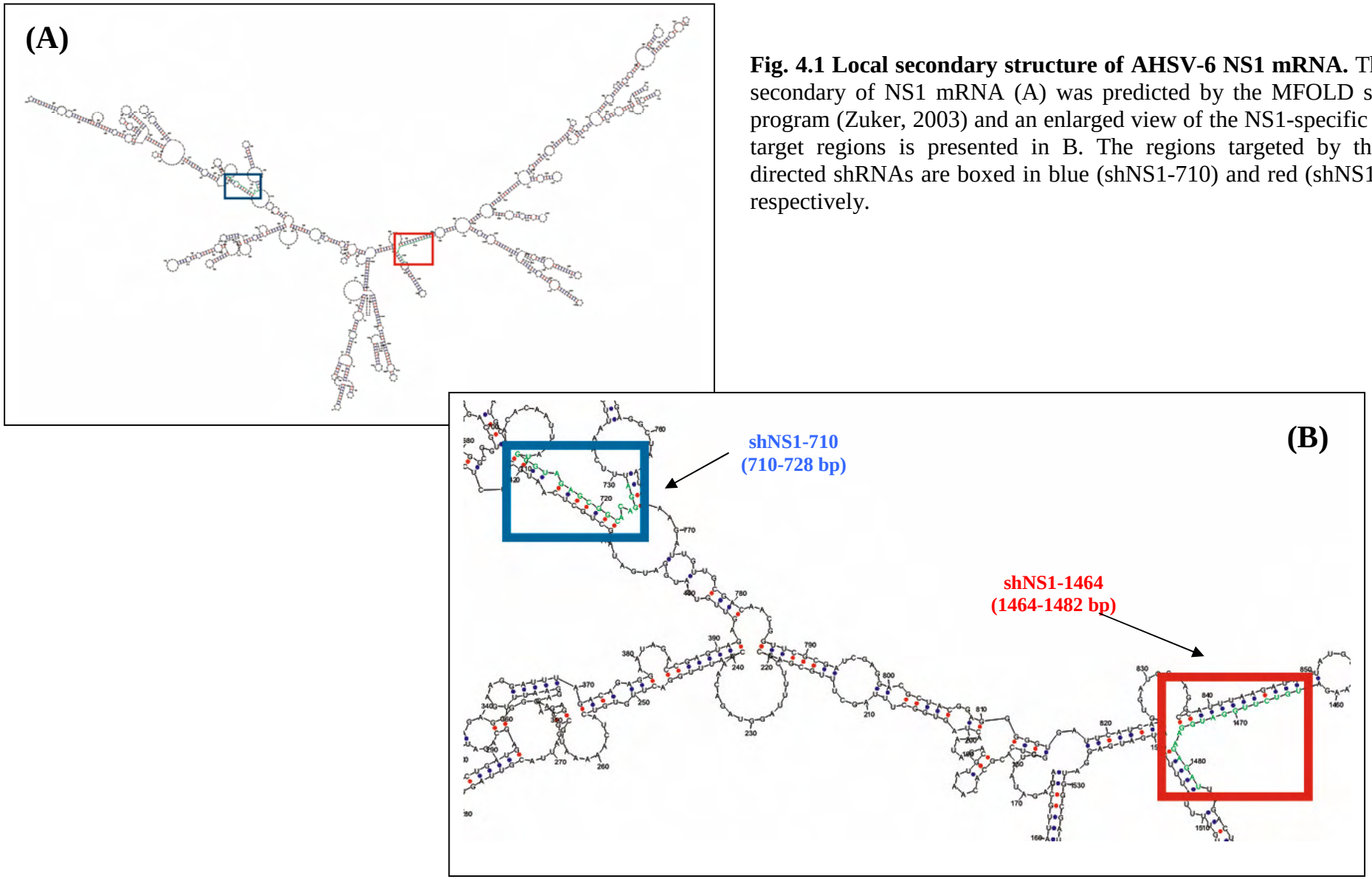

Fig. 4.1 Local secondary structure of AHSV-6 NS1 mRNA. The local secondary of NS1 mRNA (A) was predicted by the MFOLD software program (Zuker, 2003) and an enlarged view of the NS1-specific shRNA target regions is presented in B. The regions targeted by the NS1-directed shRNAs are boxed in blue (shNS1-710) and red (shNS1-1464), respectively.

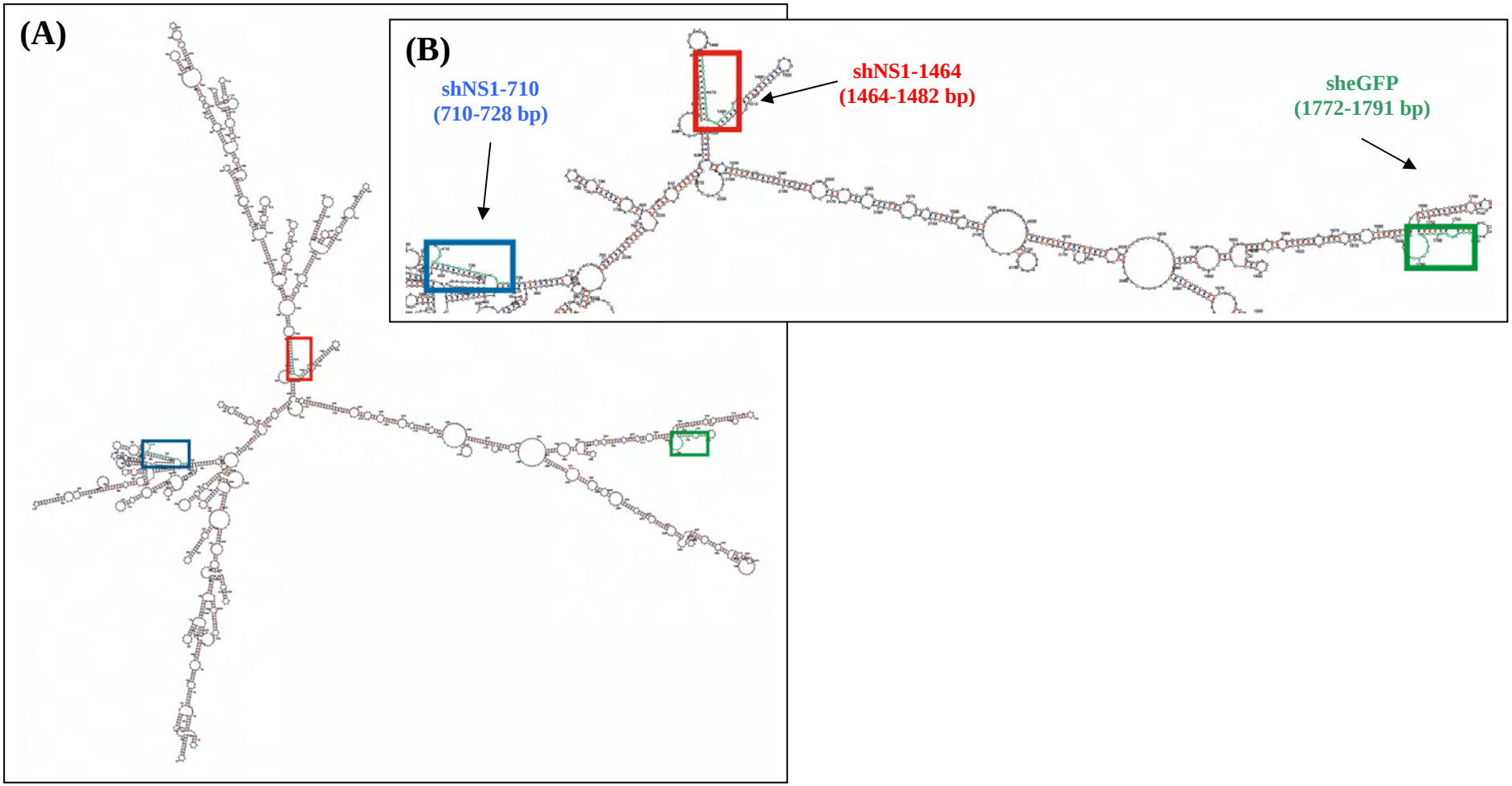

Fig. 4.2 Local secondary structure of AHSV-6 NS1-eGFP chimeric mRNA. The local secondary of NS1-eGFP chimeric mRNA (A) was predicted by the MFOLD software program (Zuker, 2003) and an enlarged view of the NS1- and eGFP-specific shRNA target regions is presented in B. The region targeted by sheGFP is boxed in green, while the regions targeted by the NS1-directed shRNAs are boxed in blue (shNS1-710) and red (shNS1-1464), respectively.

containing 6 U of Shrimp alkaline phosphatase (1 U/µl; Fermentas) and 4 µl of 10 × reaction buffer. Following incubation at 37°C for 30 min, the reaction mixtures were heated to 65°C for 15 min in order to inactivate the phosphatase enzyme.

4.2.4.3 Cloning of oligonucleotide insert DNA into pSUPER vector DNA

The digested dephosphorylated pSUPER vector and phosphorylated oligonucleotide insert DNA were ligated at 4°C for 20 h in a 10-µl reaction volume that contained 1 × ligation buffer and 1 U of T4 DNA ligase (1 U/µ1; Promega). The ratio of insert to vector DNA was typically in excess of 10:1. Competent *E. coli* DH5α cells were prepared and transformed with the ligation reaction mixtures, and transformants were selected on LB agar medium supplemented with ampicillin after incubation overnight at 37°C. Plasmid DNA was screened by restriction enzyme digestion with *Bgl*II, of which the recognition site is destroyed when the insert oligonucleotide has been cloned successfully into the pSUPER vector (Fig. 4.3). The presence and integrity of the cloned insert DNA was verified by nucleotide sequencing using the ABI PRISM® BigDye™ Terminator Cycle Sequencing Ready Reaction kit v.3.1 (Perkin-Elmer Applied Biosystems), and oligonucleotides T3 (5'-AATTAACCCTCACTAAAGGG-3') and T7 (5'-GTAATACGACTCACTATAGGGC-3') as the sequencing primers. The derived recombinant plasmids were designated pSUPER-710 and pSUPER-1464.

4.2.5 Extraction and purification of plasmid DNA

In addition to purifying plasmid DNA by CsCl-EtBr density gradient centrifugation (Chapter 2, Section 2.2.9.2), plasmid DNA was also extracted and purified using a plasmid Midiprep kit (Qiagen) according to the manufacturer's instructions. Briefly, the cells from 80 ml of an overnight culture were collected by centrifugation at 7 000 rpm for 15 min at 4°C. The cell pellet was suspended in 4 ml of Buffer P1 (50 mM Tris, 10 mM EDTA, 100 µg/ml RNaseA; pH 8), after which 4 ml of Buffer P2 (200 mM NaOH, 1% SDS) was added, and the cell lysate incubated at room temperature for 5 min. To this, 4 ml of Buffer P3 (3 M KOAc; pH 5.5) was added, and incubation was continued on ice for 15 min. Following centrifugation twice at 11 000 rpm for 30 min at 4°C, the supernatant was recovered and loaded onto a DNA-binding column, pre-equilibrated with 4 ml of Buffer QBT (750 mM NaCl, 50 mM MOPS, 15% ethanol, 0.15% TritonX-100; pH 7). The column was subsequently rinsed twice

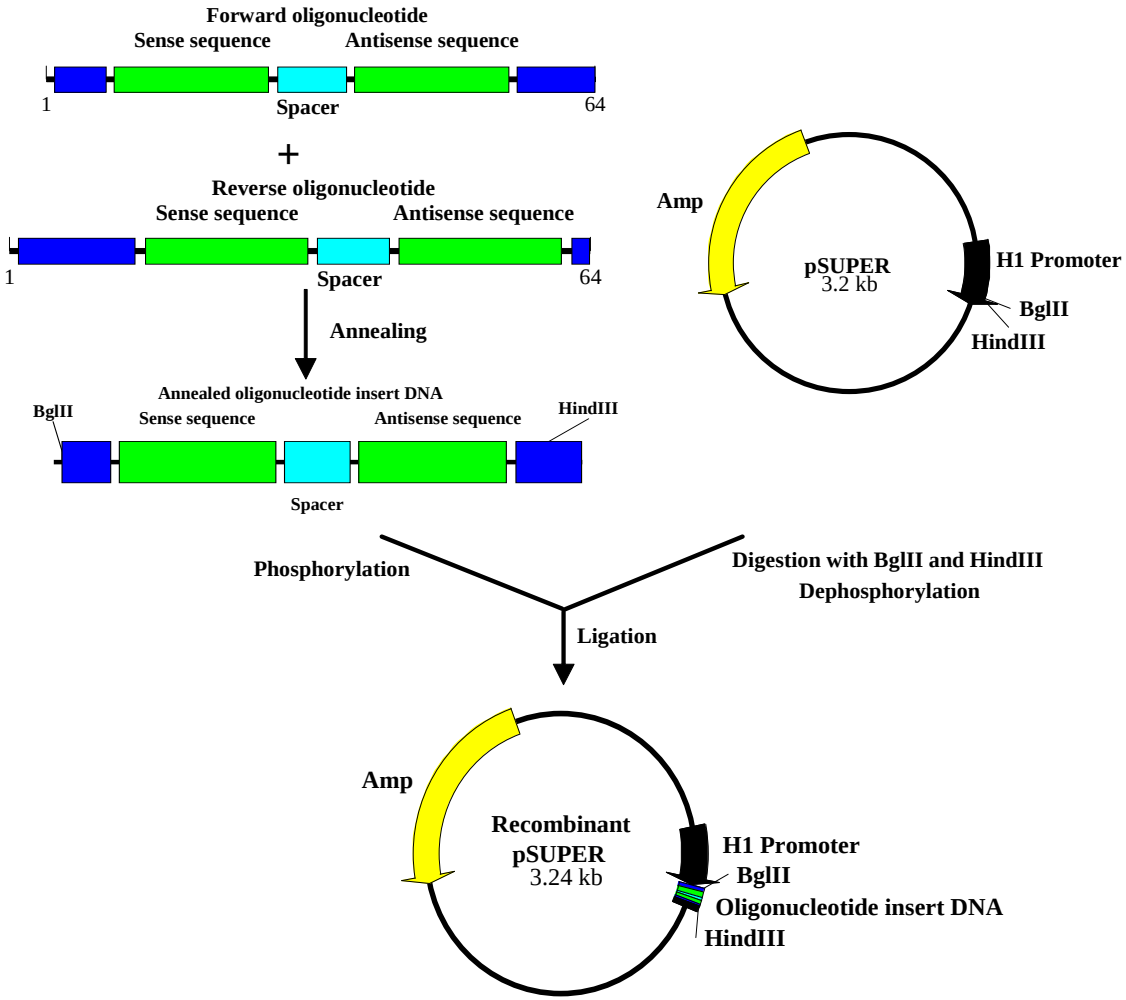

Fig. 4.3 Schematic diagram indicating the cloning strategy for cloning of the annealed forward and reverse oligonucleotides into the pSUPER shRNA delivery vector.

with 10 ml of Buffer QC (1.0 M NaCl, 50 mM MOPS, 15% ethanol; pH 7) and the plasmid DNA was eluted with 5 ml of Buffer QF (1.25 M NaCl, 50 mM Tris, 15% ethanol; pH 8.5). The purified plasmid DNA was precipitated by addition of 3.5 ml of isopropanol and collected by centrifugation at 11 000 rpm for 30 min at 4°C. The DNA pellet was washed with 70% ethanol, air-dried for 10 min and then suspended in 100 µl of 1 × TE buffer. The concentration of the purified plasmid DNA was determined spectrophotometrically using a Nanodrop instrument (Thermo Scientific) according to the manufacturer's instructions.

4.2.6 RNAi assays

4.2.6.1 Co-transfection of BHK-21 cells with pCMV-NS1-eGFP and recombinant pSUPER shRNA delivery vectors

BHK-21 cells were seeded in 24-well tissue culture dishes to reach 80% confluency within 24 h of incubation at 37°C in the presence of 5% CO_2. The BHK-21 cells were co-transfected with pCMV-NS1-eGFP and the recombinant pSUPER plasmid DNA using Lipofectamine™ 2000 (Invitrogen). For each transfection, 800 ng of purified recombinant pCMV-NS1-eGFP plasmid DNA and 2 µ1 of Lipofectamine™ 2000 reagent were each diluted in 50 µl of serum- and antibiotic-free MEM medium, incubated at room temperature for 5 min and then mixed. Similarly, 800 ng of purified recombinant pSUPER plasmid DNA and 2 µ1 of the Lipofectamine™ 2000 reagent were also each diluted in 50 µ1 of MEM medium (without serum and antibiotics) and, following incubation at room temperature for 5 min, were mixed. After incubation at room temperature for 20 min, the two solutions were mixed and then used to overlay the BHK-21 cell monolayers. The monolayers had been prepared by rinsing the cells three times with 500 µl of antibiotic-free MEM medium but containing 2.5% (v/v) FBS. After addition of 300 µ1 of the same medium, the tissue culture dishes were incubated at 37°C for 24 h in a CO_2 incubator. Untransfected BHK-21 cells and cells transfected with pCMV-NS1-eGFP only were included as controls.

4.2.6.2 Co-transfection of BHK-21 cells with pCMV-NS1 and recombinant pSUPER shRNA delivery vectors

BHK-21 cells were seeded in 35-mm-diameter wells to reach 80% confluency within 24 h of incubation at 37°C in the presence of 5% CO_2. The cells were transfected with 4 µg of purified recombinant pSUPER plasmid DNA by diluting the plasmid DNA and 10 µ1 of the Lipofectamine™ 2000 reagent separately in 250 µ1 of antibiotic- and serum-free MEM

medium. Following incubation at room temperature for 5 min, the two solutions were mixed and incubated at room temperature for 20 min. After addition of 1.5 ml of antibiotic-free MEM medium supplemented with 2.5% (v/v) FBS, the BHK-21 cell monolayers, prepared as described above, were overlayed with the DNA-lipotectamine complexes. Following incubation of the tissue culture dishes at 37°C for 24 h in a CO_2 incubator, the cells were again transfected, as described above, with 4 µg of purified pCMV-NS1 plasmid DNA. The tissue culture dishes were incubated at 37°C for a further 24 h in a CO_2 incubator. Untransfected BHK-21 cells and cells transfected with pCMV-NS1 only were included as controls.

4.2.6.3 Transfection and AHSV-6 infection of BHK-21 cells

BHK-21 cells were seeded in 35-mm-diameter wells to reach 80% confluency within 24 h of incubation at 37°C in the presence of 5% CO_2. The BHK-21 cells were then transfected with the respective recombinant pSUPER plasmid DNAs using Lipofectamine™ 2000, as described above, with the following modifications. Briefly, 4 µg of plasmid DNA was diluted in 250 µ1 of MEM medium (without serum and antibiotics) and, following incubation at room temperature for 5 min, was added to 250 µ1 of serum- and antibiotic-free MEM medium containing 10 µ1 of the Lipofectamine™ 2000 reagent. Following incubation at room temperature for 20 min, the BHK-21 cell monolayers, which had been prepared for transfection by rinsing the cells three times with 2 ml of MEM medium (without serum and antibiotics), were then overlayed with the DNA-lipofectamine complexes. After addition of 1.5 ml of MEM medium supplemented with 2.5% (v/v) FBS, but lacking antibiotics, the tissue culture dishes were incubated at 37°C for 24 h in a CO_2 incubator. The transfected cells were then infected with AHSV-6 at a multiplicity of infection (MOI) of 1 pfu/cell. Following incubation at room temperature for 1 h, the inoculum was removed and the tissue culture dishes were then incubated at 37°C for a further 24 h in a CO_2 incubator. Untransfected BHK-21 cells and cells infected with AHSV-6 only were included as controls.

4.2.7 Analysis and quantification of reporter protein expression

BHK-21 cell monolayers were observed at 24 h post-transfection for NS1-eGFP protein expression on a Zeiss Axiovert 200 fluorescent microscope fitted with the no. 10 Zeiss filter set (excitation at 450-490 nm; emission at 515-560 nm). The images were captured for separate microscope fields with a Nikon DMX 1200 digital camera. For fluorometry, the

BHK-21 cell monolayers were rinsed once with 1 × PBS and trypsinized by addition of 30 µl of Trypsin/Versene. After incubation at 37°C for 1 min, the cells were collected by centrifugation at 3 000 rpm for 10 min, rinsed with 1 × PBS and suspended in 1 ml of 1 × PBS. The relative fluorescence was determined with a BioRad Versafluor™ fluorometer (excitation at 485-495 nm; emission at 515-525 nm).

4.2.8 Semi-quantitative reverse transcriptase-polymerase chain reaction (RT-PCR)

4.2.8.1 Oligonucleotides

Gene-specific oligonucleotides were designed based on the AHSV-6 NS1 (GenBank accession no. U73658) and β2-microglobulin (β2-MG; GenBank accession no. X17002) gene sequences to yield amplicons of 130 and 138 bp, respectively. The oligonucleotides were designed using Primer 3 (Rozen and Skaletsky, 2000) and DNAMAN v.4.13 (Lynnon Biosoft), while optimal oligonucleotide pairs were analyzed by PerlPrimer v.1.1.6 (Marshall, 2004). To verify the target sequence specificity of each oligonucleotide pair, the oligonucleotide sequences were subjected to a BLASTN analysis. The oligonucleotide sequences are indicated in Table 4.2 and were synthesized by Inqaba Biotechnical Industries.

Table 4.2 Oligonucleotides used in semi-quantitative real-time PCR

Oligonucleotide	Nucleotide sequence	Tm (°C)	Annealing position	Target mRNA
β2-MG-F	5'-AGTGGAGCTGTCAGATCTGTCCTTC-3'	64.5°C	9-34	BHK β2-MG
β2-MG-R	5'-TGACCACCTTGGGCTCCTTC-3'	64.8°C	127-147	BHK β2-MG
RT-NS1-F	5'-GCCCGTTTGCCCTTATACTG-3'	62.5°C	603-623	AHSV-6 NS1
RT-NS1-R	5'-TGAAATCCTGTGCCGCTC-3'	59.9°C	733-751	AHSV-6 NS1

4.2.8.2 Total RNA isolation

Total RNA was isolated using the Aurum™ Total RNA Mini Kit (BioRad) according to the manufacturer's instructions. Briefly, the culture medium was removed from BHK-21 cell monolayers and the cells were rinsed once with 1 × PBS. Following trypsinization, the cells were collected by centrifugation at 15 000 rpm for 2 min and suspended in 350 µ1 of the supplied lysis solution. The cells were lysed by repeated vigorous pipetting and an equal volume of 70% ethanol was added. The cell lysate was centrifuged through a RNA-binding column at 15 000 rpm for 30 s and the column was then rinsed with wash solution and treated

with RNase-free DNase I (15 min at room temperature). The RNA was eluted from the column in 80 µl of the supplied elution buffer. To confirm the absence of contaminating DNA, aliquots of the RNA preparation were used in PCR reactions together with the oligonucleotides indicated in Table 4.2. The PCR reactions were performed, as described previously (Chapter 2, Section 2.2.3.2). Aliquots of the reaction mixtures were analyzed by electrophoresis on a 0.8% (w/v) agarose gel in the presence of appropriate DNA molecular weight markers.

4.2.8.3 cDNA synthesis

The total RNA was reverse-transcribed using the QuantiTect® Reverse Transcription kit (Qiagen) according to the manufacturer's instructions. Prior to cDNA synthesis, the RNA samples were incubated at 42°C for 2 min in 1 × genomic DNA Wipeout buffer (supplied in the kit), which removed any residual contaminating genomic DNA. For reverse transcription, each reaction mixture contained 10 µ1 of RNA, 4 µl of 5 × Quantiscript® RT buffer, 1 µl of Quantiscript® Reverse Transcriptase enzyme and 1 µl of RT primer mix, which comprises an optimized mixture of oligo-dT and random primers. The reaction mixtures were incubated at 42°C for 30 min, after which the enzyme was inactivated by heating to 95°C for 3 min. The cDNA was subsequently stored at -20°C.

4.2.8.4 Semi-quantitative real-time PCR

Semi-quantitative real-time PCR was performed using the QuantiTect™ SYBR® Green PCR kit (Qiagen) and the LightCycler® 480 system (Roche Diagnostics). Each reaction mixture (20 µ1) contained 1 µl of the cDNA, 10 pmol of each of the gene-specific oligonucleotides and 10 µl of 2 × SYBR® Green I PCR master mix (containing HotStar*Taq*® DNA polymerase, dNTP mixture, SYBR® Green I, ROX passive reference dye and 5 mM $MgCl_2$). The reaction mixtures were incubated at 95°C for 15 min to activate the HotStar*Taq*® DNA polymerase, and then subjected to 55 cycles of denaturation at 94°C for 15 s, annealing at 55°C for 20 s and extension at 72°C for 10 s. For each target gene, a reaction mixture from which template cDNA was omitted was included as a control. To confirm specific amplication, the amplicons were analyzed on a 2% (w/v) agarose gel in the presence of a DNA molecular weight marker, and melt-curve analysis of the amplicons were performed according to manufacturer's protocol with the LightCycler v.3.5.3 software package (Roche Diagnostics). The Relative

Expression Software Tool (REST©) (Pfaffl *et al.*, 2002) was used for data normalization and calculation of fold changes in NS1 transcripts. For these analyses, the relative expression of target (NS1) was normalized to an endogenous reference gene (β2-microglobulin) in a NS1 shRNA-treated sample relative to an experimental control (control shRNA-treated, AHSV-infected cells).

4.3 RESULTS

4.3.1 Construction of recombinant pSUPER shRNA delivery vectors

To enable expression of shRNAs for silencing of AHSV-6 NS1 gene expression in BHK-21 cells, oligonucleotides, 64 bp in length, targeting two different regions on the AHSV-6 NS1 mRNA were designed. For each targeted region, a forward and reverse oligonucleotide were chemically synthesized, annealed and phosphorylated at their 5'-ends to enable efficient ligation with pSUPER vector DNA that had been digested with both *Bgl*II and *Hind*III and dephosphorylated. Following transformation of competent *E. coli* DH5α cells with the ligation reaction mixtures, plasmid DNA was extracted from randomly selected ampicillin-resistant transformants and screened by restriction enzyme digestions.

Initial screening of recombinant pSUPER plasmid DNA was greatly facilitated as a consequence of the cloning strategy used. Since the *Bgl*II site of the vector is destroyed upon successful ligation with the oligonucleotide insert DNA, recombinant plasmid DNA could thus be readily identified based on their inability to be linearized upon digestion with *Bgl*II (Fig. 4.4A). Following screening of the plasmid DNA by *Bgl*II digestion, the uncut plasmid DNA was selected and subsequently subjected to digestion with both *Eco*RI and *Hind*III, which flank the H1 promoter and downstream insert DNA. Digestion of the putative recombinant plasmid DNAs with these enzymes resulted in the excision of a 291-bp DNA fragment, corresponding in size to the H1 promoter region (227 bp) together with the cloned oligonucleotide insert DNA (64 bp) (Fig. 4.4B, lanes 2 and 3). In contrast, digestion of the non-recombinant pSUPER plasmid DNA excised only the 227-bp H1 promoter region (Fig. 4.4B, lane 1).

To confirm that errors were not incorporated during chemical synthesis of the respective oligonucleotides, recombinant pSUPER plasmids were selected and characterized by nucleotide sequencing of both strands of the cloned insert DNA with T7 and T3 sequencing

oligonucleotides. No nucleotide differences were observed between the cloned insert DNA and their intended AHSV-6 NS1 target regions (results not shown). Recombinant plasmids containing the NS1-directed oligonucleotide insert DNA was selected, designated pSUPER-710 and pSUPER-1464, and used in all subsequent experiments. The plasmid DNA vector-expressed shRNA will be referred to as shNS1-710 and shNS1-1464, respectively.

4.3.2 Suppression of NS1-eGFP protein expression by shRNAs in BHK-21 cells

In Chapter 2 it was established that a gene-specific siRNA could be used to efficiently silence heterologous gene expression in BHK-21 cells. These studies were subsequently extended by investigating whether the constructed recombinant pSUPER shRNA delivery vectors could be used to suppress AHSV-6 NS1 gene expression. To investigate, BHK-21 cells were co-transfected with pCMV-NS1-eGFP and either pSUPER-Uneg, pSUPER-eGFP, pSUPER-710 or pSUPER-1464. The BHK-21 cell monolayers were analyzed at 24 h post-transfection by fluorescence microscopy and the NS1-eGFP fluorescence was quantified by fluorometry.

Fluorescence microscopy revealed high levels of NS1-eGFP protein expression in BHK-21 cells transfected with pCMV-NS1-eGFP and in cells co-transfected with the control non-silencing pSUPER-Uneg vector (not shown). In contrast, expression of the NS1-eGFP protein was slightly suppressed in BHK-21 cells co-transfected with the recombinant pSUPER vectors expressing an eGFP-directed shRNA and the respective NS1-directed shRNAs. Quantitative fluorometry analysis of NS1-eGFP protein expression in these BHK-21 cell monolayers indicated that sheGFP reduced expression of the chimeric protein by 10%, while shNS1-710 and shNS1-1464 reduced NS1-eGFP protein expression by 19% and 9%, respectively (Fig. 4.5). These results therefore indicated that the NS1-directed shRNAs could suppress NS1-eGFP protein expression, albeit it weakly.

4.3.3 Suppresion of NS1 mRNA expression by shRNAs in BHK-21 cells transfected with pCMV-NS1

The AHSV-6 NS1-directed shRNAs did not appear to efficiently suppress NS1-eGFP protein expression (Fig. 4.5). Since RNAi functions by silencing targeted gene expression at a post-transcriptional level, the effect of the NS1-directed shRNAs on expression of AHSV-6 NS1 mRNA transcripts was thus investigated. For this purpose, BHK-21 cell monolayers were first transfected with the recombinant pSUPER vectors expressing shNS1-710 and shNS1-1464, as

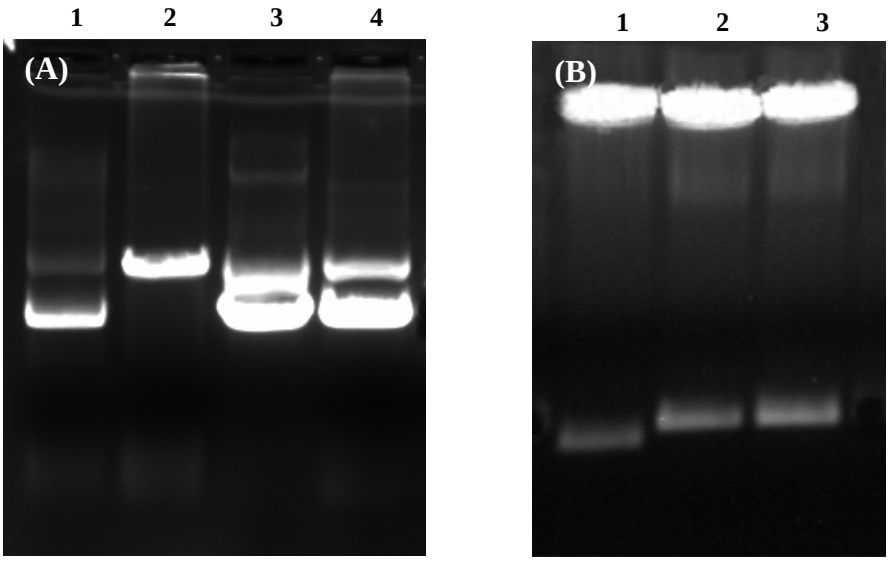

Fig. 4.4 Agarose gel electrophoretic analysis of recombinant pSUPER shRNA delivery vectors. The plasmid DNA was screened by digestion with *Bgl*II (A) and by digestion with both *Eco*RI and *Hind*III (B). (A) Lanes: 1, undigested parental pSUPER vector; 2, *Bgl*II-linearized parental pSUPER vector; 3, *Bgl*II-digested pSUPER-710; 4, *Bgl*II-digested pSUPER-1464. (B) Lanes: 1, *Hind*III- and *Eco*RI-digested parental pSUPER vector; 2, *Hind*III- and *Eco*RI-digested pSUPER-710; 3, *Hind*III- and *Eco*RI-digested pSUPER-1464.

well as with a control non-silencing shRNA (shUneg) that does not display homology with any known gene sequence. At 24 h post-transfection, the cells were transfected with the recombinant pCMV-NS1 mammalian expression vector that expresses the full-length AHSV-6 NS1 gene. Following incubation for 24 h, the cells were harvested and total RNA was isolated prior to performing reverse transcription and semi-quantitative real-time PCR. The data was analyzed using the REST© software tool (Pfaffl *et al*., 2002), as described under Materials and Methods (Section 4.2.8.4).

In contrast to BHK-21 cells transfected with the control pSUPER-Uneg shRNA delivery plasmid, NS1 mRNA expression was reduced in BHK-21 cells transfected with pSUPER-710 and pSUPER-1464. The results indicated that shNS1-710 and shNS1-1464 caused a 3.0- and 1.9-fold reduction in NS1 mRNA transcripts, respectively, as compared to cells transfected with the control plasmid pSUPER-Uneg (Fig. 4.6). These results therefore indicated that both of the NS1-directed shRNAs were indeed capable of reducing NS1 mRNA expression, albeit to different efficiencies.

4.3.4 Suppression of NS1 mRNA expression by shRNAs in BHK-21 cells infected with AHSV-6

The effect of shNS1-710 and shNS1-1464 on the abundance of AHSV-6 NS1 mRNA in virus-infected BHK-21 cells were subsequently investigated. BHK-21 cells were transfected with the recombinant pSUPER shRNA delivery vectors pSUPER-1464 and pSUPER-710, as well as with the control plasmid pSUPER-Uneg. After incubation for 24 h, the transfected cells were infected with AHSV-6 at a MOI of 1 pfu/cell. At 24 h post-infection, the cells were harvested and processed for analysis by semi-quantitative real-time PCR, using an approach similar to that described in the preceding section.

The results, presented in Fig 4.7, indicated that both the NS1-directed shRNAs reduced the amount of NS1 mRNA in the AHSV-6 infected BHK-21 cells. Whereas shNS1-710 induced a 2.6-fold reduction in NS1 mRNA transcripts, the silencing effect of shNS1-1464 on NS1 mRNA expression was weaker and resulted in a 1.2-fold reduction in NS1 mRNA transcripts. These results are in agreement with those obtained above (Fig. 4.6), indicating that shNS1-710 is more efficient than shNS1-1464 in reducing AHSV-6 NS1 mRNA expression. However, the inhibitory effect of shNS1-710 in reducing NS1 mRNA transcripts in virus-infected BHK-21 cells was slightly diminished compared to the reduction observed when the

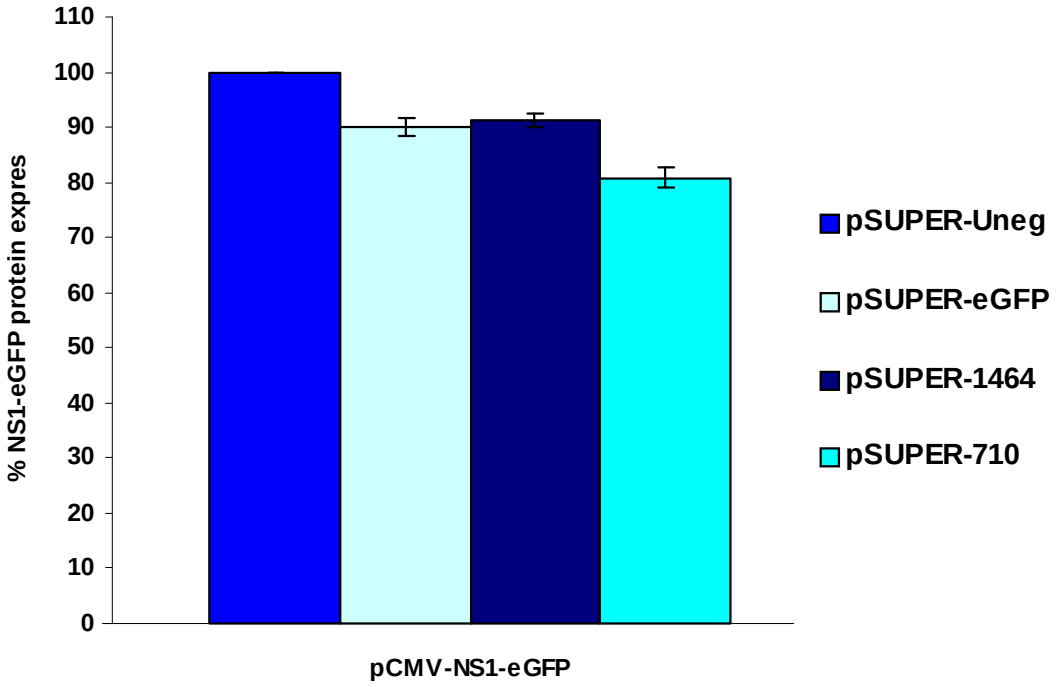

Fig. 4.5 Suppression of NS1-eGFP expression by NS1-directed shRNAs in BHK-21 cells. BHK-21 cells were co-transfected with pCMV-NS1-eGFP and pSUPER-Uneg, pSUPER-eGFP, pSUPER-1464 or pSUPER-710. At 24 h post-transfection, the cells were processed for analysis of eGFP reporter protein expression by fluorometry. The values are expressed as percentages of the value for cells co-transfected with the control non-silencing shRNA (Uneg) and represent the mean ± standard deviation (SD) from three independent experiments.

recombinant plasmid pCMV-NS1 was used in similar assays (3.0-fold vs. 2.6-fold reduction). This may reflect on differences in NS1 transcription rates between the experimental systems.

In both of the above semi-quantitative real-time PCR assays the possibility of non-specific amplification due to contaminating DNA was eliminated by performing extensive DNAse treatments and then subjecting the RNA samples to PCR amplification using the NS1 and β2-MG gene-specific oligonucleotide sets. No amplicons were obtained from the RNA samples. Moreover, the amplification specificity was verified by agarose gel electrophoresis and single amplicons of the expected size for the target and endogenous reference gene were obtained (NS1, 147 bp; β2-MG, 138 bp) (results not shown). Melt cure analyses were also performed to confirm the reproducibility of the PCR and determine the PCR efficiency (*E*). For this purpose, serial dilutions, in triplicate, of the cDNA prepared from the respective samples were subjected to semi-quantitative real-time PCR. The calculated PCR efficiencies for both targets (E_{NS1} = 1.96 And $E_{\beta2\text{-}MG}$ = 2.00) were close to the theoretic maximum and optimum efficiency of E = 2.0, indicating that the assays had a high level of reproducibility and sensitivity (Pfafll *et al*., 2002).

4.4 DISCUSSION

Of the many techniques available for the specific knock-down of genes in mammalian cells, plasmid DNA-based vectors that are capable of generating siRNA-like molecules within cells have become very appealing (Brummelkamp *et al*., 2002a; Paddison *et al*., 2002; Paul *et al*., 2002). After transfection into cells, the vector expresses shRNA, which makes a tight hairpin turn, and can be digested by Dicer to siRNA that subsequently guides the cleavage of complementary mRNA. These plasmid vector-based RNAi systems are fairly inexpensive and have been shown to inhibit multiple genes both transiently and in long-term experiments (Shlomai and Shaul, 2003; Chang *et al*., 2004; Wu *et al*., 2005; Huang *et al*., 2006; Liu *et al*., 2007). Consequently, in this part of the investigation, the use of a plasmid DNA vector-based approach to suppress expression of the AHSV-6 NS1 gene in BHK-21 cells was investigated.

To investigate, two shRNA delivery vectors, designated pSUPER-710 and pSUPER-1464, were constructed. In this system, complementary 64-nt oligonucleotides with 5’ single-stranded overhangs for ligation into the pSUPER vector were designed. The oligonucleotides

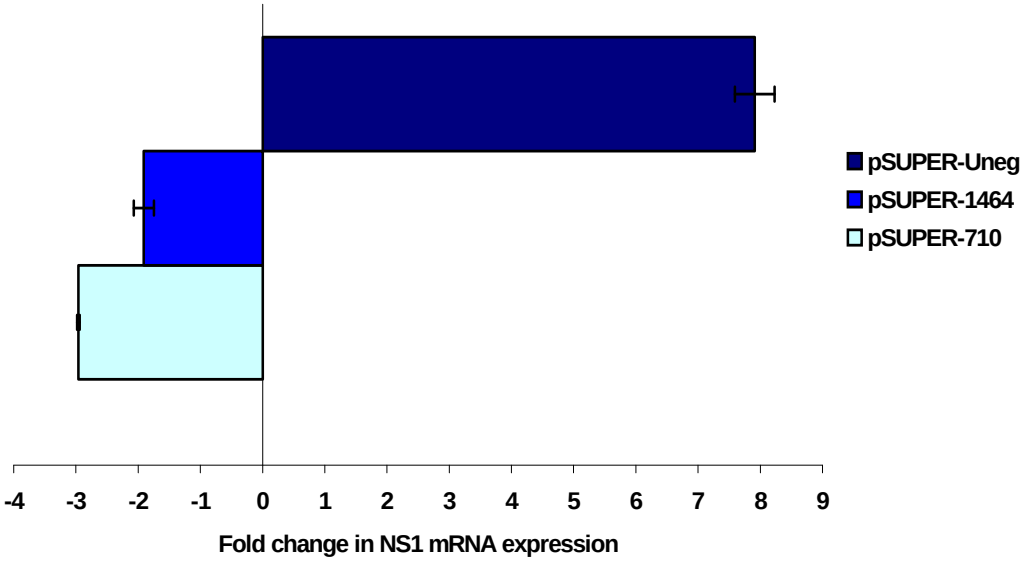

Fig. 4.6 Semi-quantitative real-time PCR analysis for relative quantification of NS1 mRNA expression in BHK-21 cells transfected with the mammalian expression plasmid pCMV-NS1. Fold changes in AHSV-6 NS1 mRNA expression levels were calculated by relative quantification of NS1 mRNA in cells transfected with recombinant pSUPER shRNA delivery vectors, expressing NS1-directed shRNAs (pSUPER-710 and pSUPER-1464) as compared with cells transfected with the control non-silencing pSUPER-Uneg vector. Real-time PCR for β2-microglobulin gene transcripts was also included in the assays as endogenous reference and used for data normalization of NS1 mRNA fold changes. The data shown are the means ± standard deviation of three experiments.

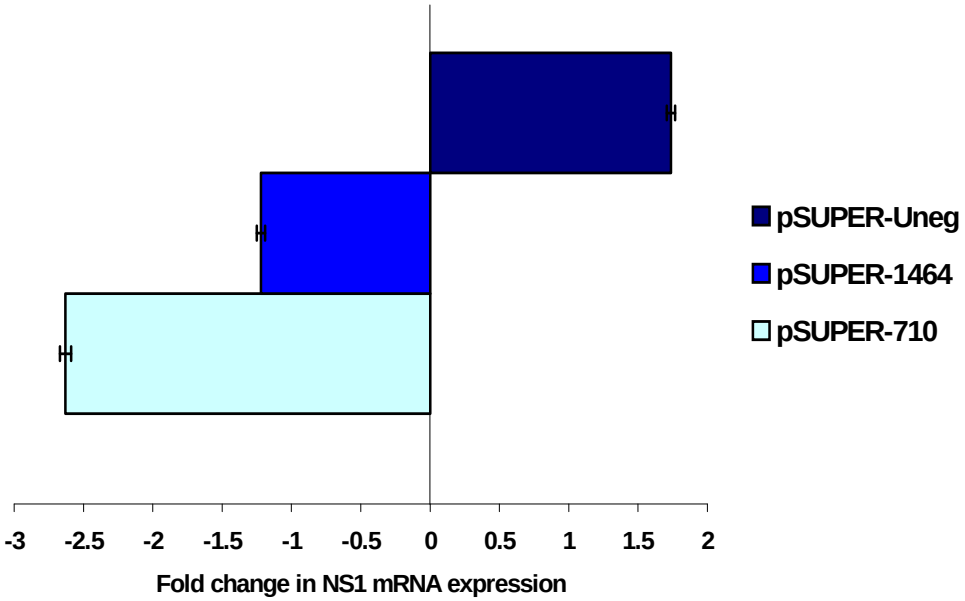

Fig. 4.7 Semi-quantitative real-time PCR analysis for relative quantification of NS1 mRNA expression in AHSV-6 infected BHK-21 cells. Fold changes in AHSV-6 NS1 mRNA expression levels were determined by semi-quantitative real-time PCR analysis, as described in the legend to Fig. 4.7. The data shown are the means ± standard deviation of three experiments.

encode 19-nt hairpin sequences specific for the AHSV-6 NS1 mRNA and were selected by making use of different siRNA design algorithms. The efficiency of the two shRNAs to mediate NS1 gene silencing was subsequently investigated and compared, following co-transfection of BHK-21 cell monolayers with the pCMV-NS1-eGFP reporter plasmid and the respective shRNA delivery vectors. Fluorometry analysis indicated that shNS1-710 and shNS1-1464 suppressed NS1-eGFP expression by 19% and 9%, respectively. Due to the weak suppression of NS1-eGFP expression and considering that RNAi functions largely through post-transcriptional gene silencing, it was next investigated whether the two NS1-directed shRNAs were indeed capable of suppressing AHSV-6 NS1 mRNA expression. For this purpose, two different approaches were adopted, *i.e.* transfection of BHK-21 cells with the recombinant pSUPER shRNA delivery vectors, followed by transfection with either the recombinant mammalian expression vector pCMV-NS1 or infection of the transfected cells with AHSV-6. The results obtained by semi-quantitative real-time PCR assays indicated that NS1 mRNA expression was reduced 3.0- and 1.9-fold by shNS1-710 and shNS1-1464, respectively, in the BHK-21 cells transfected with pCMV-NS1. In contrast, NS1 mRNA expression was suppressed slightly less efficiently in the BHK-21 cells infected with AHSV-6. In this case, NS1 mRNA expression was reduced 2.6-fold by shNS1-710 and 1.2-fold by shNS1-1464. It has been reported that the NS1 gene is transcribed at a significantly higher rate that the other viral genome segments (Huismans and Verwoerd, 1973; Van Dijk and Huismans, 1988). The reduced silencing of NS1 mRNA expression by the respective NS1-directed shRNAs in AHSV-6 infected BHK-21 cells may therefore be attributable to differences in the rate of NS1 gene transcription between the two experimental systems utilized.

From the results presented above, it is evident that although both shNS1-710 and shNS1-1464 were capable of suppressing AHSV-6 NS1 mRNA expression, they differed in their silencing efficiency. These results are in agreement with several previous reports, indicating that RNAi effector molecules targeted to different sites on the same mRNA differ in their silencing efficiency (Holen *et al*., 2002; Harborth *et al*., 2003; Vickers *et al*., 2003; Scherer *et al*., 2004; Lambeth *et al*., 2007). It is unlikely that the observed difference in silencing efficiency between the two NS1-directed shRNAs is due to differences in transfection efficiency, since, in at least two different assays (using cells transfected with pCMV-NS1 and cells infected with AHSV-6), shNS1-710 consistently suppressed NS1 mRNA expression more efficiently than did shNS1-1464. At present, there is still a lack of clear understanding of the

mechanisms that determine gene silencing efficiency of a given RNAi effector molecule. It is, however, likely to involve the primary sequence and secondary RNA structure of the RNAi effector molecule (Schwarz *et al.*, 2003; Reynolds *et al.*, 2004; Taxman *et al.*, 2006) and the target mRNA (Bohula *et al.*, 2003; Kretschmer-Kazemi Far and Sczakiel, 2003). Indeed, several reports have argued that local secondary structures in the target mRNAs may restrict the accessibility of RISC and attenuate or even abolish RNAi efficiency (Luo and Chang, 2004; Heale *et al.*, 2005; Schubert *et al.*, 2005; Overhof *et al.*, 2005). Although care was taken to select accessible NS1 mRNA target sites, as predicted with the MFOLD software programme (Zuker, 2003), it is difficult to accurately model the complex secondary structure of mRNA (Lima *et al.*, 1992; Stein, 2001; Kawasaki *et al.*, 2003). Since these models should therefore be viewed as merely predictive, it is thus plausible that the target site of shNS1-1464 on the NS1 mRNA transcript was less accessible for interaction with the RISC/shNS1-1464 complex due to local secondary structure constraints.

Although both shNS1-710 and shNS1-1464 suppressed expression of AHSV-6 NS1 mRNA, they did not induce a significant reduction in NS1-eGFP reporter protein expression. As indicated above, the NS1-directed shRNAs might have been ineffective due to changes in the local secondary structures of the target regions in the NS1 mRNA compared to those in the NS1-eGFP chimeric mRNA. This was especially noticeable for the target region of shNS1-710. Whereas the target region in the NS1-eGFP mRNA appeared to be comprised of a region rich in hairpin-loop structures in close proximity to each other (Fig. 4.2), the identical region in the NS1 mRNA was structurally less complex and the target region appeared to be more readily accessible (Fig. 4.1). Notably, Wu *et al.* (2004) reported that for some human genes analyzed, the protein levels were not affected despite a sharp reduction in the corresponding mRNA levels. It was concluded that long-lived proteins may show only a modest knock-down even if the RNAi effect at the mRNA level is readily detectable. In this regard, it is important to note that the NS1 protein, which is synthesized in a large excess over other proteins in orbivirus-infected cells and rapidly polymerizes into tubules (Nel and Huismans, 1991), is also a stable, major constituent of the infected cells throughout the infectious cycle (Huismans, 1979; Huismans and Els, 1979). Unfortunately, the unavailability of an anti-AHSV NS1 antibody precluded Western blot analyses whereby the suppression of NS1 protein levels in the experimental systems utilized in this investigation could be investigated and compared. Nevertheless, the results appear to suggest that the value of RNAi as a tool for functional studies of such stable, long-lived proteins may be weakened.

Interestingly, the results obtained in this part of the investigation also suggested that shRNAs may not be as effective as chemically synthesized siRNAs to suppress gene expression. Several reports have claimed that shRNAs are as effective and even more effective than siRNAs to mediate gene silencing (Scherer *et al.*, 2004; Siolas *et al.*, 2005; Vlassov *et al.*, 2007), while others have claimed the opposite (Bridge *et al.*, 2003). It should be kept in mind that there are no specific guidelines for the design of shRNAs. Since shRNAs are processed by Dicer intracellularly to siRNAs, it has generally been recommended that shRNA design should be based on the design rules for siRNAs (Amarzguioui *et al.*, 2005). However, several recent reports have demonstrated that although a given siRNA sequence can effectively suppress expression of a target gene, a corresponding DNA-expressed shRNA may not perform equally (Peng *et al.*, 2005; Lambeth *et al.*, 2007). In this investigation, a chemically synthesized siRNA directed to the eGFP reporter gene (eGFP-siRNA) was previously shown to suppress NS1-eGFP protein expression by 55% (Chapter 2), but when expressed as a shRNA, NS1-eGFP protein expression was reduced by only 10% (this Chapter, Fig. 4.5). Several factors may account for the difference in NS1-eGFP protein suppression observed by the eGFP-directed siRNA compared to the corresponding shRNA. The difference may be due to decreased transfection efficiency of the plasmid DNA compared to that of siRNA. In contrast to plasmid DNA, which has a high molecular mass and highly charged characteristics, the chemically synthesized siRNA is much smaller and thus enter cells more easily (Schiffelers *et al.*, 2004; Judge *et al.*, 2005). Also, in the case of shRNA delivery vectors, the plasmid DNA must first be transcribed by the cellular machinery to generate shRNA transcripts that then need to be processed by Dicer into siRNAs and, in addition, the amount of shRNA transcripts generated in the transfected cells by the plasmid vector DNA cannot be controlled. In contrast, chemically synthesized siRNAs allow for precise control of the amount of the siRNA and immediate gene silencing due to their delivery directly into the cell cytoplasm (Elbashir *et al.*, 2002; Mittal, 2004). Moreover, Taxman *et al.* (2006) reported that none of the algorithms frequently used for siRNA design showed a statistically significant ability to discriminate between effective and ineffective shRNA. Thus, the absence of satisfactory shRNA design tools may be another factor in the difference observed for siRNA versus expressed shRNA to mediate silencing of the chimeric NS1-eGFP protein.

In conclusion, the results obtained in this part of the investigation indicated that shRNA-mediated silencing of the AHSV-6 NS1 gene in mammalian BHK-21 cells is tractable. However, the results also highlighted several aspects that warrant further investigation. These

include the selection of optimal NS1 target sequences for increased NS1 gene silencing efficiency and the use of alternative shRNA delivery vectors to mediate persistent long-term gene silencing. The latter may be used to overcome problems associated with the abundance and longetivity of the NS1 protein in infected cells. These aspects will be discussed in greater detail in the following Chapter.

CHAPTER 5

CONCLUDING REMARKS

RNA interference (RNAi) is an evolutionary conserved mechanism of post-transcriptional gene silencing produced by double-stranded (ds) RNA (Fire *et al.*, 1998; Tuschl *et al.*, 1999). Currently, RNAi is widely used both as a powerful approach for the analysis of viral gene function (López *et al.*, 2005; Campagna *et al.*, 2005; Wirblich *et al.*, 2006) and as a strategy for gene silencing-based antiviral therapeutics (Haasnoot *et al.*, 2003; Stram and Kuzntzova, 2006). As compared with other gene silencing reagents such as antisense oligonucleotides, ribozymes and intrabodies (Nahreini *et al.*, 2004; Robishaw *et al.*, 2004; Owens *et al.*, 2004; Vascotto *et al.*, 2005), short interfering RNAs (siRNAs) have become the most widely used gene silencing reagents for manipulating gene activity in mammalian systems (Elbashir *et al.*, 2002; Scherer *et al.*, 2004; Cullen, 2006). In addition to exogenous delivery of chemically synthesized siRNAs into mammalian cells (Elbashir *et al.*, 2001a; Caplen *et al.*, 2001), active siRNAs can also be generated from endogenous vector-expressed short hairpin RNAs (shRNAs) (Brummelkamp *et al.*, 2002a; Paddison *et al.*, 2002). Consequently, the aim of this investigation was essentially to develop a plasmid DNA vector-based RNAi assay whereby expression of the NS1 gene of AHSV-6 could be silenced with shRNAs in mammalian BHK-21 cells. The details of the results obtained in the course of achieving this objective have been discussed in the individual Chapters. The new information that has evolved during this investigation will be briefly summarized and suggestions regarding future research in this field will be made.

Results obtained during the course of this investigation indicated that the two shRNAs directed to the AHSV-6 NS1 gene were capable of reducing NS1 mRNA expression. Whereas shNS1-710 induced a 2.6-fold reduction in NS1 mRNA expression in virus-infected cells, shNS1-1464 was less efficient and induced a 1.2-fold reduction in NS1 mRNA expression (Chapter 4). It has previously been reported that shRNA-mediated silencing of AHSV-9 NS2 gene expression induced a 4.1-fold reduction in NS2 mRNA expression (Nieuwoudt, 2008). Thus, the results obtained may suggest that there is room for improvement in searching for the "ideal" sequence in NS1 that may yield optimum silencing effectivity. However, this may not be a trivial matter as a major problem in the RNAi field concerns the design of effective shRNAs. Notably, two studies have described approaches whereby the efficiency of a shRNA can be enhanced (Kim *et al.*, 2005; Siolas *et al.*, 2005). In the study by Kim *et al.* (2005), a set of chemically synthesized siRNAs of varying length was used to silence target gene expression. The optimum silencing efficiency was found for siRNAs being 27 nt in length. The 27-nt siRNAs were purportedly also suitable to target sites that were refractory to

silencing by 21-nt siRNAs, and did not activate the interferon response or protein kinase R (PKR). Similarly, Siolas *et al*. (2005) reported that 29-nt shRNAs were particularly potent inducers of RNAi. The improved efficiencies of these longer RNAi effector molecules, which were reported to be up to 100-fold more potent than the corresponding conventional 21-nt siRNAs, was postulated to result from their recognition and cleavage by Dicer, followed by their subsequently more efficient incorporation into the RISC complex. It was suggested that providing the RNAi machinery with a Dicer substrate presumably results in more efficient incorporation of the active 21-nt RNAi effector molecule into RISC (Kim *et al*., 2005; Siolas *et al*. 2005). Consequently, based on these findings, it was recently proposed that shRNA design should proceed according to the following steps: (i) selection of the desired 21-nt siRNA sequence using the most current design rules; (ii) extension of the above sequence towards the 3' end of the target for a duplex length of 25-29 bp; and (iii) capping of the 3' end of the duplex with a loop, preferably one derived from a naturally occurring miRNA (Amarzguioui *et al*., 2005). Since the screening of effective shRNAs is still an empirical process, future research should allow for the screening of an increased number of candidate shRNAs and these should be designed by taking the above recommendations into account.

Despite the shRNA-mediated reduction in AHSV-6 mRNA expression being readily detectable, a corresponding reduction in NS1 protein levels could not be demonstrated due to the lack of an anti-NS1 antibody. Nevertheless, the NS1-directed shRNAs were shown to mediate silencing of the NS1-eGFP reporter protein, albeit weakly (9-19%). Although differences in the local secondary structure of the target sequences in the native NS1 and chimeric NS1-eGFP mRNAs may account for the weak correlation between these results, the results also hinted at the importance of the abundance and half-life of the target protein in evaluating RNAi efficiency. The NS1 protein is the most abundantly expressed protein during virus infection (Huismans, 1979) and the NS1-rich tubules are major constituents of the infected cells throughout the viral infectious cycle (Huismans and Els, 1979). Previous reports have indicated that siRNA-mediated silencing of highly abundant proteins requires a higher dosage of the siRNA or multiple (2 to 3 times) transfections of the mammalian cells with the siRNA, while in the case of proteins with long half-lives the assays have to be performed over a longer period of time in order to detect a knock-down effect on the protein level (Ritter *et al*., 2003; Choi *et al*., 2005). The pSUPER shRNA delivery vector used in this investigation lacks a selectable marker for mammalian cells and therefore does not allow for persistent gene silencing. Persistent long-term silencing of AHSV-6 NS1 gene expression may be obtained

by making use of other plasmid DNA, lentiviral or retroviral shRNA expression vectors that allows for antibiotic-based selection of transductants that stably express the relevant shRNAs (Brummelkamp *et al*., 2002b; Rubinson *et al*., 2003; Schuck *et al*., 2004; Wadhwa *et al*., 2004; Cullen, 2006). The use of such vector systems should allow RNAi assays to be performed over a longer period of time that is permissible with the pSUPER shRNA delivery vector. This may make it possible to suppress NS1 mRNA expression to such an extent where no new protein synthesis will be initiated, thus allowing for detailed characterization of the resulting loss-of-function phenotype.

In this investigation, low expression levels in BHK-21 cells necessitated that the eGFP and chimeric NS1-eGFP genes had to be recloned from mammalian expression vectors and expressed in *S. frugiperda* insect cells by means of baculovirus recombinants in order to allow for their characterization (Chapter 3). In this regard, it is interesting to note that although the baculovirus system was initially classified as being non-infectious to mammalian cells (O'Reilly *et al*., 1992), it has subsequently been reported that baculovirus can be used to deliver heterologous genes into numerous mammalian cells, including BHK cells (Ghosh *et al*., 2002; Huser and Hofmann, 2003; Cheng *et al*., 2004; Phillips *et al*., 2005; Hu, 2005). The transduction efficiencies may vary depending on the cell types, but it has been reported to be up to 95% for BHK-21 cells (Cheng *et al.*, 2004; Hu, 2005). Moreover, it has also been reported that enhanced gene transfer efficiency could be obtained in a variety of cell lines when using a recombinant baculovirus expressing the surface glycoprotein of vesicular stomatitis virus (VSV G) (Lu *et al*., 2006). Recently, Philipps *et al*. (2005) described the construction of a derivative pFastBac1™ vector in which the baculovirus polyhedrin promoter was replaced with the p10 promoter, and the cytomegalovirus immediate early enhancer and promoter was then cloned upstream of the baculovirus p10 promoter. Using this vector system, the expression yields in *S. frugiperda* cells were comparable to that determined for the unmodified pFastBac1™ vector and a high expression level in mammalian cells (CHO and HEK-293) was achieved after transduction of the cells with the recombinant baculovirus (Philipps *et al*., 2005). A future avenue of research may therefore be to construct such derivative baculovirus vectors that will allow the expression of the target protein in both insect and mammalian cells, thus eliminating additional cloning steps into mammalian expression vectors. The baculovirus-transduced mammalian cells may also be used to screen for effective target gene-specific RNAi effector molecules by making use of an approach similar to that described in this investigation (Chapter 2). An extension of this research may

also entail construction of recombinant baculoviruses that can serve as alternative vehicles for shRNA delivery. Based on their high transduction efficiency of mammalian cells, they may overcome the low transfection efficiency often associated with plasmid DNA shRNA delivery vectors (Schiffelers *et al*., 2004; Judge *et al*., 2005).

As indicated previously, one of the major drawbacks of research with AHSV has been the lack of a suitable reverse genetics system that would allow genetic manipulation of the virus. However, during the course of finalizing this dissertation, it was reported that it is possible to recover infectious bluetongue virus (BTV) wholly from single-stranded (ss) RNA synthesized *in vitro* using BTV core particles (Boyce and Roy, 2007). These results not only indicated that the viral ssRNA is infectious, but it also suggested a means for establishing a helper virus-independent reverse genetics system for orbiviruses. Consequently, the development of a reverse genetics system for BTV was recently reported (Boyce *et al*., 2008). It was demonstrated that infectious BTV could be recovered entirely from *in vitro*-synthesized T7 transcripts, derived from cDNA clones, which had been synthesized in the presence of a cap analogue. Moreover, the reverse genetics system was shown to allow for the generation of BTV mutants in a consistent genetic background (Boyce *et al*., 2008). Clearly, the development and establishment of such a reverse genetics system for AHSV would be of great benefit to research in this field. Not only will such a system allow for the introduction of specific mutations into the genome segments of AHSV thereby enhancing understanding of the functions of the viral proteins in the replicating virus, but it will also allow for the mapping of regulatory sequences that, amongst other, control the replication and packaging of the respective genome segments.

In conclusion, a plasmid DNA vector-based gene silencing assay has been developed for the suppression of AHSV-6 NS1 gene expression in BHK-21 cells by means of shRNAs. Having established this technology, future studies should be directed at optimizing the assay and using the developed assay to investigate not only NS1 protein function, but also the function of other AHSV proteins during the replication cycle of the virus. It can be envisaged that the development of a reverse genetics system for AHSV, combined with the use of RNAi-based gene silencing technologies, will become a dominant future research area and should facilitate greatly molecular studies of individual proteins in the context of the whole virus.

CONGRESS CONTRIBUTIONS DURING THE COURSE OF THIS STUDY

Conference contributions

1. **Roos, H.J.**, Huismans, H. and Theron, J. (2004) Silencing of the African horse sickness serotype 6 NS1 gene with cognate siRNAs in mammalian cell culture. Joint Congress of the South African Genetics Society (SAGS) and the South African Society for Microbiology (SASM), 4-7 April 2004, Stellenbosch.

2. **Roos, H.J.**, Huismans, H. and Theron, J. (2004) Inhibition of African horse sickness virus NS1 gene expression in mammalian cells using short interfering RNA (siRNAs). The 43rd Annual Conference of the Microscopy Society of Southern Africa (MSSA), 30 November-3 December 2004, Pretoria.

3. **Roos, H.J.**, Huismans, H. and Theron, J. (2006) Silencing of the nonstructural gene NS1 of African horse sickness virus by RNA interference. The 14th Biennial Congress of the South African Society for Microbiology (SASM), 9-12 April 2006, Pretoria.

Refereed published conference proceeding

1. Roos, H.J., Huismans, H., Hall, A.N. and Theron, J. (2004). Inhibition of African horse sickness virus NS1 gene expression in mammalian cells using short interfering RNA (siRNA). Proceedings of the Electron Microscopy Society of Southern Africa **34**, 40.

REFERENCES

Altschul, S.F., Madden, T.L., Schaffer, A.A., Zhang, J., Zhang, Z., Miller, W. and Lipman, D.J. (1997). Gapped BLAST and PSI-BLAST: A new generation of protein database search programs. *Nucl. Acids Res*. **25**, 3389-3402.

Amarzguioui, M. and Prydz, H. (2004). An algorithm for selection of functional siRNA sequences. *Biochem. Biophys. Res. Commun.* **316**, 1050-1058.

Amarzguioui, M., Holen, T., Babaie, E. and Prydz, H. (2003). Tolerance for mutations and chemical modifications in a siRNA. *Nucl. Acids Res.* **31**, 589-595.

Amarzguioui, M., Rossi, J.J. and Kim, D. (2005). Approaches for chemically synthesized siRNA and vector-mediated RNAi. *FEBS Lett*. **579**, 5974-5981.

Anzola, J.V., Xu, Z., Asamizu, T. and Nuss, D.L. (1987). Segment-specific inverted repeats found adjacent to conserved terminal sequences in wound tumor virus genome and defective interfering RNAs. *Proc. Natl. Acad. Sci. USA* **84**, 350-357.

Arias, C.F., Déctor, M.A., Segovia, L., López, T., Camacho, M., Isa, P., Espinosa, R. and López, S. (2004). RNA silencing of rotavirus gene expression. *Virus Res*. **102**, 43-51.

Bansal, O.B., Stokes, A., Bansal, A., Bishop, D. and Roy, P. (1998). Membrane organization of bluetongue virus nonstructural glycoprotein NS3. *J. Virol.* **72**, 3362-3369.

Bantounas, I., Phylactou, L.A. and Uney, J.B. (2004). RNA interference and the use of small interfering RNA to study gene function in mammalian systems. *J. Mol. Endocrinol.* **33**, 545-557.

Barnard, J.H. (1998). Epidemiology of African horse sickness and the role of the zebra in South Africa. *Arch. Virol.* (*Suppl.*) **14**, 13-19.

Basak, A.K., Gouet, P., Grimes, J., Roy, P. and Stuart, D. (1996). Crystal structure of the top domain of African horse sickness virus VP7: Comparison with Bluetongue virus VP7. *J. Virol.* **70**, 3797-3806.

Basak, A.K., Stuart, D.I. and Roy, P. (1992). Preliminary crystallographic study of bluetongue virus capsid protein, VP7. *J. Mol. Biol.* **228**, 687-689.

Beaton, A.R., Rodriguez, J., Reddy, Y.K. and Roy, P. (2002). The membrane trafficking protein calpactin forms a complex with bluetongue virus protein NS3 and mediates virus release. *Proc. Natl. Acad. Sci. USA* **99**,13154-13159.

Bentley, L., Fehrsen, J., Jordaan, F., Huismans, H. and du Plessis, D.H. (2000). Identification of antigenic regions on VP2 of African horsesickness virus serotype 3 by using phage-displayed epitope libraries. *J. Gen. Virol.* **81**, 993-1000.

Bernstein, E., Caudy, A.A., Hammond, S.M. and Hannon, G.J. (2001). Role for a bidentate ribonuclease in the initiation step of RNA interference. *Nature* **409**, 363-366.

Bernstein, E., Kim, S.Y., Carmell, M.A., Murchison, E.P., Alcorn, H., Li, M.Z., Mills, A.A., Elledge, S.J., Anderson, K.V. and Hannon, G.J. (2003). Dicer is essential for mouse development. *Nature Genet*. **35**, 215-217.

Bitko, V. and Barik, S. (2001). Phenotypic silencing of cytoplasmic genes using sequence-specific double-stranded short interfering RNA and its application in the reverse genetics of wild type negative-strand RNA viruses. *BMC Microbiol.* **1**, 1-11.

Blumenstiel, J.P. and Hartl, D.L. (2005). Evidence for maternally transmitted small interfering RNA in the repression of transposition in *Drosophila virilis*. *Proc. Natl. Acad. Sci. USA* **102**, 15965-15970.

Bohula, E.A., Salisbury, A.J., Sohail, M., Playford, M.P., Riedemann, J., Southern, E.M. and Macaulay, V.M. (2003). The efficacy of small interfering RNAs targeted to the type 1 insulin-like growth factor receptor (IGF1R) is influenced by secondary structure in the IGF1R transcript. *J. Biol. Chem.* **278**, 15991-15997.

Borden, E.C., Shope, R.E. and Murphy, F.A. (1971). Physicochemical and morphological relationships of some arthropod-borne viruses to bluetongue virus - a new taxonomic group. Electron microscopic studies. *J. Gen. Virol.* **13**, 273-283.

Boyce, M. and Roy, P. (2007). Recovery of infectious bluetongue virus from RNA. *J. Virol*. **81**, 2179-2186.

Boyce, M., Celma, C. and Roy, P. (2008). Development of reverse genetics systems for bluetongue virus: Recovery of infectious virus from synthetic RNA transcripts. *J. Virol*. (published online ahead of print on 18 June 2008).

Boyce, M., Wehrfritz, J., Noad, R. and Roy, P. (2004). Purified recombinant Bluetongue virus VP1 exhibits RNA replicase activity. *J. Virol*. **78**, 3994-4002.

Boyle, J.S. and Lew, A.M. (1995). An inexpensive alternative to glassmilk for DNA purification. *Tends Genet.* **11**, 8.

Bremer, C.W., Huismans, H. and van Dijk, A.A. (1990). Characterization and cloning of the African horsesickness virus genome. *J. Gen. Virol.* **71**, 793-799.

Bremer, C.W. (1976). A gel electrophoretic study of the protein and nucleic acid components of African horsesickness virus. *Onderstepoort J. Vet. Res.* **43**, 193-200.

Bridge, A.J., Pebernard, S., Ducraux, A., Nicoulaz, A-L. and Iggo, R. (2003). Induction of an interferon response by RNAi vectors in mammalian cells. *Nature Genet.* **34**, 263-264.

Brookes, S.M., Hyatt, A.D. and Eaton, B.T. (1993). Characterization of virus inclusion bodies in bluetongue virus-infected cells. *J. Gen. Virol.* **74**, 525-530.

Brown, S.E., Morrison, H.G., Karabatsos, N. and Knudson, D.L. (1991). Genetic relatedness of two new Orbivirus serogroups: Orungo and Lebombo. *J. Gen. Virol.* **72**, 1065-1072.

Brummelkamp, T.R., Bernards, R. and Agami, R. (2002a). A system for stable expression of short interfering RNAs in mammalian cells. *Science* **296**, 550-553.

Brummelkamp, T.R., Bernards, R. and Agami, R. (2002b). Stable suppression of tumorgenicity by virus-mediated RNA interference. *Cancer Cell* **2**, 243-247.

Burger, L. (2006). Silencing African horsesickness virus VP7 protein expression *in vitro* by RNA interference. M.Sc Dissertation, Department of Microbiology and Plant Pathology, Faculty of Biological and Agricultural Sciences, University of Pretoria, South Africa.

Burroughs, J.N., O'Hara, R.S., Smale, C.J., Hamblin, C., Walton, A., Armstrong, R. and Mertens, P.P.C. (1994). Purification and properties of virus particles, infectious subviral particles, cores and VP7 crystals of African horsesickness virus serotype 9. *J. Gen. Virol.* **75**, 1849-1857.

Calisher, C.H. and Mertens, P.P.C. (1998). Taxonomy of African horse sickness viruses. *Arch. Virol.* (*Suppl.*) **14**, 3-11.

Campagna, M., Eichwald, C., Vascotto, F. and Burrone, O.R. (2005). RNA interference of rotavirus segment 11 mRNA reveals the essential role of NSP5 in the virus replicative cycle. *J. Gen. Virol.* **86**, 1481-1487.

Caplen, N.J., Parrish, S., Imani, F., Fire, A. and Morgan, R.A. (2001). Specific inhibition of gene expression by small double-stranded RNAs in vertebrate and invertebrate systems. *Proc. Natl. Acad. Sci. USA* **98**, 9742-9747.

Carmell, M.A., Xuan, Z., Zhang, M.Q. and Hannon, G.J. (2002). The Argonaute family: Tentacles that reach into RNAi: developmental control, stem cell maintenance and tumorgenesis. *Gene Dev.* **16**, 2733-2742.

Carmona, S., Ely, A., Crowther, C., Moolla, N., Salazar, F.H., Marion, P.L., Ferry, N., Weinberg, M.S. and Arbuthnot, P. (2005). Effective inhibition of HBV replication *in vivo* by anti-HBx short hairpin RNAs. *Mol. Ther*. **13**, 411-421.

Carroll, S.S., Benseler, F. and Olse, D.B. (1996). Preparation and use of synthetic oligoribonucleotides as tools for study of viral polymerases. *Methods Enzymol*. **275**, 365-382.

Castanotto, D., Li, H. and Rossi, J.J. (2002). Functional siRNA expression from transfected PCR products. *RNA* **8**, 1454-1460.

Cerutti, L., Mian, N. and Bateman, A. (2000). Domains in gene silencing and cell differentiation proteins: The novel PAZ domain and redefinition of the Piwi domain. *Trends Biochem. Sci.* **25**, 481-482.

Chang, H.S., Lin, C.H., Chen, Y.C. and Yu, W.C.Y. (2004). Using siRNA technique to generate transgenic animals with spatiotemporal and conditional gene knockdown. *Am. J. Pathol*. **165**, 1535-1541.

Chen, W., Liu, M., Jiao, Y., Yan, W., Wei, X., Chen, J., Fei, L., Liu, Y., Zuo, X., Yang, F., Lu, Y. and Zheng, Z. (2006). Adenovirus-mediated RNA interference against foot-and-mouth disease virus infection both *in vitro* and *in vivo*. *J. Virol*. **80**, 3559-3566.

Chen, W., Yan, W., Du, Q., Fei, L., Liu, M., Ni, Z., Sheng, Z. and Zheng, Z. (2004). RNA interference targeting VP1 inhibits foot-and-mouth disease virus replication in BHK-21 cells and suckling mice. *J. Virol.* **78**, 6900-6907.

Cheng, T., Xu, C-Y., Wang, Y-B., Chen, M., Wu, T., Zhang, J. and Xia, N-S. (2004). A rapid and efficient method to express target genes in mammalian cells by baculovirus. *World J. Gastroenterol.* **10**, 1612-1618.

Choi, I., Cho, B.R., Kim, D., Miyagawa, S., Kubo, T., Kim, J.Y., Park, C.G., Hwang, W.S., Lee, J.S. and Ahn, C. (2005). Choice of the adequate detection time for the accurate evaluation of the efficiency of siRNA-induced gene silencing. *J. Biotechnol*. **120**, 251-261.

Chuma, T., Le Blois, H., Sanchez-Vizcaino, J.M., Diaz-Laviada, M. and Roy, P. (1992). Expression of the major core antigen VP7 of African horsesickness virus by a recombinant baculovirus and its use as a group-specific diagnostic reagent. *J. Gen. Virol.* **73**, 925-931.

Ciccarone, V.C., Polayes, D. and Luckow, V.A. (1997). In: Generation of recombinant baculovirus DNA using baculovirus shuttle vector. U. Reischt (Ed.), pp. 38-96. Humana Press Inc., New Jersey.

Coetzer, J.A.W. and Erasmus, B.J. (1994). African horse sickness. In: Infectious diseases of live-stock with special reference to Southern Africa. J.A.W. Coetzer, G.R. Thomson and R.C. Tustin (Eds.), pp. 460-475. Oxford University Press, Cape Town.

Cogoni, C., Irelan, J.T., Schumacker, M., Schmidhauser, T.J., Selker, E.U. and Macino, G. (1996). Transgene silencing of the *al-1* gene in vegetative cells of *Neurospora* is mediated by a cytoplasmic effector and does not depend on DNA-DNA interactions or DNA methylation. *EMBO J.* **15**, 3153-3163.

Colbère-Garapin, F., Blondel, B., Sualnier, A., Pelletier, I. and Labadie, K. (2005). Silencing viruses by RNA interference. *Microbes Infect.* **7**, 767-775.

Cowley, J.A. and Gorman, B.M. (1987). Genetic reassortants for identification of the genome segment coding for the bluetongue virus haemagglutinin. *J. Virol.* **61**, 2304-2306.

Cowley, J.A., Walker, P.J. and Gorman, B.M. (1992). Recognition sites in assembly of bluetongue viruses. In: Bluetongue, African horse sickness and related orbiviruses. Proceedings of the Second International Symposium. T.E. Walton and B.I. Osborn (Eds.), pp. 423-432. CRC Press, London.

Cullen, B.R. (2006). Induction of stable RNA interference in mammalian cells. *Gene Ther.* **13**, 503-508.

Czauderna, F., Fechtner, M., Dames, S., Aygün, H., Klippel, A., Pronk, G.J., Giese, K. and Kaufmann, J. (2003). Structural variations and stabilizing modifications of synthetic siRNAs in mammalian cells. *Nucl. Acids Res.* **31**, 2705-2716.

De Los Santos, T., Wu, Q., De Avila Botton, S. and Grubman, M.J. (2005). Short hairpin RNA targeted to the highly conserved 2B nonstructural protein coding region inhibits replication of multiple serotypes of foot-and-mouth disease virus. *Virol.* **335**, 222-231.

De Waal, P.J. and Huismans, H. (2005). Characterization of the nucleic acid binding activity of inner core protein VP6 of African horse sickness virus. *Arch. Virol.* **150**, 2037-2050.

Déctor, M.A., Romero, P., López, S. and Arias, C.F. (2002). Rotavirus gene silencing by small interfering RNAs. *EMBO Rep.* **3**, 1175-1180.

Devaney, M.A., Kendall, J. and Grubman, M.J. (1988). Characterization of a non-structural phosphoprotein of two orbiviruses. *Virus Res.* **11**, 151-164.

Doench, J.G., Petersen, C.P. and Sharp, P.A. (2003). siRNAs can function as miRNAs. *Genes Dev.* **17**, 438-442.

Donze, O. and Picard, D. (2002). RNA interference in mammalian cells using siRNAs synthesized with T7 RNA polymerase. *Nucl. Acids Res.* **30**, e46.

Dorsett, Y. and Tuchl, T. (2004). siRNAs: Applications in functional genomics and potential as therapeutics. *Nature Rev. Drug Discov.* **3**, 318-329.

Dykxhoorn, D.M., Novina, C.D. and Sharp, P.A. (2003). Killing the messenger: Short RNAs that silence gene expression. *Nature Rev. Mol. Cell. Biol.* **4**, 457-467.

Eaton, B.T., Hyatt, A.D. and Brookes, S.M. (1990). The replication of bluetongue virus. *Curr. Top. Microbiol. Immunol.* **162**, 89-118.

Eaton, B.T., Hyatt, A.D. and White, J.R. (1987). Association of bluetongue virus with the cytoskeleton. *Virol.* **157**, 107-116.

Eaton, B.T., Hyatt, A.D. and White, J.R. (1988). Localization of the nonstructural protein NS1 in bluetongue virus-infected cells and its presence in virus particles. *Virol.* **163**, 527-537.

El Hasnaoui, H., El Harrak, M., Zientara, S., Laviada, M. and Hamblin, C. (1998). Serological and virological responses in mules and donkeys following inoculation with African horse sickness virus serotype 4. *Arch. Virol.* (*Suppl.*) **14**, 29-36.

Elbashir, S.M., Harborth, J., Lendeckel, W., Yalcin, A., Weber, K. and Tuschl, T. (2001a). Duplexes of 21-nucleotide RNAs mediate RNA interference in cultured mammalian cells. *Nature* **411**, 494-498.

Elbashir, S.M., Lendeckel, W. and Tuschl, T. (2001b). RNA interference is mediated by 21 and 22-nucleotide RNAs. *Genes Dev.* **15**, 188-200.

Elbashir, S.M., Martinez, J., Patkaniowska, A., Lendeckel, W. and Tuschl, T. (2001c). Functional anatomy of siRNAs for mediating efficient RNAi in *Drosophila melanogaster* embryo lysate. *EMBO J.* **20**, 6877-6888.

Elbashir, S.M., Harborth, J., Weber, K. and Tuschl, T. (2002). Analysis of gene functions in somatic mammalian cells with small interfering RNAs. *Methods* **26**, 199-213.

Erasmus, B.J. (1976). A new approach to polyvalent immunization against African horsesickness. Proceeding of the Fourth International Conference of Equine Infectious Diseases, Lyon, pp. 401-403. Veterinary Publications, Inc., New Jersey.

Erasmus, B.J. (1994). African horse sickness vaccine information. Circular to veterinary surgeons in practice in South Africa. Onderstepoort Biological Products, Department of Agriculture, Republic of South Africa.

Erasmus, B.J., Young, E., Pieterse, L.M. and Boshoff, S.T. (1978). The susceptibility of zebra and elephants to African horsesickness virus. *J. Equine Med. Surg.* (*Suppl.*) **1**, 409-413.

Fassi-Fihri, O., El Harrak, M. and Fassi-Fehri, M.M. (1998). Clinical, virological and immune responses of normal and immunosuppressed donkeys (*Equus asinus africanus*) after inoculation with African horse sickness virus. *Arch. Virol.* (*Suppl.*) **14**, 49-56.

Fire, A., Xu, S., Montgomery, M.K., Kostas, S.A., Driver, S.E. and Mello, C.C. (1998). Potent and specific genetic interference by double-stranded RNA in *Caenorhabditis elegans*. *Nature* **391**, 806-811.

Floyd-Smith, G., Slattery, E. and Lengyel, P. (1981). Interferon action: RNA cleavage pattern of a (2'-5') oligoadenylate-dependent endonuclease. *Science* **212**, 1030-1032.

Forzan, M., Marsh, M. and Roy, P. (2007). Bluetongue virus entry into the cells. *J. Virol*. **81**, 4819-4827.

Forzan, M., Wirblich, C. and Roy, P. (2004). A capsid protein of nonenveloped bluetongue virus exhibits membrane fusion activity. *Proc. Natl. Acad. Sci. USA* **101**, 2100-2105.

Francki, R.I.B., Fauquet, C.M., Knudson, D.L. and Brown, F. (1991). Classification and nomenclature of viruses: Fifth report of the International Committee on Taxonomy of Viruses. *Arch. Virol. (Suppl.)* **2**, 12-23.

French, T.J., Inumaru, S. and Roy, P. (1989). Expression of two related nonstructural proteins of bluetongue virus (BTV) type 10 in insect cells by a recombinant baculovirus: Production of polyclonal ascetic fluid and characterization of the gene product in BTV-infected BHK cells. *J. Virol.* **63**, 3270-3278.

Ge, Q., Filip, L., Bai, A., Nguyen, T., Eisen, H.N. and Chen, J. (2004). Inhibition of influenza virus production in virus-infected mice by RNA interference. *Proc. Natl. Acad. Sci. USA* **101**, 8676-8681.

Ghosh, M.K., Borca, M.V. and Roy, P. (2002). Virus-derived tubular structure displaying foreign sequences on the surface elicit $CD4^+$ Th cell and protective humoral responses. *Virol*. **302**, 383-392.

Gitlin, L. and Andino, R. (2003). Nucleic acid-based immune system: Antiviral potential of mammalian RNA silencing. *J. Virol.* **77**, 7159-7165.

Gitlin, L., Karelsky, S. and Andino, R. (2002). Short interfering RNA confers intracellular antiviral immunity in human cells. *Nature* **418**, 430-434.

Goodbourn, S., Didcock, L. and Randall, R.E. (2000). Interferons: Cell signaling, immune modulation, antiviral response and viral countermeasures. *J. Gen. Virol.* **81**, 2341-2364.

Gorman, B.M. (1992). An overview of orbiviruses. In: Bluetongue, African horse sickness and related orbiviruses, Proceedings of the Second International symposium. T.E Walton and. B.I. Osburn (Eds.), pp. 335-348. CRC Press, London.

Gorman, B.M. and Taylor, J. (1985). Orbiviruses. In: Field's Virology. B.N. Fields and D.M. Knipe (Eds.), pp. 275-278. Raven Press, New York.

Gorman, B.M., Taylor, J., Brown, K. and Meltzer, A.J. (1977). Laboratory studies of orbiviruses. Structure and genetics of orbiviruses. *Annu. Rep. Qld. Inst. Med. Res.* **32**, 15.

Gould, A.R. and Hyatt, A.D. (1994). The orbivirus genus, diversity, structure, replication and phylogenetic relationships. *Comp. Immunol. Microbiol. Infect. Dis.* **17**, 163-188.

Grimes, J.M., Burroughs, J.N., Gouet, P., Diprose, J.M., Malby, R., Zientara, S., Mertens, P.P. and Stuart, D.I. (1998). The atomic structure of the bluetongue virus core. *Nature* **395**, 470-478.

Grubman, M.J. and Lewis, S.A. (1992). Identification and characterization of the structural and non-structural proteins of African horse sickness virus and determination of the genome coding assignments. *Virol.* **186**, 444-451.

Haasnoot, P.C., Cupac, D. and Berkhout, B. (2003). Inhibition of virus replication by RNA interference. *J. Biomed. Sci.* **10**, 607-616.

Hall, T.A. (1999). BioEdit: A user-friendly biological sequence alignment editor and analysis program for Windows 95/98/NT. *Nucl. Acids Symp. Ser.* **41**, 95-98.

Hammond, S.M., Bernstein, E., Beach, D. and Hannon, G.J. (2000). An RNA-directed nuclease mediates post-transcriptional gene silencing in *Drosophila* cells. *Nature* **404**, 293-296.

Hammond, S.M., Boettcher, S., Caudy, A.A., Kobayashi, R. and Hannon, G.J. (2001). Argonaute2, a link between genetic and biochemical analyses of RNAi. *Science* **293**, 1146-1150.

Hannon, G.J. (2002). RNA interference. *Nature* **418**, 244-251.

Harborth, J., Elbashir, S.M., Bechert, K., Tuschl, T. and Weber, K. (2001). Identification of essential genes in cultured mammalian cells using small interfering RNAs. *J. Cell. Sci.* **114**, 4557-4565.

Harborth, J., Elbashir, S.M., Vandenburgh, K., Manninga, H., Scaringe, S.A., Weber, K. and Tuschl, T. (2003). Sequence, chemical, and structural variation of small interfering RNAs and short hairpin RNAs and the effect on mammalian gene silencing. *Antisense Nucl. Acid Drug Dev*. **13**, 83-105.

Hassan, S.H., Wirblich, C., Forzan, M. and Roy, P. (2001). Expression and functional characterization of bluetongue virus VP5 protein: Role in cellular permeabilization. *J. Virol.* **75**, 8356-8367.

Hassan, S.S. and Roy, P. (1999). Expression and functional characterization of bluetongue virus VP2 protein: Role in cell entry. *J. Virol.* **73**, 9832-9842.

Hayama, E. and Li, J.K. (1994). Mapping and characterization of antigenic epitopes and the nucleic acid-binding domains of VP6 protein of bluetongue viruses. *J. Virol.* **68**, 3604-3611.

Heale, B.S., Soifer, H.S., Bower, C. and Rossi, J.J. (2005). siRNA target site secondary structure predictions using local stable substructures. *Nucl. Acids Res.* **33**, e30.

Heggestadt, A.D., Notterpek, L. and Fletcher, B.S. (2004). Transposon-based RNAi delivery system for generating knockdown cell lines. *Biochem. Biophys. Res. Commun*. **316**, 643-650.

Hewat, E.A., Booth, T.F. and Roy, P. (1992a). Structure of bluetongue virus particles by cryoelectron microscopy. *J. Struct. Biol.* **109**, 61-69.

Hewat, E.A., Booth, T.F., Wade, R.H. and Roy, P. (1992b). 3-D reconstruction of bluetongue virus tubules using cryoelectron microscopy. *J. Struct. Biol.* **108**, 35-48.

Higuchi, M., Tsutsumi, R., Higashi, H. and Hatakeyama, M. (2004). Conditional gene silencing utilizing the *lac* repressor reveals a role of SHP-2 in *cagA*-positive *Helicobacter pylori* pathogenicity. *Cancer Sci*. **95**, 442-447.

Ho, H.Y., Cheng, M.L., Wang, Y.H. and Chiu, D.T. (2006). Flow cytometry for assessment of the efficacy of siRNA. *Cytometry* **69**, 1054-1061.

Holen, T., Amarzguioui, M., Wiiger, M.T., Babaie, E. and Prydz, H. (2002). Positional effects of short interfering RNAs targeting the human coagulation trigger tissue factor. *Nucl. Acids Res.* **30**, 1757-1766.

Hommel, J.D., Sears, R.M., Georgescu, D., Simmons, D.L. and DiLeoni, R.J. (2003). Local gene knockdown in the brain using viral-mediated RNA interference. *Nature Med.* **9**, 1539-1544.

Horscroft, N. and Roy, P. (2000). NTP-binding and phosphohydrolase activity associated with purified bluetongue virus non-structural protein NS2. *J. Gen. Virol*. **81**, 1961-1965.

Howell, P.G. (1960). The 1960 epizootic in the Middle East and SW Asia. *J. S. Afr. Vet. Med. Assoc.* **31**, 329-334.

Howell, P.G. (1962). The isolation and identification of further antigenic types of African horse sickness virus. *Onderstepoort J. Vet. Res.* **29**, 139-149.

Hu, Y-C. (2005). Baculovirus as a highly efficient expression vector in insect and mammalian cells. *Acta Pharmacol. Sin.* **26**, 405-416.

Huang, J., Jiang, P., Li, Y., Xu, J., Jiang, W. and Wang, X. (2006). Inhibition of porcine reproductive and respiratory syndrome virus replication by short hairpin RNA in MARC-145 cells. *Vet. Microbiol.* **115**, 302-310.

Huismans, H. (1979). Protein synthesis in bluetongue virus-infected cells. *Virol.* **92**, 385-396.

Huismans, H. and Els, H.J. (1979). Characterization of the tubules associated with the replication of the three different orbiviruses. *Virol.* **92**, 397-406.

Huismans, H. and Erasmus, B.J. (1981). Identification of the serotype-specific and group-specific antigens of bluetongue virus. *Onderstepoort J. Vet. Res.* 48, 1-8.

Huismans, H. and Van Dijk, A.A. (1990). Bluetongue virus structural components. *Curr. Top. Microbiol. Immunol.* **162**, 21-37.

Huismans, H. and Verwoerd, D.W. (1973). Control of transcription during expression of the bluetongue virus genome. *Virol.* **52**, 81-88.

Huismans, H., Van der Walt, N.T., Cloete, M. and Erasmus, B.J. (1983). The biochemical and immunological characterization of bluetongue virus outer capsid polypeptides. In: Double-stranded RNA viruses. R.W. Compans and D.H.L. Bishop (Eds.), pp. 165-172, Elsevier, New York.

Huismans, H., Van der Walt, N.T., Cloete, M. and Erasmus, B.J. (1987a). Isolation of a capsid protein of bluetongue virus that induces a protective immune response in sheep. *Virol.* **157**, 172-179.

Huismans, H., Van Dijk, A.A. and Bauskin, A.R. (1987b). *In vitro* phosphorylation and purification of a nonstructural protein of bluetongue virus with affinity for single-stranded RNA. *J. Virol.* **61**, 3589-3595.

Huismans, H., van Dijk, A.A. and Els, H.J. (1987c). Uncoating of parental bluetongue virus to core and subcore particles in infected L cells. *Virol.* **157**, 180-188.

Huser, A. and Hofmann, C. (2003). Baculovirus vectors: Novel mammalian cell gene-delivery vehicles and their applications. *Am. J. Pharmacogenomics* **3**, 53-63.

Hyatt, A.D. and Eaton, B.T. (1988). Ultrastructural distribution of the major capsid proteins within bluetongue virus and infected cells. *J. Gen. Virol.* **69**, 805-815.

Hyatt, A.D., Brookes, S.M., Gould, A.R. and Eaton, B.T. (1992). Morphogenesis of bluetongue viruses: Development of a model for the site of virus synthesis, translocation and release from infected tissue culture cells. In: Bluetongue, African horse sickness and related orbiviruses. Proceedings of the Second International Symposium. T.E. Walton and B.I. Osburn (Eds.), pp. 358-365. CRC Press, London.

Hyatt, A.D., Eaton, B.T. and Brookes, S.M. (1989). The release of bluetongue virus from infected cells and their super-infection by progeny virus. *Virol.* **173**, 21-34.

Hyatt, A.D., Zhao, Y. and Roy, P. (1993). Release of bluetongue virus-like particles from insect cells is mediated by BTV nonstructural protein NS3/NS3A. *Virol.* **193**, 592-603.

Jackson, A.L. and Linsley, P.S. (2004). Noise amidst the silence: Off-target effects of siRNAs. *Trends Genet* **20**, 521-524.

Jackson, A.L., Bartz, S.R., Schelter, J., Kobayashi, S.V., Burchard, J., Mao, M., Li, B., Cavet, G. and Linsley, P.S. (2003). Expression profiling reveals off-target gene regulation by RNAi. *Nature Biotech.* **21**, 635-637.

Jaronczyk, K., Carmichael, J.B. and Hobman, T.C. (2005). Exploring the functions of RNA interference pathway proteins: Some functions are more RISC than others? *Biochem. J.* **387**, 561-571.

Judge, A.D., Sood, V., Shaw, J.R., Fang, D., McClintock, K. and MacLachlan, I. (2005). Sequence-dependent stimulation of the mammalian innate immune response by synthetic siRNA. *Nature Biotech.* **23**, 457-462.

Kar, A.K., Bishnupriya, B. and Roy, P. (2007). Bluetongue virus RNA binding protein NS2 is a modulator of viral replication and assembly. *BMC Mol. Biol*. **8**:1.

Kar, A.K., Ghosh, M. and Roy, P. (2004). Mapping the assembly pathway of Bluetongue virus scaffolding protein VP3. *Virol.* **324**, 387-399.

Kar, A.K., Iwatani, N. and Roy, P. (2005). Assembly and intracellular localization of the bluetongue virus core protein VP3. *J. Virol.* **79**, 11487-11495.

Kawasaki, H., Suyama, E., Lyo, M. and Taira, K. (2003). siRNAs generated by recombinant human Dicer induce specific and significant but target site-independent gene silencing in human cells. *Nucl. Acids Res.* **31**, 981-987.

Kaykas, A. and Moon, R.T. (2004). A plasmid-based system for expressing small interfering RNA libraries in mammalian cells. *BMC Cell Biol*. **5**, 16-37.

Keene, K.M., Foy, B.D., Sanchez-Vargas, I., Beaty, B.J., Blair, C.D. and Olson, K.E. (2004). RNA interference acts as a natural antiviral response to O'nyong-nyong virus (*Alphavirus*; Togaviridae) infection of *Anopheles gambiae*. *Proc. Natl. Acad. Sci. USA* **101**, 17240-17245.

Kennerdell, J.R. and Carthew, R.W. (1998). Use of dsRNA-mediated genetic interference to demonstrate that frizzled and frizzled 2 act in the wingless pathway. *Cell* **95**, 1017-1026.

Khvorova, A., Reynolds, A. and Jayasena, S.D. (2003). Functional siRNAs and miRNAs exhibit strand bias. *Cell* **115**, 209-216.

Kim, D., Longo, M., Han, Y., Lundberg, P., Cantin, E. and Rossi, J.J. (2004). Interferon induction by siRNAs and ssRNAs synthesized by phage polymerase. *Nature Biotech.* **22**, 321-325.

Kim, D.H., Behlke, M.A., Rose, S.D., Chang, M-S., Choi, S. and Rossi, J.J. (2005). Synthetic dsRNA Dicer substrates enhance RNAi potency and efficacy. *Nature Biotech.* **23**, 222-226.

Kitts, P.A. and Possee, R.D. (1993). A method for producing recombinant baculovirus expression vectors at high frequency. *BioTechniques* **14**, 810-817.

Kitts, P.A., Ayres, M.D. and Possee, R.D. (1990). Linearization of baculovirus DNA enhances the recovery of recombinant virus expression vectors. *Nucl. Acids Res*. **18**, 5667-5672.

Knudson, D.L. and Monath, T.P. (1990). Orbiviruses. In: Field's Virology. B.N. Fields and D.M. Knipe (Eds.), pp. 1405-1433. Raven Press, New York.

Koonin, E.V., Gorbalenya, A.E. and Chumakov, K.M. (1989). Tentative identification of RNA-dependent RNA polymerases of dsRNA viruses and their relationship to positive strand RNA viral polymerases. *FEBS Lett.* **252**, 42-46.

Kooter, J.M., Matzke, M.A. and Meyer, P. (1999). Listening to silent gene: Transgene silencing, gene regulation and pathogen control. *Trends Plant Sci.* **4**, 340-347.

Kretschmer-Kazemi Far, R. and Sczakiel, G. (2003). The activity of siRNA in mammalian cells is related to structural target accessibility: A comparison with antisense oligonucleotides. *Nucl. Acids Res.* **31**, 4417-4424.

Kuttenkeuler, D. and Boutrous, M. (2004). Genome-wide RNAi as a route to gene function in *Drosophila*. *Funct. Genom. Proteom.* **3**, 168-176.

Laegreid, W.W. (1996). African horsesickness. In: Virus infections of Vertebrates, Vol. 6. Virus Infections of Equines. M.J. Studdert (Ed.), pp. 101-123. Elsevier Press, Amsterdam.

Laemmli, U.K. (1970). Cleavage of structural proteins during the assembly of the head of bacteriophage T4. *Nature* **227**, 680-685.

Lambeth, L.S., Moore, R.J., Muralitharan, M.S. and Doran, T.J. (2007). Suppression of bovine viral diarrhea virus replication by small interfering RNA and short hairpin RNA-mediated RNA interference. *Vet. Microbiol.* **119**, 132-143.

Larke, N., Murphy, A., Wirblich, C., Teoh, D., Estcourt, M.J., McMichael, A.J., Roy, P. and Hanke, T. (2005). Induction of human immunodeficiency virus type 1-specific T cells by a bluetongue virus tubule-vectored vaccine prime-recombinant modified virus Ankara boost regimen. *J. Virol.* **79**, 14822-14833.

Le Blois, H., French, T., Mertens, P.P.C., Burroughs, J.N. and Roy, P. (1992). The expressed VP4 protein of bluetongue virus binds GTP and is the candidate guanylyl transferase of the virus. *Virol.* **189**, 757-761.

Lecastas, G. (1968). Electron microscopic study of the formation of bluetongue virus. *Onderstepoort J. Vet. Res.* **35**, 139-149.

Lee, N.S., Dohjima, T., Bauer, G., Li, H., Li, M.J., Ehsani, A., Salvaterra, P. and Rossi, J.J. (2002). Expression of small interfering RNAs targeted against HIV-1 *rev* transcripts in human cells. *Nature Biotech.* **20**, 500-505.

Li, G., Xiang, Y., Sabapathy, K. and Silverman, R.H. (2003). An apoptotic signaling pathway in the interferon antiviral response mediated by RNase L and c-Jun NH_2-terminal kinase. *J. Biol. Chem.* **279**, 1123-1131.

Lima, W.F., Monia, B.P., Ecker, D.J. and Freier, S.M. (1992). Implication of RNA structure on antisense oligonucleotide hybridization kinetics. *Biochem.* **31**, 12055-12061.

Liu, J., Carmell, M.A., Fabiola, V.R., Marsden, C.G., Thomson, J.M., Song, J.J., Hammond, S.M., Joshua-Tor, L. and Hannon, G.J. (2004). Argonaute2 is the catalytic engine of mammalian RNAi. *Science* **305**, 1437-1441.

Liu, Y.P., Haasnoot, J. and Berkhout, B. (2007). Design of short hairpin RNAs for HIV-1 inhibition. *Nucl. Acids Res*. **35**, 5683-5693.

López, T., Camacho, M., Zayas, M., Nájera, R., Sánchez, R., Arias, C.F. and López, S. (2005). Silencing the morphogenesis of rotavirus. *J. Virol.* **79**, 184-192.

Loudon, P.T. and Roy, P. (1991). Assembly of five bluetongue virus proteins expressed by recombinant baculoviruses: Inclusion of the largest protein VP1 in the core and virus-like particles. *Virol*. **180**, 798-802.

Lu, L., Ho, Y. and Kwang, J. (2006). Suppression of porcine arterivirus replication by baculovirus-delivered shRNA targeting nucleoprotein. *Biochem. Biophys. Res. Commun.* **340**, 1178-1183.

Lubroth, J. (1988). African horse sickness and the epizootic in Spain 1987. *Equine Pract.* **10**, 26-33.

Luckow, V.A., Lee, S.C., Barry, G.F. and Olins, P.O. (1993). Efficient generation of infectious recombinant baculoviruses by site-specific transposon-mediated insertion of foreign genes into a baculovirus genome propagated in *Escherichia coli*. *J. Virol.* **67**, 4566-4579.

Luo, K.Q. and Chang, D.C. (2004). The gene-silencing efficiency of siRNA is strongly dependent on the local structure of mRNA at the targeted region. *Biochem. Biophys. Res. Commun.* **318**, 303-310.

Lymperopoulus, K., Noad, R., Tosi, S., Nethisinghe, S., Brierley, I. and Roy, P. (2006). Specific binding of Bluetongue virus NS2 to different viral plus-strand RNAs. *Virol*. **353**, 17-26.

Lymperopoulus, K., Wirblich, C., Brierley, I. and Roy, P. (2003). Sequence specificity in the interaction of Bluetongue virus non-structural protein 2 NS2 with viral RNA. *J. Biol. Chem.* **278**, 31722-31730.

Manche, L., Green, S.R., Schmedt, C. and Mathews, M.B. (1992). Interactions between double-stranded RNA regulators and the protein kinase DAI. *Mol. Cell. Biol.* **12**, 5238-5248.

Maree, F.F. and Huismans, H. (1997). Characterization of tubular structures composed of nonstructural protein NS1 of African horsesickness virus expressed in insect cells. *J. Gen. Virol.* **78**, 1077-1082.

Maree, S., Durbach, S. and Huismans, H. (1998). Intracellular production of African horsesickness virus core-like particles by expression of the two major core proteins, VP3 and VP7, in insect cells. *J. Gen. Virol.* **79**, 333-337.

Markotter, W., Theron, J. and Nel, L.H. (2004). Segment-specific inverted repeat sequences in bluetongue virus are required for interaction with the virus non-structural protein NS2. *Virus Res.* **105**, 1-9.

Marshall, J.J. and Roy, P. (1990). High level expression of the two outer capsid proteins of bluetongue virus serotype 10: Their relationship with the neutralization of virus infection. *Virus Res.* **15**, 189-195.

Marshall, O.J. (2004). PerlPrimer: Cross-platform, graphical primer design for standard, bisulphite and real-time PCR. *Bioinformatics* **20**, 2471-2472.

Martinez, J. and Tuschl, T. (2004). RISC is a 5' phosphomonoester-producing RNA endonuclease. *Genes Dev.* **18**, 975-980.

Martinez, J., Patkaniowska, A., Urlaub, H., Luhrmann, R. and Tuschl, T. (2002). Single-stranded antisense siRNAs guide target RNA cleavage in RNAi. *Cell* **110**, 563-574.

Martinez-Torrecuadrada, J.L., Diaz-Laviada, M., Roy, P., Sanchez, C., Vela, C., Sanchez-Vizcaino, J.M. and Casal, J.I. (1996). Full protection against African horsesickness (AHS) in horses induced by baculovirus-derived AHS virus serotype 4 VP2, VP5 and VP7. *J. Gen. Virol.* **77**, 1211-1221.

Martinez-Torrecuadrada, J.L., Iwata, H., Venteo, A., Casal, I. and Roy, P. (1994). Expression and characterization of two outer capsid proteins of African horsesickness virus: The role of VP2 in virus neutralization. *Virol.* **202**, 348-359.

Martinez-Torrecuadrada, J.L., Langeveld, J.P.M., Meloen, R.H. and Casal, J.I. (2001). Definition of neutralizing sites on African horse sickness virus serotype 4 VP2 at the level of peptides. *J. Gen. Virol.* **82**, 2415-2424.

Martinez-Torrecuadrada, J.L., Langeveld, J.P.M., Venteo, A., Sanz, A., Dalsgaard, K., Hamilton, W.D.O., Meloen, R.H. and Casal, J.I. (1999). Antigenic profile of African horse sickness virus serotype 4 VP5 and identification of a neutralizing epitope shared with bluetongue virus and epizootic hemorrhagic disease virus. *Virol.* **257**, 449-459.

Matsukura, S., Jones, P.A. and Takai, D. (2003). Establishment of conditional vectors for hairpin siRNA knockdown. *Nucl. Acids Res.* **31**, e77.

Matsuura, Y., Possee, R.D., Overton, H.A. and Bishop, D.H.L. (1987). Baculovirus expression vectors: The requirements for high level expression of proteins, including glycoproteins. *J. Gen. Virol.* **68**, 1233-1250.

Matthews, R.E.F. (1982). Classification and nomenclature of viruses. Fourth report of the International Committee on Taxonomy of viruses. *Intervirol.* **17**, 1-200.

McCown, M., Diamond, M.S. and Pekosz, A. (2003). The utility of siRNA transcripts produced by RNA polymerase I in down regulating viral gene expression and replication of negative and positive-strand RNA viruses. *Virol.* **313**, 514-524.

McIntosh, B.M. (1958). Immunological types of horse sickness virus and their significance in immunization. *Onderstepoort J. Vet. Res.* **27**, 465-538.

Meister, G. and Tuschl, T. (2004). Mechanisms of gene silencing by double-stranded RNA. *Nature* **431**, 343-349.

Mellor, P.S. (1994). Epizootiology and vectors of African horse sickness. *Comp. Immun. Microbiol. Infect. Dis.* **17**, 287-296.

Mellor, P.S. and Hamblin, C. (2004). African horse sickness. *Vet. Res.* **35**, 445-466.

Mellor, P.S., Boorman, J., Wilkinson, P.J. and Martinez-Gomez, F. (1983). Potential vectors of bluetongue and African horse sickness viruses in Spain. *Vet. Rec.* **112**, 229-230.

Mertens, P.P.C. (2000). Orbiviruses and coltiviruses - general features. In: Encyclopedia of Virology. R.G. Webster and A. Ganoff (Eds.), pp. 1043-1061. Academic Press, London.

Mertens, P. (2004). The dsRNA viruses. *Virus Res.* **101**, 3-13.

Mertens, P.P.C. and Diprose, J. (2004). The bluetongue virus core: A nano-scale transcription machine. *Virus Res.* **101**, 29-43.

Mirchamsy, H. and Hazrati, A. (1973). A review of the aetiology and pathology of African horse sickness. *Arch. Inst. Razi.* **25**, 23-46.

Mittal, V. (2004). Improving the efficiency of RNA interference in mammals. *Nature Rev. Genet.* **5**, 355-365.

Mizukoshi, N., Sakamoto, K., Iwata, A., Tsuchiya, T., Ueda, S., Apiwatnakorn, B., Kamada, M. and Fukusho, A. (1993). The complete nucleotide sequence of African horsesickness virus serotype 4 (vaccine strain) segment 4, which encodes the minor core protein VP4. *Virus Res.* **28**, 299-306.

Mocellin, S. and Provenzano, M. (2004). RNA interference learning gene knock-down from cell physiology. *J. Translational Med.* **2**, 1-6.

Modrof, J., Lymperopoulos, K. and Roy, P. (2005). Phosphorylation of Bluetongue virus nonstructural protein 2 is essential for formation of viral inclusion bodies. *J. Virol*. **79**, 10023-10031.

Monastyrskaya, K., Booth, T., Nel, L. and Roy, P. (1994). Mutation of either of two cysteine residues or deletion of the amino or carboxy terminus of nonstructural protein NS1 of bluetongue virus abrogates virus-specific tubule formation in insect cells. *J. Virol.* **68**, 2169-2178.

Myers, J.W., Jones, J.T., Meyer, T. and Ferrel, J.E. (2003). Recombinant Dicer efficiently converts large dsRNA into siRNAs suitable for gene silencing. *Nature Biotech.* **21**, 324-328.

Nahreini, P., Hanson, A.J., Andreatta, C.P., Koustas, W.T. and Prasad, K.N. (2004). Altering cellular signaling pathways enhance gene silencing activity of shRNA, shRNA.ribozyme, and shRNA.antisense in neuroblastoma cells. *Cell. Mol. Neurobiol.* **24**, 781-792.

Napoli, C., Lemieux, C. and Jorgensen, R. (1990). Introduction of a chalcone synthase gene into Petunia results in reversible co-suppression of homologous genes *in trans*. *Plant Cell* **2**, 279-289.

Nason, E.L., Rothagel, R., Mukherjee, S.K., Kar, A.K., Forzan, M., Prasad, V. and Roy, P. (2004). Interactions between the inner and outer capsids of bluetongue virus. *J. Virol.* **78**, 8059-8067.

Nel, L.H. and Huismans, H. (1991). Synthesis of the virus-specified tubules of epizootic haemorrhagic disease virus using a baculovirus expression system. *Virus Res.* **19**, 139-152.

Ngo, H., Tschudi, C., Gull, K. and Ullu, E. (1998). Double-stranded RNA induces mRNA degradation in *Trypanosoma brucei*. *Proc. Natl. Acad. Sci. USA* **95**, 14687-14692.

Nieuwoudt, M.A. (2008). Silencing of African horse sickness virus NS2 gene expression using vector-derived short hairpin RNAs. M.Sc Dissertation, Department of Microbiology and Plant Pathology, Faculty of Biological and Agricultural Sciences, University of Pretoria, South Africa.

Nykänen, A., Haley, B. and Zamore, P.D. (2001). ATP requirements and small interfering RNA structure in the RNA interference pathway. *Cell* **107**, 309-321.

O'Reilly, D.R., Miller, L.K. and Luckow, V.A. (1992). An overview of baculoviruses, choosing a transfer plasmid and parent virus, methods for vector construction and gene expression. In: Baculo-expression vectors: A laboratory manual. D.R. O'Reilly, L.K. Miller and V.A. Luckow (Eds.), pp. 1-36. W.H. Freeman and Company, New York.

Oellerman, R.A. (1970). Plaque formation by African horse sickness virus and characterization of its RNA. *Onderstepoort J. Vet. Res.* **37**, 137-144.

Oellermann, R.A., Els, H.J. and Erasmus, B.J. (1970). Characterisation of African horsesickness virus. *Arch. Gesamte Virusforsch* **29**, 163-174.

Overhoff, M., Alken, M., Kretschmer-Kazemi Far, R., Lemaitre, M., Lebleu, B., Sczakiel, G. and Robbins, I. (2005). Local RNA target structure influences siRNA efficacy: A systematic global analysis. *J. Mol. Biol.* **348**, 871-881.

Owens, R.J., Limn, C. and Roy, P. (2004). Role of arbovirus nonstructural protein in cellular pathogenesis and virus release. *J. Virol.* **78**, 6649-6656.

Paddison, P.J., Caudy, A.A. and Hannon, G.J. (2002). Stable suppression of gene expression by RNAi in mammalian cells. *Proc. Natl. Acad. Sci. USA* **99**, 1443-1448.

Parker, J.S., Roe, S.M. and Barford, D. (2005). Structural insights into mRNA recognition from a PIWI domain-siRNA guide complex. *Nature* **434**, 663-666.

Paul, C.P., Good, P.D., Winer, I. and Engelke, D.R. (2002). Effective expression of small interfering RNA in human cells. *Nature Biotech.* **20**, 505-508.

Paule, M.R. and White, R.J. (2000). Transcription by RNA polymerase I and III. *Nucl. Acids Res.* **28**, 1283-1298.

Peng, J., Zhao, Y., Mai, J., Pang, W.K., Wei, X., Xhang, P. and Xu, Y. (2005). Inhibition of hepatitis B virus replication by various RNAi constructs and their pharmacodynamic properties. *J. Gen. Virol.* **86**, 3227-3234.

Pfaffl, M.W., Horgan, G.W. and Dempfle, L. (2002). Relative expression software tool (REST) for group-wise comparison and statistical analysis of relative expression results in real-time PCR. *Nucl. Acids Res.* **30**, e36.

Pham, J.W., Pellino, J.L., Lee, Y.S., Carthew, R.W. and Sontheimer, E.J. (2004). A Dicer-2-dependent 80S complex cleaves targeted mRNAs during RNAi in *Drosophila. Cell* **117**, 83-94.

Philipps, B., Forstner, M. and Mayr, L.M. (2005). A baculovirus expression vector system for simultaneous protein expression in insect and mammalian cells. *Biotechnol. Prog*. **21**, 708-711.

Possee, R.D. (1997). Baculoviruses as expression vectors. *Curr. Opin. Biotechnol.* **8**, 569-572.

Prasad, B.V.V., Yamaguchi, S. and Roy, P. (1992). Three-dimensional structure of single-shelled bluetongue virus. *J. Virol.* **66**, 2135-2142.

Provost, P., Dishart, D., Doucet, J., Frendewey, D., Samuelson, B. and Radmark, O. (2002). Ribonuclease activity and RNA binding of recombinant human Dicer. *EMBO J.* **21**, 5864-5874.

Qin, X-F., An, D.S., Chen, I.S.Y. and Baltimore, D. (2003). Inhibiting HIV-1 infection in human T cells by lentiviral-mediated delivery of small interfering RNA against CCR5. *Proc. Natl. Acad. Sci. USA* **100**, 183-188.

Rafyi, A. (1961). Horse sickness. *Bull. Off. Int. Epizoot.* **56**, 216-250.

Ramadevi, N. and Roy, P. (1998). Bluetongue virus core protein VP4 has nucleoside triphosphate phosphohydrolase activity. *J. Gen. Virol.* **79**, 2475-2480.

Ramadevi, N., Burroughs, N.J., Mertens, P.P., Jones, I.M. and Roy, P. (1998). Capping and methylation of mRNA by purified recombinant VP4 protein of bluetongue virus. *Proc. Natl. Acad. Sci. USA* **95**, 13537-13542.

Randall, G., Grakoui, A. and Rice, C.M. (2003). Clearance of replicating hepatitis C virus replicon RNAs in cell culture by small interfering RNAs. *Proc. Natl. Acad. Sci USA* **100**, 235-240.

Rao, C.D., Kiuchi, A. and Roy, P. (1983). Homologous terminal sequences of the genome double-stranded RNAs of bluetongue virus. *J. Virol.* **46**, 378-383.

Reynolds, A., Leake, D., Boese, Q., Scaringe, S., Marshall, W.S. and Khvorova, A. (2004). Rational siRNA design for RNA interference. *Nature Biotech.* **22**, 326-330.

Ritter, U., Damm-Welk, C., Fuchs, U., Bohle, R.M., Borkhardt, A. and Woessmann, W. (2003). Design and evaluation of chemically synthesized siRNA targeting the NPM-ALK fusion site in anaplastic large cell lymphoma (ALCL). *Oligonucleotides* **13**, 365-373.

Robishaw, J.D., Guo, Z.P. and Wang, Q. (2004). Ribozymes as tools for suppression of G protein gamma subunits. *Methods Mol. Biol.* **237**, 169-180.

Rosen, H.R. and Gretch, D.R. (1999). Hepatitis C virus: Current understanding and prospects for future therapies. *Mol. Med. Today* **5**, 393-399.

Roy, P. and Sutton, G. (1998). New generation of African horse sickness virus vaccines based on structural and molecular studies of the virus particles. *Arch. Virol.* **14**, 177-202.

Roy, P. (1992). Bluetongue virus proteins. *J. Gen. Virol.* **73**, 3051-3064.

Roy, P. (2001). Orbiviruses. In: Field's Virology. Fourth Edition. D.M. Knipe, P.M. Howley, D.E. Griffin, R.A. Lamb, M.A. Martin (Eds.), pp. 1852-1857. Lippincott Williams and Wilkins, Philadelphia.

Roy, P., Adachi, A., Urakawa, T., Booth, T.F. and Thomas, C.P. (1990). Identification of bluetongue virus VP6 as nucleic acid binding protein and the localization of VP6 in virus infected cells. *J. Virol.* **64**, 1-8.

Roy, P., Callis, J. and Erasmus, B.J. (1993). Protection of sheep against bluetongue disease after vaccination with core-like and virus-like particles: Evidence for homologous and partial heterologous protection. *Proc. Annu. Mtg. US Anim. Health Assoc.* **97**, 88-93.

Roy, P., French, T. and Erasmus, B.J. (1992). Protective efficacy of virus-like particles for bluetongue disease. *Vaccine* **10**, 28-32.

Roy, P., Fukusho, A., Ritter, D.G. and Lyons, D. (1988). Evidence for genetic relationship between RNA and DNA viruses from the sequence homology of a putative polymerase gene of bluetongue virus with that of vaccinia virus: Conservation of RNA polymerase genes from diverse species. *Nucl. Acids Res.* **16**, 11759-11767.

Roy, P., Mertens, P.P.C. and Casal, I. (1994). African horse sickness virus structure. *Comp. Immunol. Microbiol. Infect. Dis.* **17**, 243-273.

Rozen, S. and Skaletsky, H. (2000). Primer3 on the WWW for general users and for biologist programmers. *Methods Mol. Biol.* **132**, 365-386.

Rubinson, D.A., Dillon, C.P., Kwiatkowski, A.V., Sievers, C., Yang, L., Kopinja, J., Zhang, M., McManus, M.T., Gertler, F.B., Scott, M.L. and Van Parijs, L. (2003). A lentivirus-based system to functionally silence genes in primary mammalian cells, stem cells and transgenic mice by RNA interference. *Nature Genet.* **33,** 401-406.

Sambrook, J., Fritch, E.F. and Maniatis, T. (1989). Molecular cloning: A laboratory manual. Second edition. Cold Spring Harbour Laboratory Press, Cold Spring Harbor, New York.

Sandy, P., Ventura, A. and Jacks, T. (2005). Mammalian RNAi: A practical guide. *BioTechniques* **39**, 215-224.

Saxena, S., Jonsson, Z.O. and Dutta, A. (2003). Small RNAs with imperfect match to endogenous mRNA repress translation. Implications for off-target activity of small inhibitory RNA in mammalian cells. *J. Biol. Chem.* **278**, 44312-44319.

Scacheri, P.C., Rozenblatt-Rosen, O., Caplen, N.J., Wolfsberg, T.G., Umayam, L., Lee, J.C., Hughes, C.M., Shanmugam, K.S., Bhattacharjee, A., Meyerson, M. and Collins, F.S. (2004). Short interfering RNAs can induce unexpected and divergent changes in the levels of untargeted proteins in mammalian cells. *Proc. Natl. Acad. Sci. USA* **101**, 1892-1897.

Scanlen, M., Paweska, J.T., Verschoor, J.A. and Van Dijk, A.A. (2002). The protective efficacy of a recombinant VP2-based African horse sickness subunit vaccine candidate is determined by adjuvant. *Vaccine* **20**, 1079-1088.

Scherer, L.J., Yildiz, Y., Kim, J., Cagnon, L., Heale, B. and Rossi, J.J. (2004). Rapid assessment of anti-HIV siRNA efficacy using PCR-derived Pol III shRNA cassettes. *Mol. Ther.* **10**, 597-603.

Schiffelers, R.M., Ansari, A., Xu, J., Zhou, Q., Tang, Q., Storm, G., Molema, G., Lu, P.Y., Scaria, P.V. and Woodle, M.C. (2004). Cancer siRNA therapy by tumor selective delivery with ligand-targeted sterically stabilized nanoparticle. *Nucl. Acids Res.* **32**, e149.

Schubert, S., Grünweller, A., Erdmann, V.A. and Kurreck, J. (2005). Local RNA target structure influences siRNA efficacy: Systematic analysis of intentionally designed binding regions. *J. Mol. Biol.* **348**, 883-893.

Schuck, S., Manninen, A., Honsho, M., Fullekrug, J. and Simons, K. (2004). Generation of single and double knock-downs in polarized epithelial cells by retrovirus-mediated RNA interference. *Proc. Natl. Acad. Sci. USA* **101**, 4912-4917.

Schwarz, D.S., Hutvágner, G., Du, T., Xu, Z., Aronin, N. and Zamore, P.D. (2003). Asymmetry in the assembly of the RNAi enzyme complex. *Cell* **115**, 199-208.

Schwarz, D.S., Tomari, Y. and Zamore, P.D. (2004). The RNA-induced silencing complex is a Mg^{2+}-dependent endonuclease. *Curr. Biol.* **14**, 787-791.

Shen, C., Buck, A.K., Liu, X., Winkler, M. and Reske, S.N. (2003). Gene silencing by adenovirus-delivered siRNA. *FEBS Lett.* **539**, 111-114.

Shlomai, A. and Shaul, Y. (2003). Inhibition of hepatitis B virus expression and replication by RNA interference. *Hepatol.* **37**, 764-770.

Silvestri, L.S., Taraporewala, Z.F. and Patton, J.T. (2004). Rotavirus replication: Plus templates for double-stranded RNA synthesis are made in viroplasms. *J. Virol.* **78**, 7763-7774.

Siolas, D., Lerner, C., Burchard, J., Ge, W., Linsley, P.S., Paddison, P.J., Hannon, G.J. and Cleary, M.A. (2005). Synthetic shRNAs as potent RNAi triggers. *Nature Biotech.* **23**, 227-231.

Sledz, C.A., Holko, M., de Veer, M.J., Silverman, R.H. and Williams, B.R. (2003). Activation of the interferon system by short-interfering RNAs. *Nature Cell Biol.* **5**, 834-839.

Smith, G.E., Summers, M.D. and Fraser, M.J. (1983). Production of human beta interferon in insect cells infected with a baculovirus expression vector. *Mol. Cell. Biol.* **3**, 2156-2165.

Song, J.J., Smith, S.K., Hanno, G.J. and Joshua-Tor, L. (2004). Crystal structure of Argonaute and its implications for RISC Slicer activity. *Science* **305**, 1434-1437.

Stark, G.R., Kerr, I.M., Williams, B.R., Silverman, R.H. and Schreiber, R.D. (1998). How cells respond to interferons. *Annu. Rev. Biochem.* **67**, 227-264.

Stassen, L., Huismans, H. and Theron, J. (2007). Silencing of African horse sickness virus VP7 protein expression in cultured cells by RNA interference. *Virus Genes* **35**, 777-783.

Stauber, N., Martinez-Costas, J., Sutton, G., Monasturskaya, K. and Roy, P. (1997). Bluetongue virus VP6 protein binds ATP and exhibits an RNA-dependent ATPase function and a helicase activity that catalyze the unwinding of double-stranded RNA substrates. *J. Virol.* **71**, 7220-7226.

Stein, C.A. (2001). The experimental use of antisense oligonucleotides: A guide for the perplexed. *J. Clin. Invest.* **108**, 641-644.

Stoltz, M.A., van der Merwe, C.F., Coetzee, J. and Huismans, H. (1996). Subcellular localization of the nonstructural protein NS3 of African horsesickness virus. *Onderstepoort J. Vet. Res.* **63**, 57-61.

Stone-Marchat, M.A., Moss, S.R., Burrage, T.O., Barber, M.L. and Roy, P. (1996). Immunization with VP2 is sufficient for protection against lethal challenge with African horse sickness virus type 4. *Virol.* **220**, 219-222.

Stram, Y. and Kuzntzova, L. (2006). Inhibition of viruses by RNA interference. *Virus Genes* **32**, 299-306.

Stuart, D.I. and Grimes, J.M. (2006). Structural studies on orbivirus protein and particles. *Curr. Top. Microbiol. Immunol*. **309**, 221-244.

Stuart, D.I., Gouet, P., Grimes, J., Malby, R., Diprose, J., Zientara, S., Burroughs, J.N. and Mertens, P.P.C. (1998). Structural studies of orbivirus particles. *Arch. Virol.* **14**, 235-250.

Summers, M.D. and Smith, G.E. (1987). A manual of methods for Baculovirus vectors and insect cell culture procedures. *Texan Agric. Exp. Station Bull.* No. 1555.

Sutton, G., Grimes, J.M. and Roy, P. (2007). Bluetongue virus VP4 is an RNA-capping assembly line. *Nature Struct. Mol. Biol.* **14**, 449-451.

Szweykowska-Kulinska, Z., Jarmolowski, A. and Figlerowicz, M. (2003). RNA interference and its role in the regulation of eukaryotic gene expression. *Acta. Biochim. Pol*. **50**, 217-229.

Tan, B.H., Nason, E., Staeuber, N., Jiang, W., Monastryrskaya, K. and Roy, P. (2001). RGD tripeptide of bluetongue virus VP7 protein is responsible for core attachment to *Culicoides* cells. *J. Virol.* **75**, 3937-3947.

Tan, F.L. and Yin, J.Q. (2004). RNAi, a new therapeutic strategy against viral infection. *Cell Res.* **14**, 460-466.

Tanaka, S. and Roy, P. (1994). Identification of domains in bluetongue virus VP3 molecules essential for the assembly of virus cores. *J. Virol*. **68**, 2795-2802.

Taraporewala, Z., Chen, D. and Patton, J. (2001). Multimers of the bluetongue virus non-structural protein NS2 possess nucleotidyl phosphatase activity: Similarities between NS2 and rotavirus NSP2. *Virol.* **280**, 221-231.

Taxman, D.J., Livingstone, L.R., Zhang, J., Conti, B.J., Iocca, H.A., Williams, K.L., Lich, J.D., Ting, J.P-Y. and Reed, W. (2006). Criteria for effective design, construction, and gene knockdown by shRNA vectors. *BMC Biotechnol.* **6**, 7.

Theron, J. and Nel, L.H. (1997). Stable protein-RNA interaction involves the terminal domains of bluetongue virus mRNA, but not the terminally conserved sequences. *Virol*. **299**, 134-142.

Theron, J., Uitenweerde, J.M., Huismans, H. and Nel, L.H. (1994). Comparison of the expression and phosphorylation of the non-structural protein NS2 of three different orbiviruses: Evidence that the phosphorylation modulates ssRNA-binding and involves an ubiquitous cellular kinase. *J. Gen. Virol.* **75**, 3401-3411.

Thomas, C.P., Booth, T.F. and Roy, P. (1990). Synthesis of bluetongue viral-coded phosphoprotein and formation of inclusion bodies by recombinant baculovirus in insect cells: It binds the single-stranded RNA species. *J. Gen. Virol.* **71**, 2073-2083.

Tomari, Y. and Zamore, P.D. (2005). Perspective: machines for RNAi. *Genes Dev.* **19**, 517-529.

Tomari, Y., Du, T., Haley, B., Schwarz, D., Bennett, R., Cook, H., Koppetsch, B., Theurkauf, W. and Zamore, P. (2004). RISC assembly defects in the *Drosophila* RNAi mutant *armitage*. *Cell* **116**, 831-841.

Tomori, O., Baba, S. Adu, F. and Adenji, J. (1992). An overview and perspective on orbivirus disease prevalence and occurrence of vectors in Africa. In: Bluetongue, African horse sickness and related orbiviruses, Proceedings of the Second International symposium. T.E. Walton and B.I. Osburn (Eds.), pp. 23-33. CRC Press, London.

Turnbull, P.J., Cormack, S.B. and Huismans, H. (1996). Characterization of the gene encoding core protein VP6 of two African horsesickness virus serotypes. *J. Gen. Virol.* **77**, 1421-1423.

Tuschl, T., Zamore, P.D., Lehmann, R., Bartel, D.P. and Sharp, P.A. (1999). Targeted mRNA degradation by double-stranded RNA *in vitro. Genes Dev.* **13**, 3191-3197.

Ui-Tei, K., Naito, Y., Takahashi, F., Haraguchi, T., Ohki-Hamazaki, H., Juni, A., Ueda, R. and Salgo, K. (2004). Guidelines for the selection of highly effective siRNA sequences for mammalian and chick RNA interference. *Nucl. Acids Res.* **32**, 936-948.

Uitenweerde, J.M., Theron, J., Stoltz, M.A. and Huismans, H. (1995). The multimeric nonstructural NS2 proteins of Bluetongue virus, African horsesickness virus, and Epizootic hemorrhagic disease virus differ in their single-stranded RNA-binding ability. *Virol.* **209**, 624-632.

Urakawa, T. and Roy, P. (1988). Bluetongue virus tubules made in insect cells by recombinant baculoviruses: Expression of NS1 gene of bluetongue virus serotype 10. *J. Virol*. **62**, 3919-3927.

Urakawa, T., Ritter, G.D. and Roy, P. (1989). Expression of largest RNA segment and synthesis of VP1 protein of bluetongue virus in insect cells by recombinant baculovirus: Association of VP1 protein with RNA polymerase activity. *Nucl. Acids Res.* **17**, 7395-7401.

Valdes, J.V., Sampieri, A., Sepulveda, J. and Vaca, L. (2003). Using double-stranded RNA to prevent *in vitro* and *in vivo* viral infections by recombinant baculovirus. *J. Biol. Chem.* **278**, 19317-19324.

Van de Wetering, M., Oving, I., Muncan, V., Pon Fong, M.T., Brantjes, H., van Leenen, D., Holstege, F.C., Brummelkamp, T.R., Agami, R. and Clevers, H. (2003). Specific inhibition of gene expression using a stably integrated, inducible small-interfering RNA vector. *EMBO Rep.* **4**, 609-615.

Van Dijk, A.A. and Huismans, H. (1988). *In vitro* transcription and translation of bluetongue virus mRNA. *J. Gen. Virol.* **69**, 573-581.

Van Niekerk, M., Smit, C.C., Fick, W.C., van Staden, V. and Huismans, H. (2001). Membrane association of African horsesickness virus nonstructural protein NS3 determines its cytotoxicity. *Virol.* **279**, 499-508.

Van Rensburg, L.B.J., De Clerk, J., Groenewald, H.B. and Botha, W.S. (1981). An outbreak of African horse sickness in dogs. *J. S. Afr. Vet. Med. Assoc.* **52**, 323-325.

Van Staden, V. and Huismans, H. (1991). A comparison of the genes which encode nonstructural protein NS3 of different orbiviruses. *J. Gen. Virol.* **72**, 1073-1090.

Van Staden, V., Smith, C.C., Stoltz, M.A., Maree, F.F. and Huismans, H. (1998). Characterization of two African horse sickness virus nonstructural proteins, NS1 and NS3. *Arch. Virol.* (*Suppl.*) **14**, 251-258.

Van Staden, V., Stoltz, M.A. and Huismans, H. (1995). Expression of nonstructural protein NS3 of African horsesickness virus (AHSV): Evidence for a cytotoxic effect of NS3 in insect cells, and characterization of the gene products in AHSV-infected Vero cells. *Arch. Virol.* **140**, 289-306.

Vascotto, F., Visintin, M., Cattaneo, A. and Burrone, O.R. (2005). Design and selection of an intrabody library produced de-novo for the non-structural protein NSP5 of rotavirus. *J. Immunol. Methods* **301**, 31-40.

Venter, G.J., Graham, S.D. and Hamblin, C. (2000). African horse sickness epidemiology: Vector competence of South African *Culicoides* species for virus serotypes 3, 5 and 8. *Med. Vet. Entomol.* **14**, 245-250.

Verwoerd, D.W. and Huismans, H. (1969). On the relationship between bluetongue, African horsesickness and reoviruses: Hybridization studies. *Onderstepoort J. Vet. Res.* **36**, 175-179.

Verwoerd, D.W., Els, H.J., De Villiers, E.M. and Huismans, H. (1972). Structure of bluetongue virus capsid. *J. Virol.* **10**, 783-794.

Vickers, T.A., Koo, S., Bennett, C.T., Crooke, S.T., Dean, N.M. and Baker, B.F. (2003). Efficient reduction of target RNAs by small interfering RNA and RNase H-dependent antisense agents. A comparative analysis. *J. Biol. Chem.* **278**, 7108-7118.

Visintin, M., Quondam, M. and Cattaneo, A. (2004). The intracellular antibody capture technology: Towards the high-throughput selection of functional intracellular antibodies for target validation. *Methods* **34**, 200-214.

Vlassov, A.V., Korba, B., Farrar, K., Mukerjee, S., Seyhan, A.A., Ilves, H., Kaspar, R., Kazakov, S.A. and Johnston, B.H. (2007). shRNAs targeting hepatitis C: Effects of sequence and structural features, and comparison with siRNA. *Oligonucleotides* **17**, 223-236.

Vreede, F.T. and Huismans, H. (1998). Sequence analysis of the RNA polymerase gene of African horse sickness virus. *Arch. Virol.* **143**, 413-419.

Wade-Evans, A.M., Pullen, L., Hamblin, C., O'Hara, R., Burroughs, J.N. and Mertens, P.P.C. (1997). African horsesickness virus VP7 subunit vaccine protects mice against a lethal, heterologous serotype challenge. *J. Gen. Virol.* **78**, 1611-1616.

Wadhwa, R., Kaul, S.C., Miyagishi, M. and Taira, K. (2004). Vectors for RNA interference. *Curr. Opin. Mol. Ther.* **6**, 367-372.

Walters, D.K. and Jelinek, D.F. (2002). The effectiveness of double-stranded short inhibitory RNAs (siRNAs) may depend on the method of transfection. *Antisense Nucl. Acid Drug Dev.* **12**, 411-418.

Weil, D., Garçon, L., Harper, M., Duménil, D., Dautry, F. and Kress, M. (2002). Targeting the kinesin Eg5 to monitor siRNA transfection in mammalian cells. *BioTechniques* **33**, 1244-1248.

Welby, M.P., Baylis, M., Rawlings, P. and Mellor, P.S. (1996). Effects of temperature on the rate of virogenesis of African horse sickness virus in *Culicoides* (Diptera: Ceratopogonidae) and its significance in relation to the epidemiology of the disease. *Med. Vet. Entomol.* **86**, 715-720.

Werk, D., Schubert, S., Lindig, V., Grunert, H.P., Zeichhardt, H., Erdmann, V.A. and Kurreck, J. (2005). Developing an effective RNA interference strategy against a plus-strand RNA virus: Silencing of coxsackievirus B3 and its cognate coxsackievirus-adenovirus receptor. *Biol. Chem.* **386**, 857-863.

Wetzel, H., Nevill, E.M. and Erasmus, B.J. (1970). Studies on the transmission of African horsesickness. *Onderstepoort J. Vet. Res.* **37**, 165-168.

Wianny, F. and Zernicka-Goetz, M. (2000). Specific interference with gene function by double-stranded RNA in early mouse development. *Nature Cell Biol.* **2**, 70-75.

Wilkins, C., Dishongh, R., Moore, S.C., Whitt, M.A., Chow, M. and Machaca, K. (2005). RNA interference is an antiviral defense mechanism in *Caenorhabditis elegans. Nature* **436**, 1044-1047.

Wirblich, C., Bhattacharya, B. and Roy, P. (2006). Nonstructural protein 3 of Bluetongue virus assists virus release by recruiting ESCRT-1 protein Tsg101. *J. Virol.* **80**, 460-473.

Wu, M., Wu, R., Hung, C., Cheng, T., Tsai, W. and Chang, W. (2005). Simple and efficient DNA vector-based RNAi systems in mammalian cells. *Biochem. Biophys. Res. Commun.* **330**, 53-59.

Wu, V., Chen, S., Iwata, H., Compas, R. and Roy, P. (1992). Multiple glycoproteins synthesized by the smallest RNA segment (S10) of bluetongue virus. *J. Virol.* **12**, 7104-7112.

Wu, W., Hodges, E., Redelius, J. and Höög, C. (2004). A novel approach for evaluating the efficiency of siRNAs on protein levels in cultured cells. *Nucl. Acids Res.* **32**, e17.

Xia, H., Mao, Q., Paulson, H.L. and Davidson, B.L. (2002). siRNA-mediated gene silencing *in vitro* and *in vivo*. *Nature Biotech.* **20**, 1006-1010.

Xuan, B., Qian, Z., Hong, J. and Huang, W. (2006). EsiRNAs inhibit Hepatitis B virus replication in mice model more efficiently than synthesized siRNAs. *Virus Res.* **118**, 150-155.

Yang, D., Buchholz, F., Huang, Z., Goga, A., Chen, C-Y., Brodsky, F.M. and Bishop, J.M. (2002). Short RNA duplexes produced by hydrolysis with *Escherichia coli* RNase III mediate effective RNA interference in mammalian cells. *Proc. Natl. Acad. Sci. USA* **99**, 9942-9947.

Yang, W., Wang, Q., Howell, K.L., Lee, J.T., Murray, J.M. and Nishikura, K. (2005). ADAR1 RNA deaminase limits short interfering RNA efficacy in mammalian cells. *J. Biol. Chem.* **280**, 3946-3953.

Yin, J., Li, G., Ren, X. and Herrler, G. (2007). Select what you need: A comparative evaluation of the advantages and limitations of frequently used expression systems for foreign genes. *J. Biotechnol*. **127**, 335-347.

Yu, J.Y., DeRuiter, S.L. and Turner, D.L. (2002). RNA interference by expression of short-interfering RNAs and hairpin RNAs in mammalian cells. *Proc. Natl. Acad. Sci. USA* **99**, 6047-6052.

Zamore, P.D. (2001). Thirty-three years later, a glimpse at the ribonuclease III active site. *Mol. Cell*. **8**, 1158-1160.

Zamore, P.D., Tuschl, T., Sharp, P.A. and Bartel, D.P. (2000). RNAi: Double-stranded RNA directs the ATP-dependent cleavage of mRNA at 21 to 23 nucleotide intervals. *Cell* **101**, 25-33.

Zhang, G., Gurtu, V. and Kain, S.R. (1996). An enhanced green fluorescent protein allows sensitive detection of gene transfer in mammalian cells. *Biochem. Biophys. Res. Commun*. **227**, 707-711.

Zhang, H., Fabrice, A.K., Jaskiewicz, L., Westhof, E. and Filipowicz, W. (2004). Single processing centre models for human Dicer and bacterial RNase III. *Cell* **118**, 57-68.

Zhang, H., Kolb, F.A., Brondani, V., Billy, E. and Filipowicz, W. (2002). Human Dicer preferentially cleaves dsRNA at their termini without a requirement for ATP. *EMBO J.* **21**, 5875-5885.

Zuker, M. (2003). MFOLD web server for nucleic acid folding and hybridization prediction. *Nucl. Acids Res.* **31**, 3406-3415.